

(Gargèse, 14 May 2015)

Passive imaging of crust and mantle structure

**R. van der Hilst¹, M. de Hoop², H.J. Yao^{1,3}, H. Huang^{1,4},
M. Chen^{1,2}, S. Burdick^{1,5}, C. Yu¹**

¹ Massachusetts Institute of Technology (MIT)

² Now at: Rice University

³ Now at: University of Science and Technology China (USTC)

⁴ Now at: CGG Veritas, Houston

⁵ Now at: University of Maryland

Research sponsored by



Overview of lecture:

1. Introduction/background

2. Ambient noise and surface wave tomography (MIT, 2005-2015)

- Traditional transmission tomography:

- combining ambient noise and earthquake data
- quantifying and correcting for uneven noise distribution
- azimuthal anisotropy
- radial anisotropy

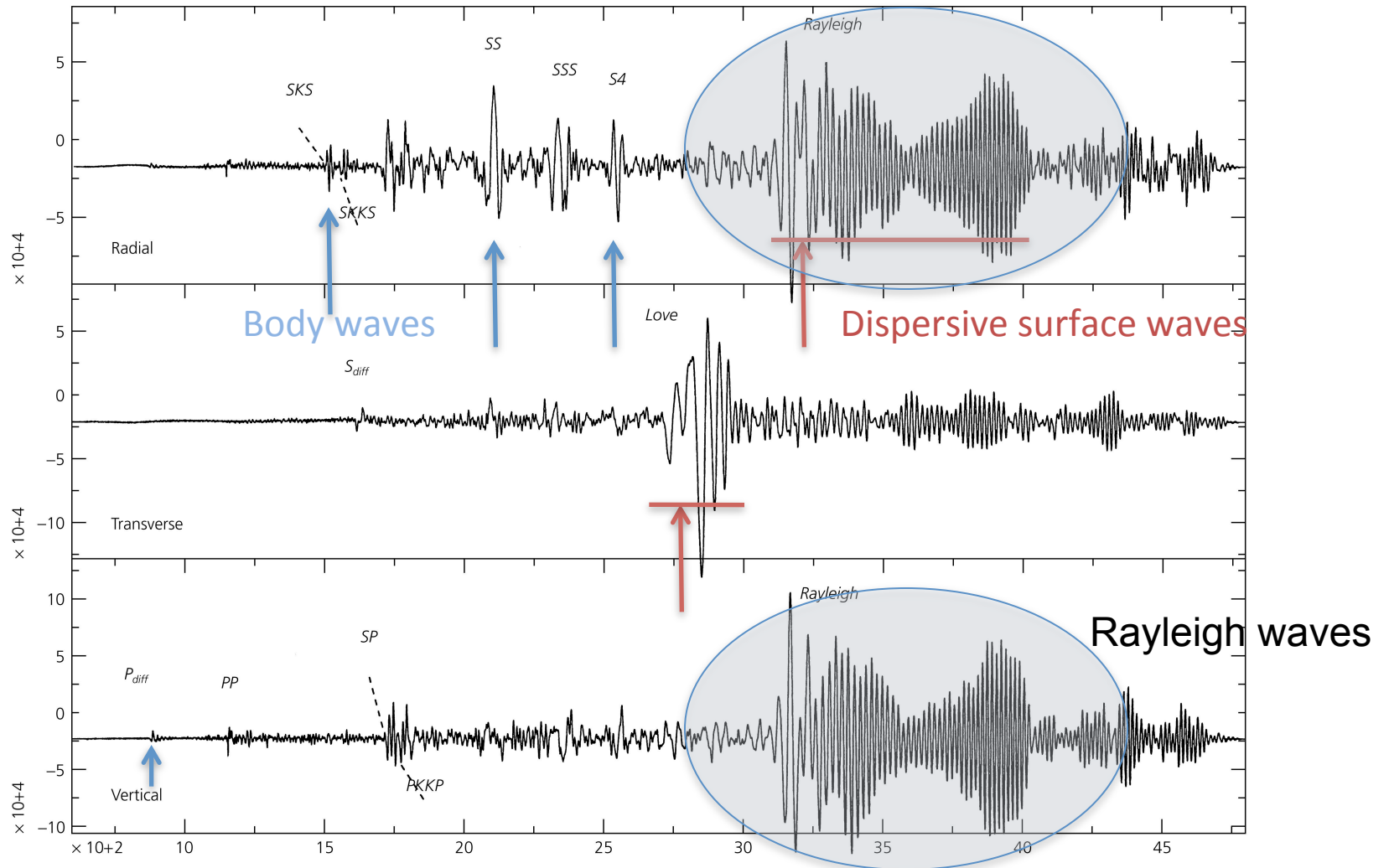
- Eikonal tomography

- Adjoint tomography with ambient noise data

3. Interferometry of teleseismic body waves – concept

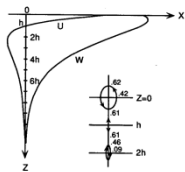
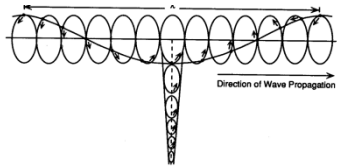
4. Imaging with multiples – just some thoughts ...

Figure 2.7-1: Seismograms recorded at a distance of 110°, showing surface waves.

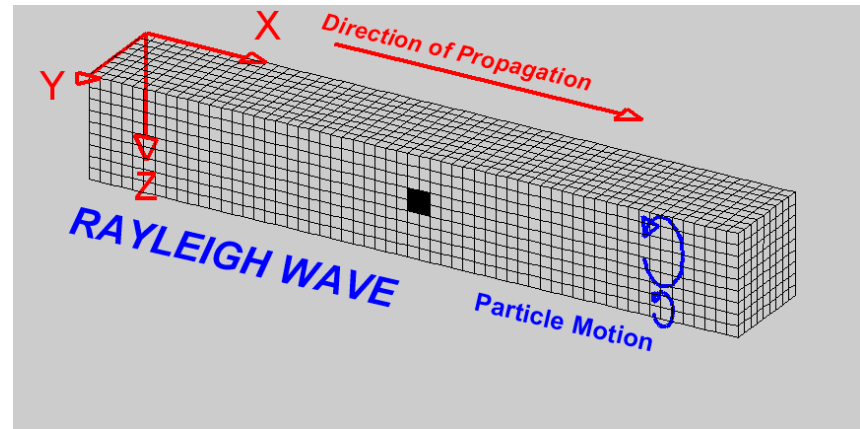


From Stein and Wyession

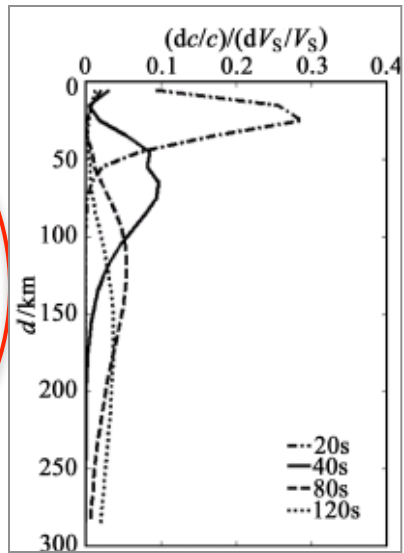
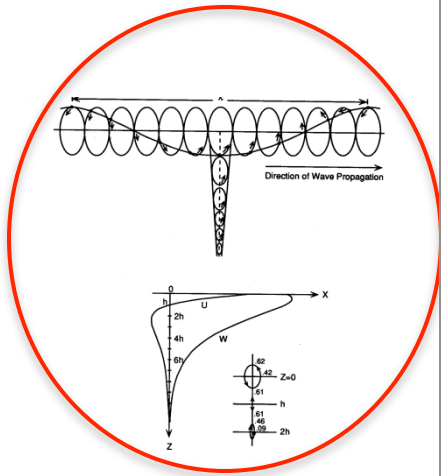
'Surface and guided waves': waves trapped in the shallow layers or a wave guide (such as Love waves in the Earth, acoustic waves in the oceanic SOFAR,)



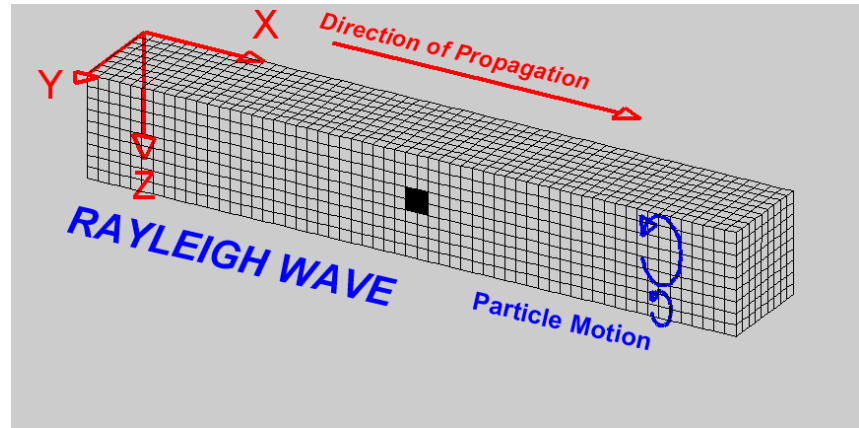
Eigenfunction



'Surface and guided waves': waves trapped in the shallow layers or a wave guide (such as Love waves in the Earth, acoustic waves in the oceanic SOFAR,)



frequency proxy for depth



Overview of lecture:

1. Introduction/background

2. Ambient noise and surface wave tomography (MIT, 2005-2015)

- Traditional transmission tomography:

- combining ambient noise and earthquake data
- quantifying and correcting for uneven noise distribution
- azimuthal anisotropy
- radial anisotropy

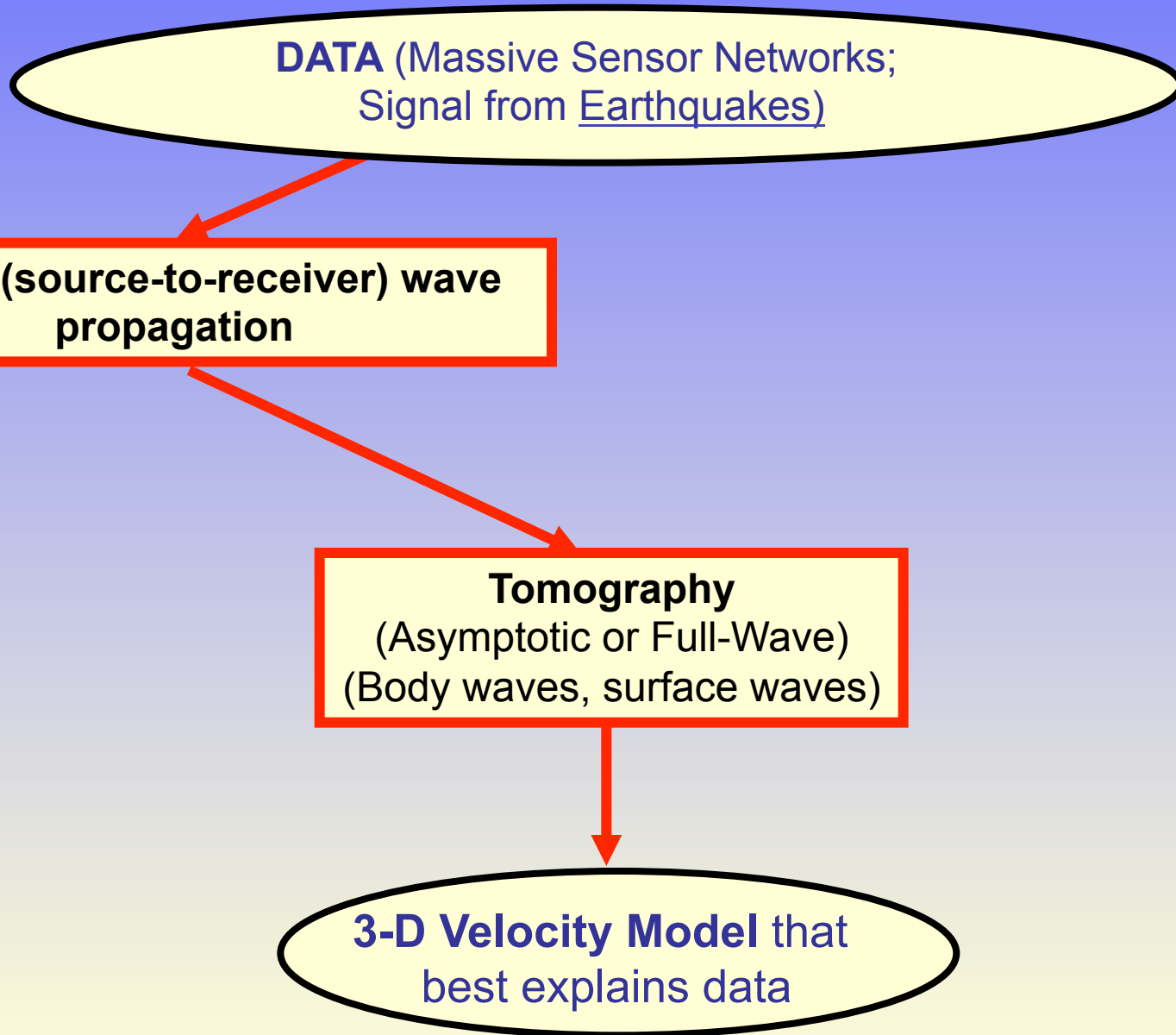
- Eikonal tomography

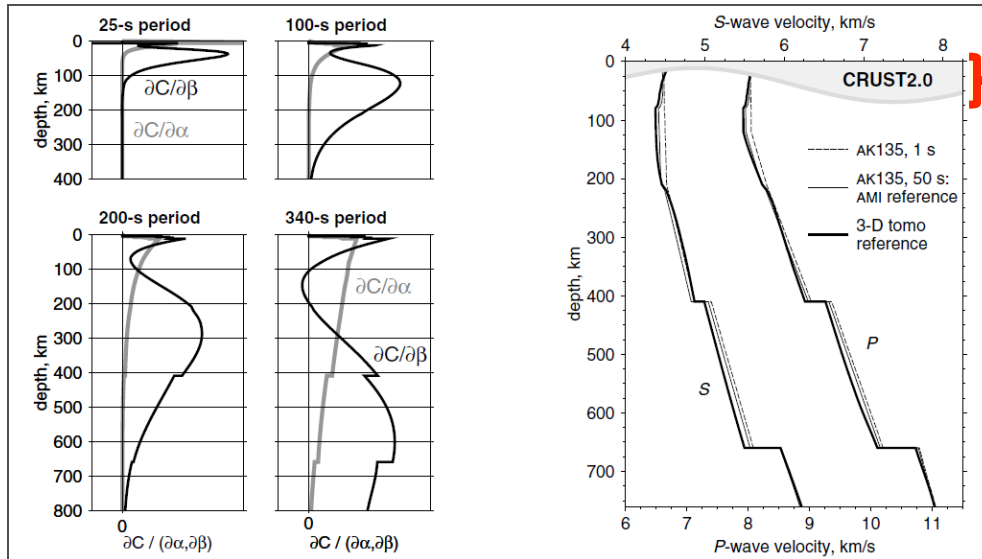
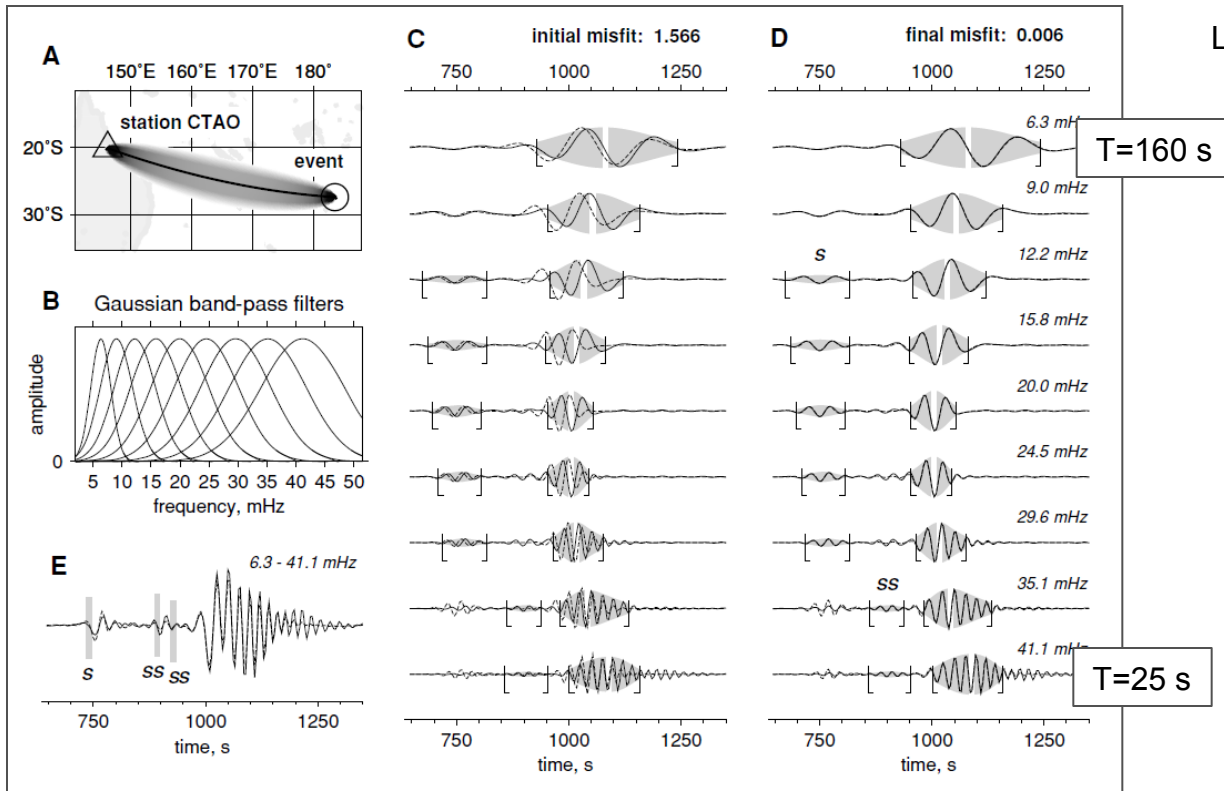
- Adjoint tomography with ambient noise data

3. Interferometry of teleseismic body waves

4. Imaging with multiples

Traditional Approach to Tomography



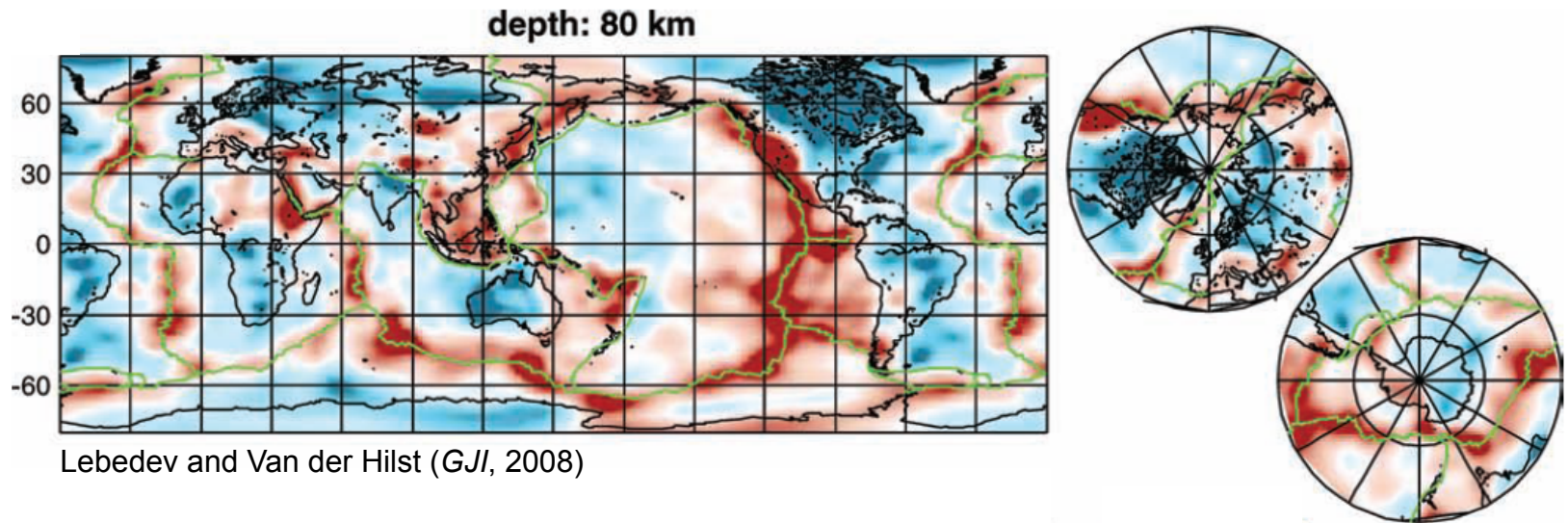
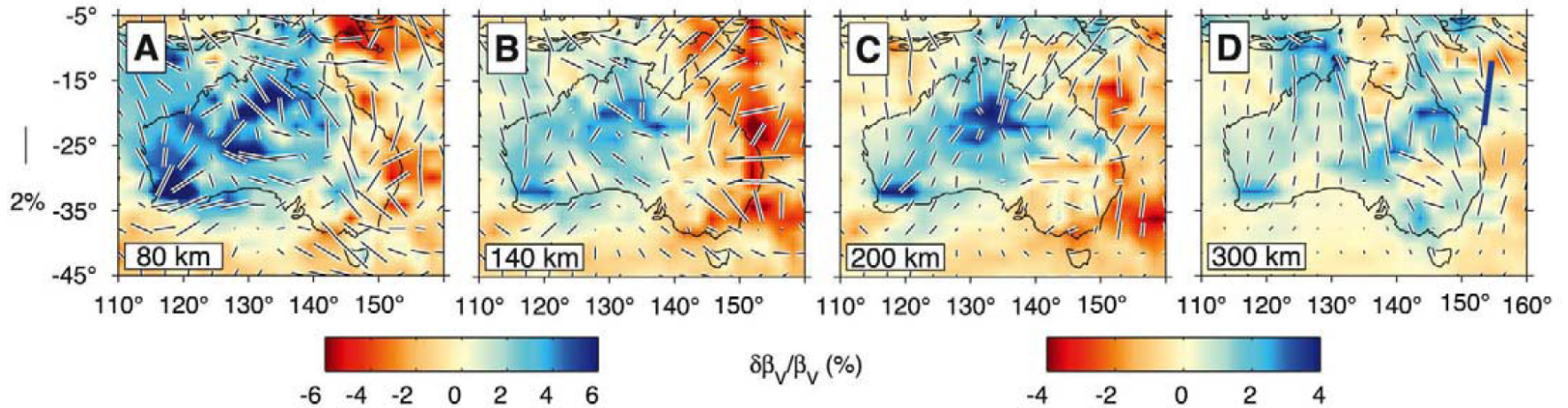


Crust = Problem!

Examples from traditional surface wave tomography with earthquake waves: relatively low frequencies → deep structures

T > 30 s → upper mantle

Simons and Van der Hilst (*EPSL*, 2008)



Lebedev and Van der Hilst (*GJI*, 2008)

Ambient Noise Tomography

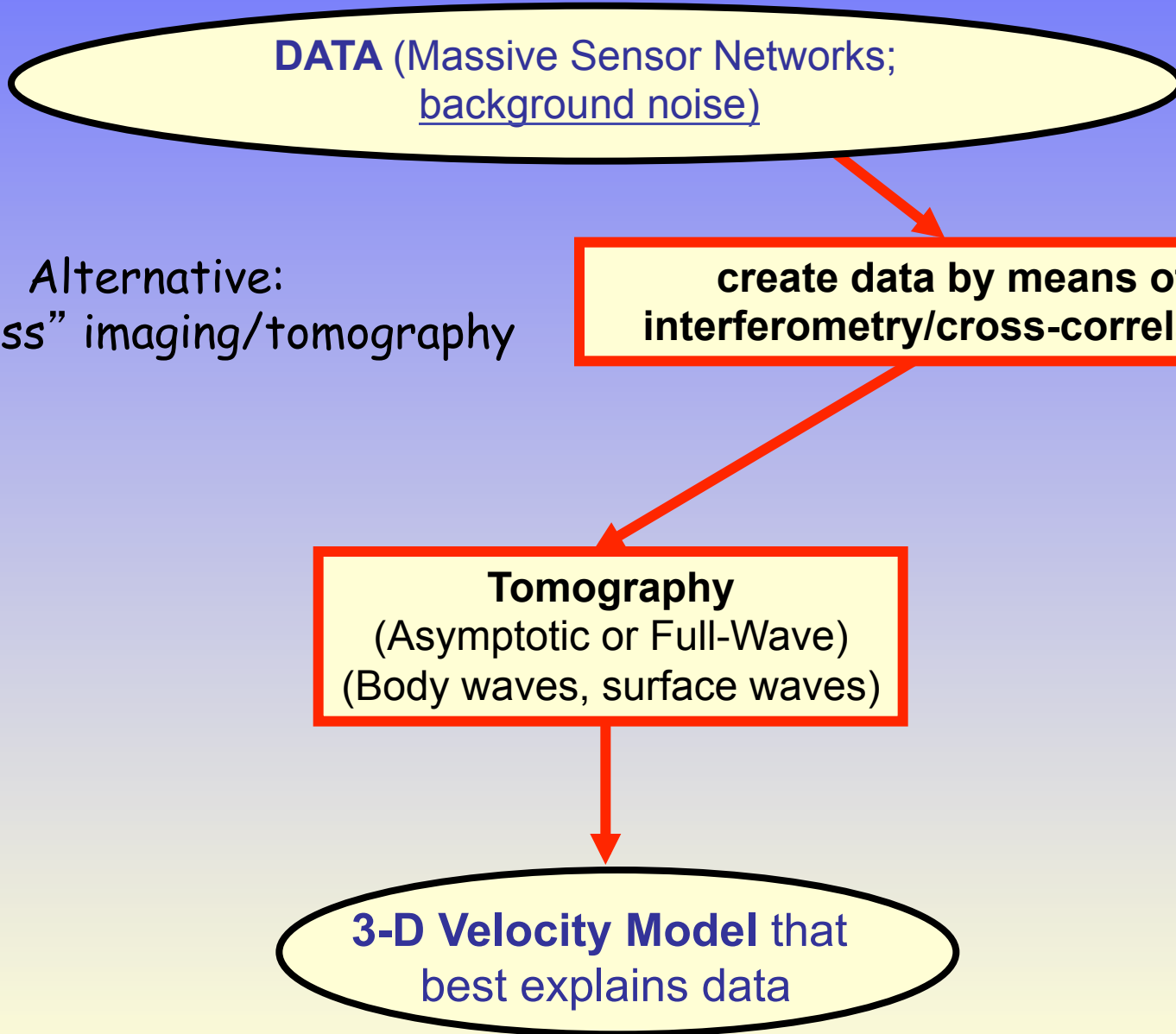
DATA (Massive Sensor Networks;
background noise)

Alternative:
“sourceless” imaging/tomography

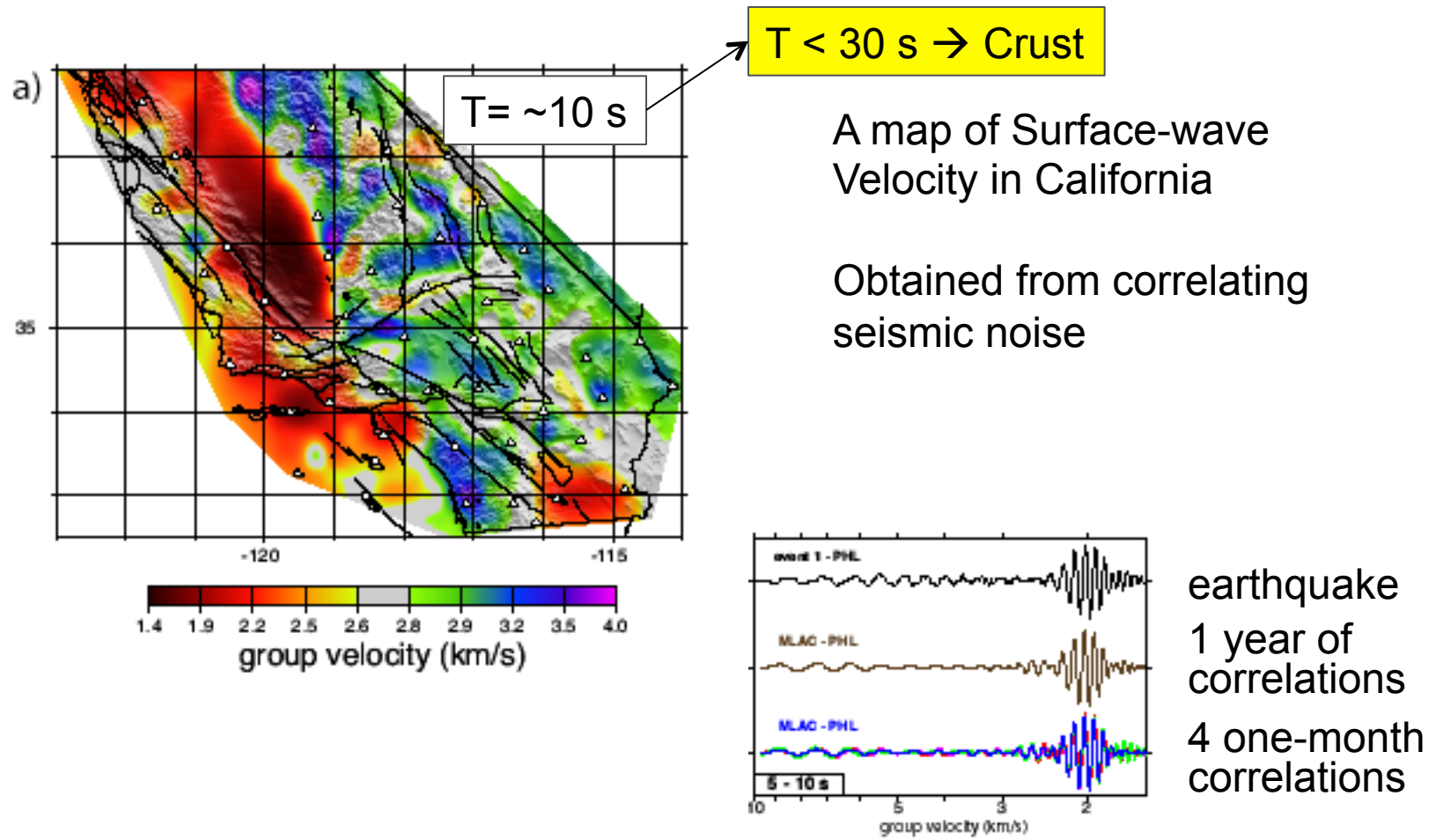
**create data by means of
interferometry/cross-correlation**

Tomography
(Asymptotic or Full-Wave)
(Body waves, surface waves)

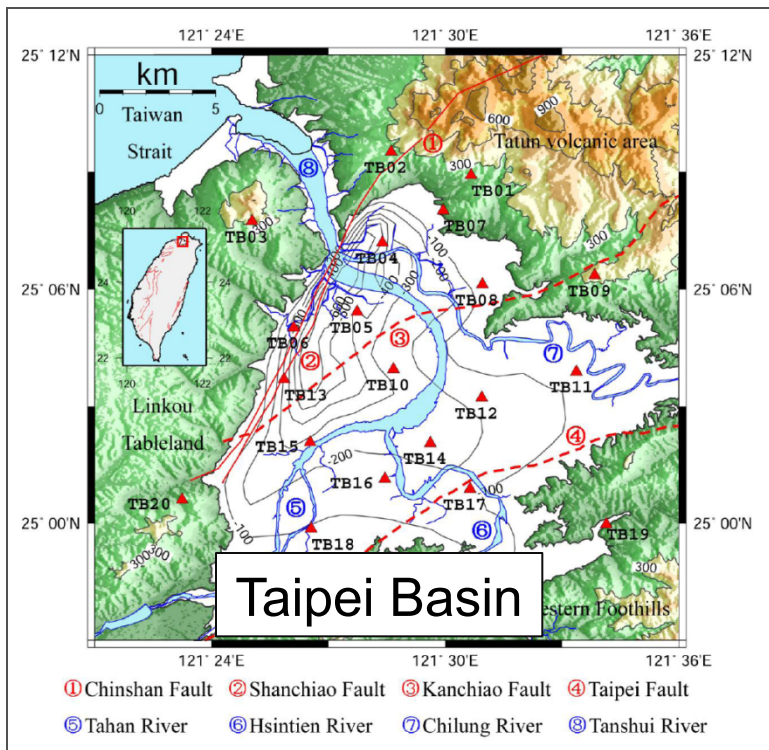
3-D Velocity Model that
best explains data



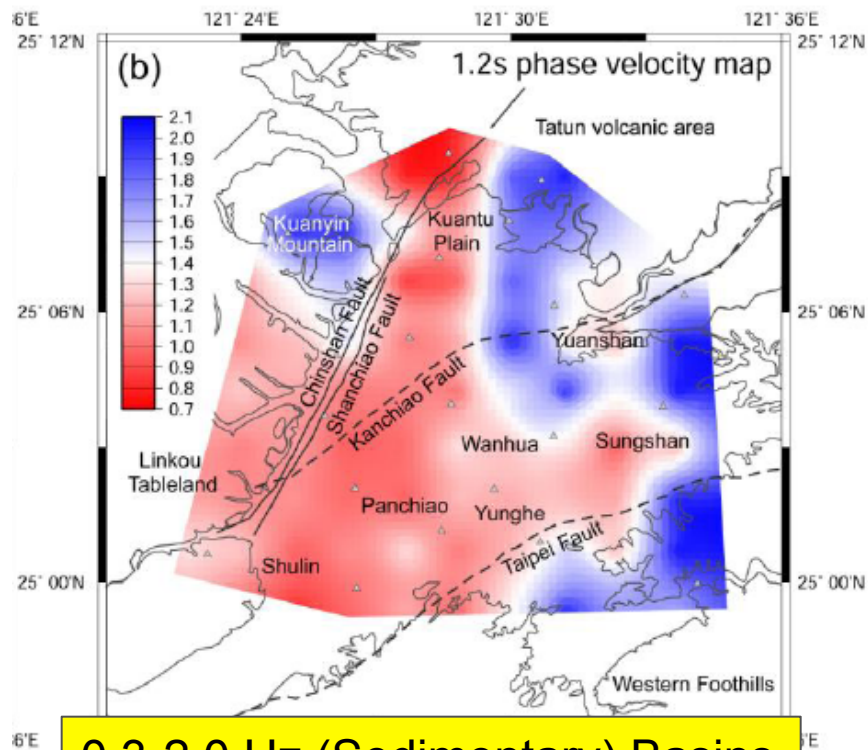
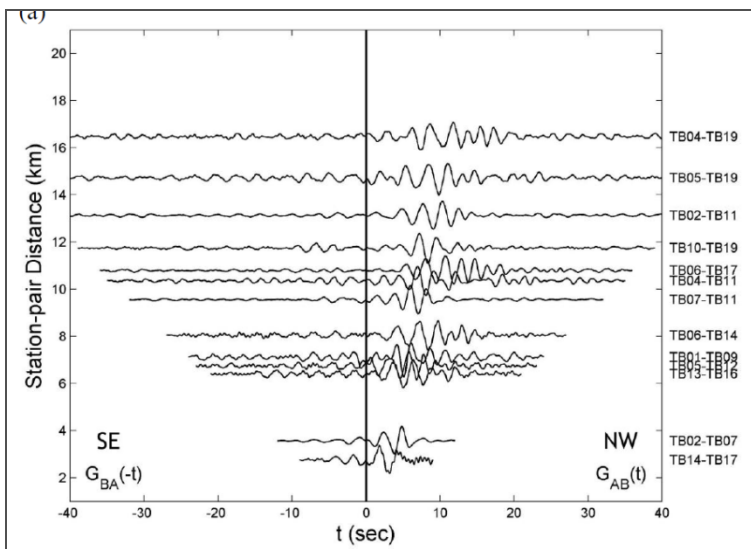
Shapiro, N.M., M. Campillo, L. Stehly, and M.H. Ritzwoller, 2005, High-Resolution Surface-Wave Tomography from Ambient Seismic Noise: *Science* **307**:1615-1618



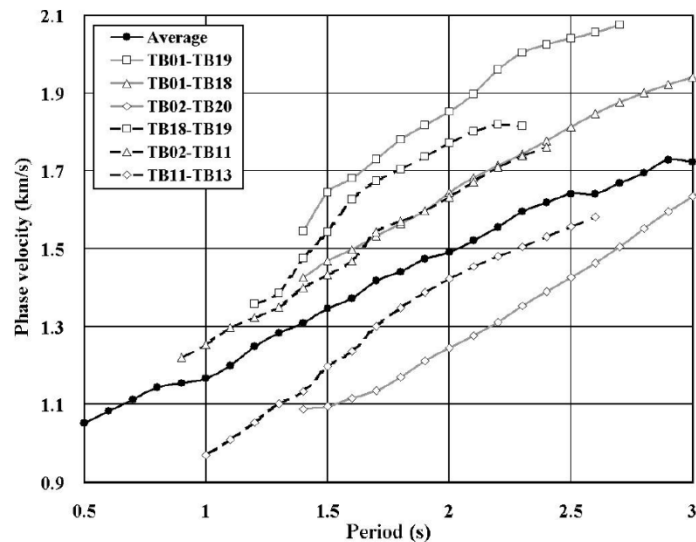
also Sabra, et al Surface wave tomography from microseisms in Southern California
Geophys Res Lett **32** (2005)



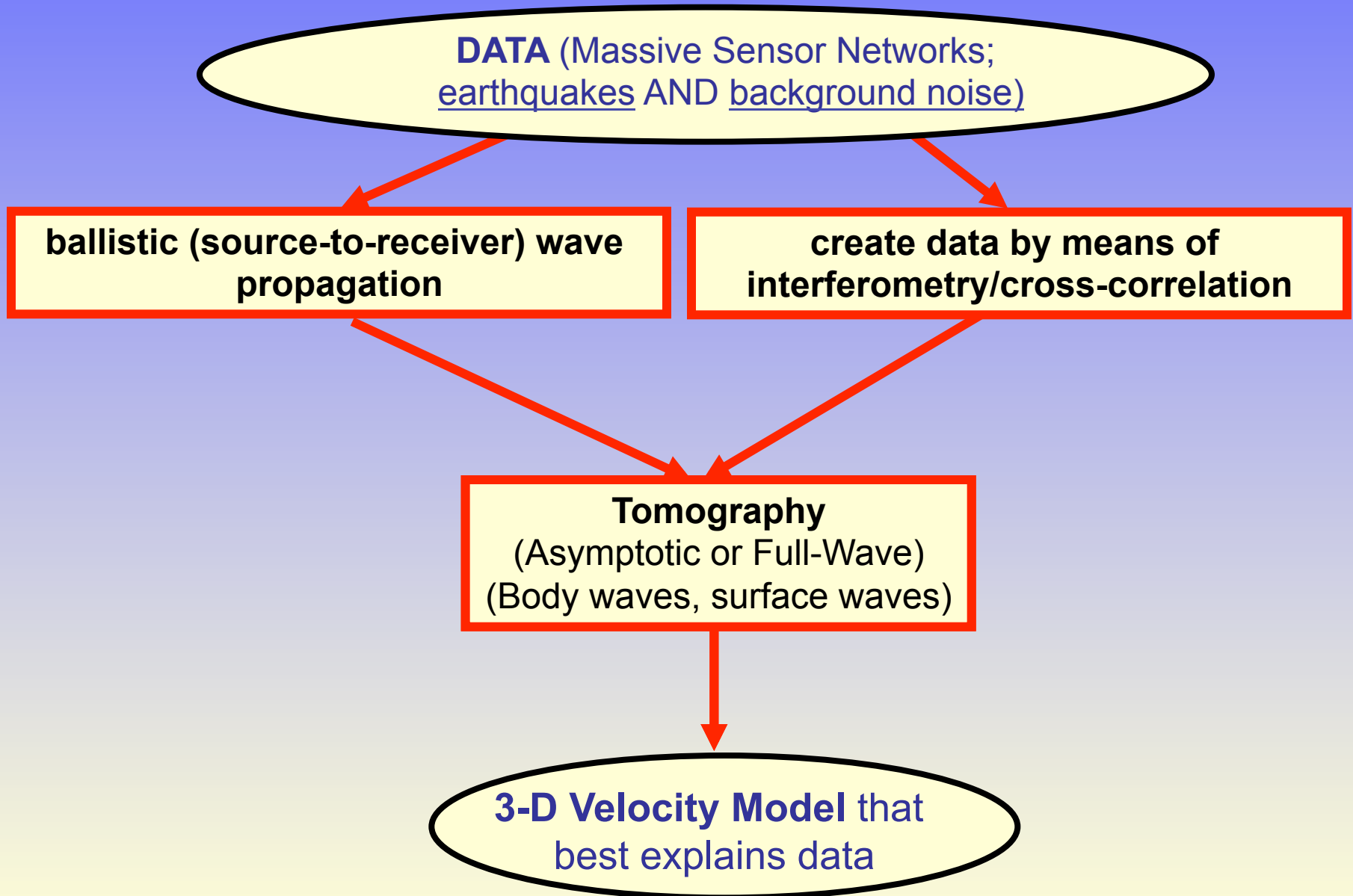
Huang et al. (BSSA, 2010)



0.3-2.0 Hz (Sedimentary) Basins



Use both 'active' and 'passive' data



Field Projects Sichuan & Yunnan Provinces and E. Tibet (2003-2004)

Crust-Mantle study E Tibet – SW China



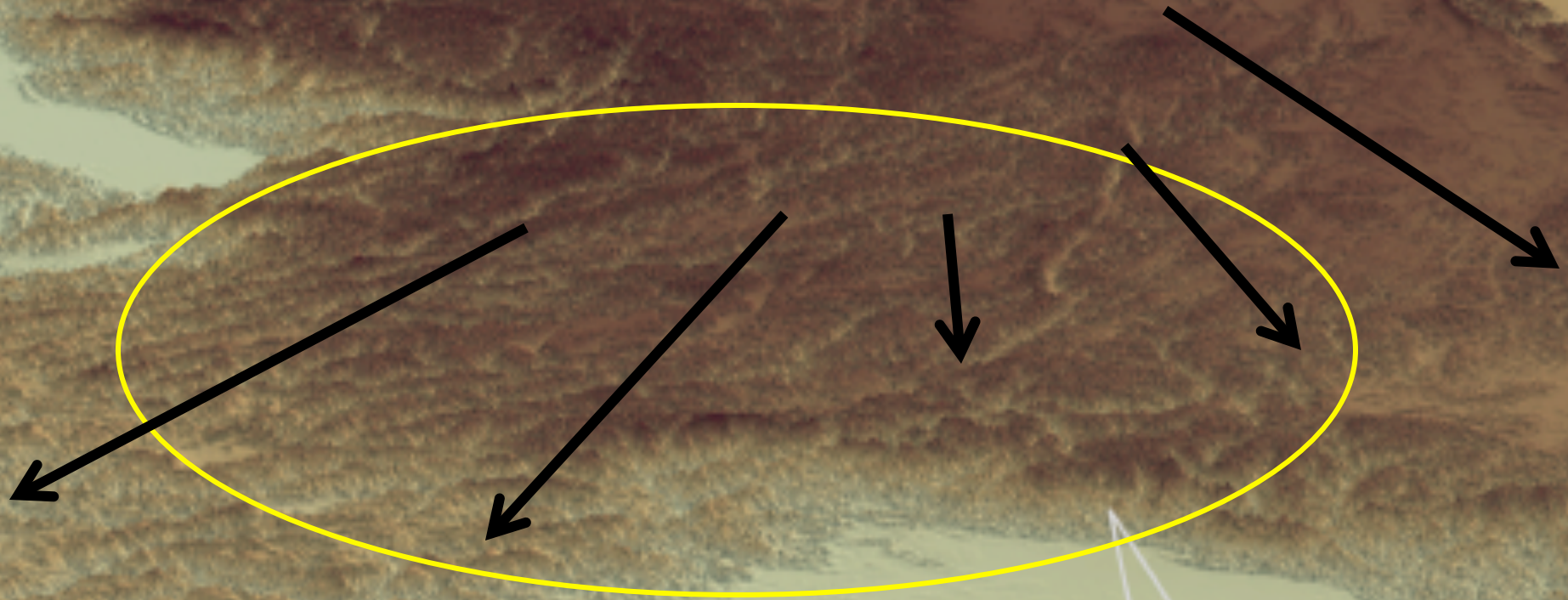
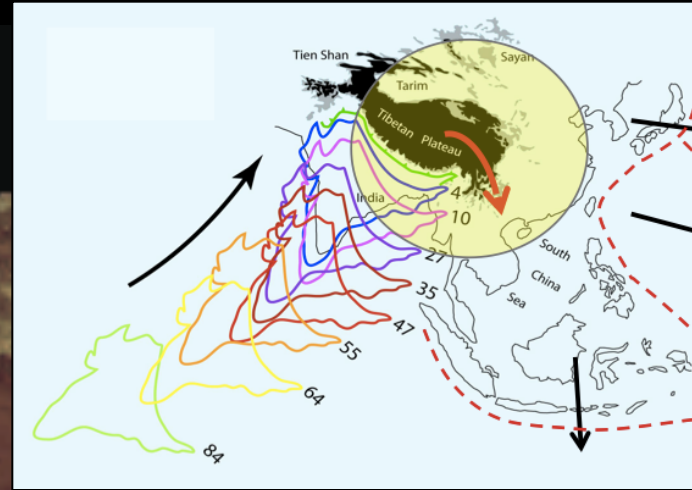
Why SE Tibet?

1. understanding eastward expansion of plateau

→ N

India

Tibetan Plateau

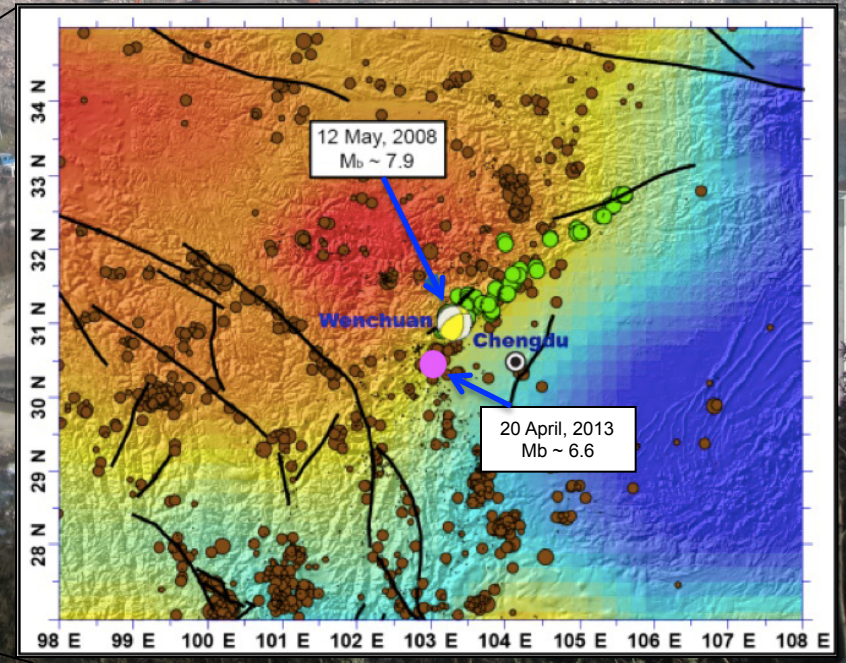
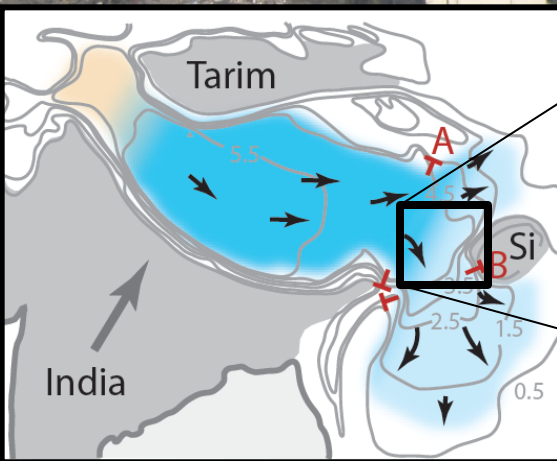
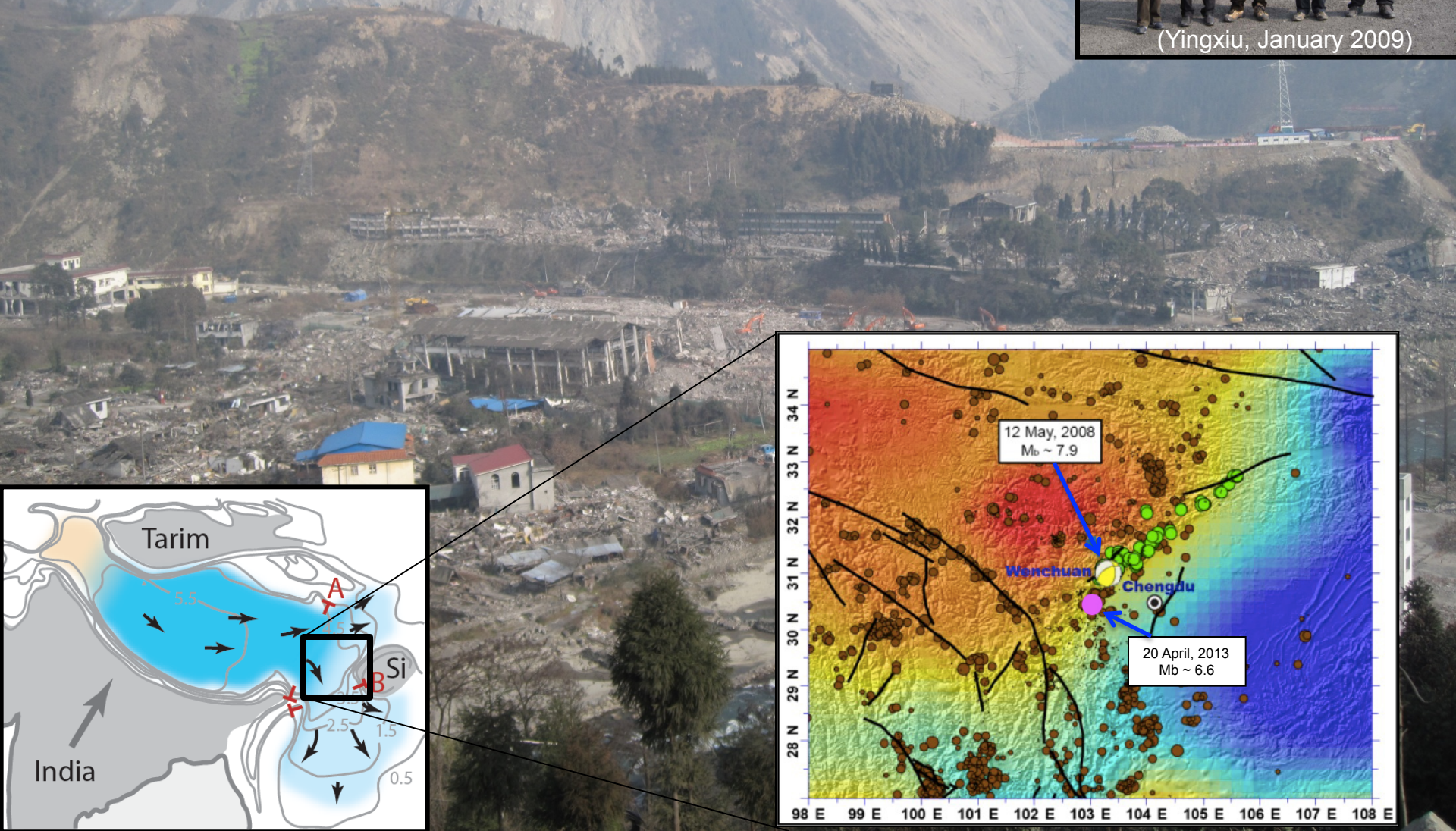
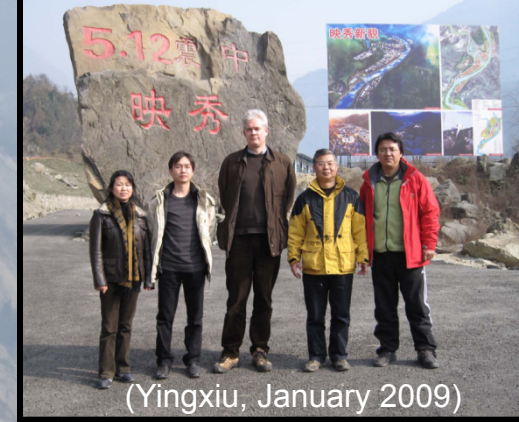


Why SE Tibet?

2. Southern end of Trans China Seismicity Belt

E.g. Sichuan, 12 May 2008

~80,000 people killed ...

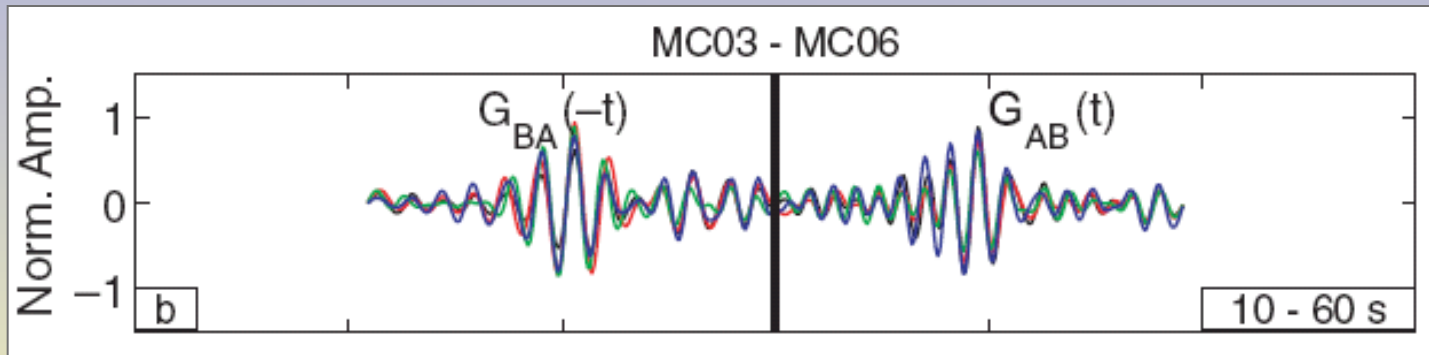


Interferometry:

long-term noise correlation \rightarrow new data
for crustal tomography

$$\frac{dC_{AB}(t)}{dt} \approx -\hat{G}_{AB}(t) + \hat{G}_{BA}(-t) \approx -G_{AB}(t) + G_{BA}(-t).$$

G = Green's function

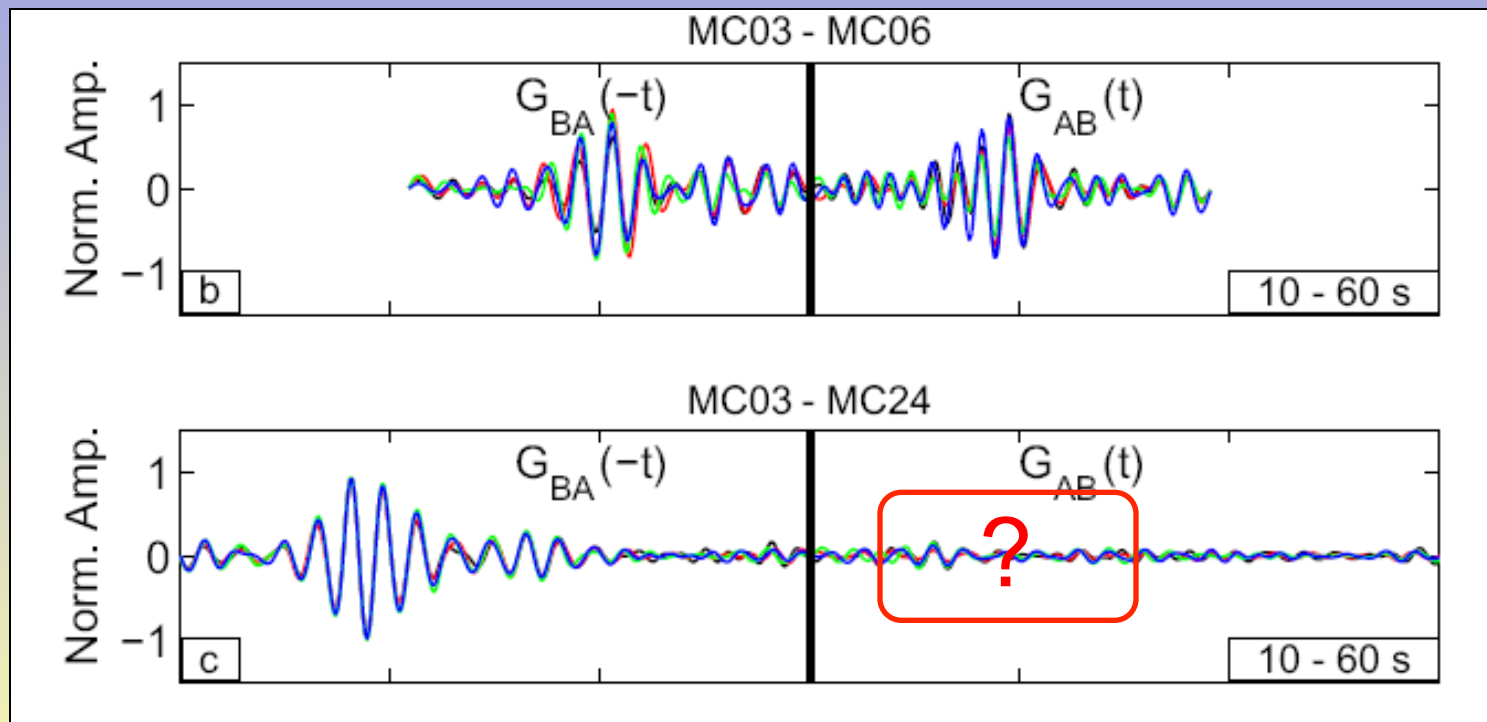


Yao et al. (*GJI*, 2006)

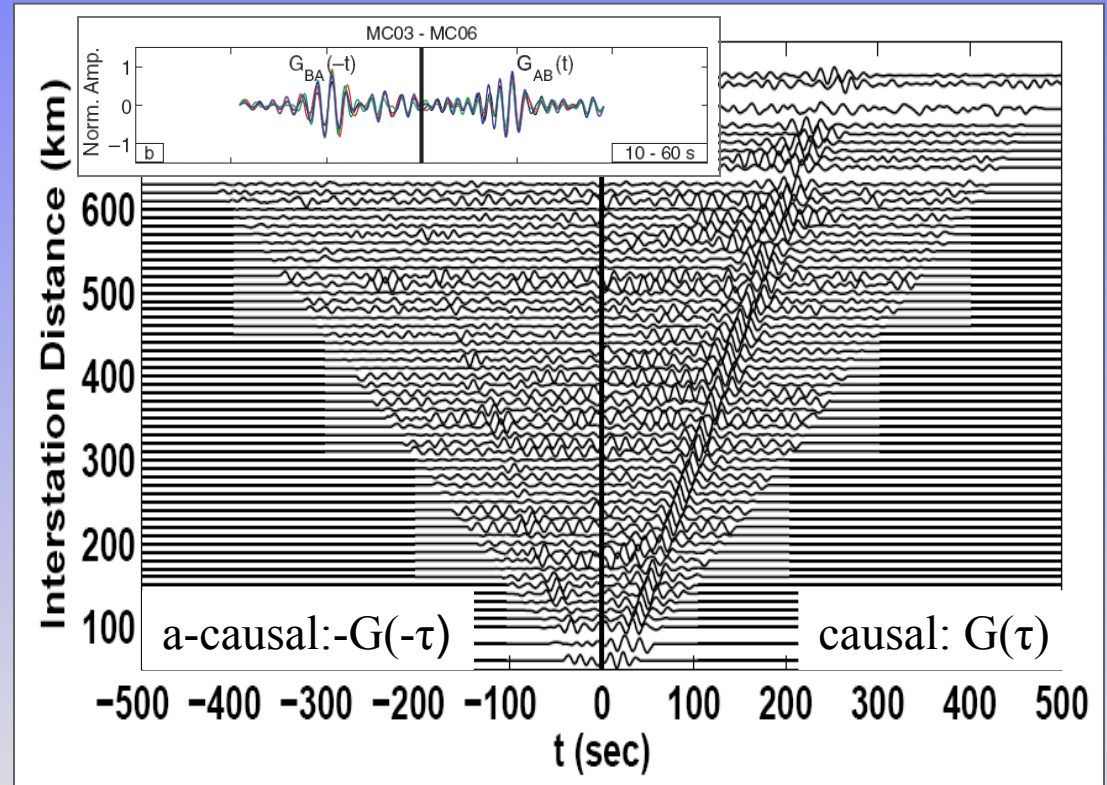
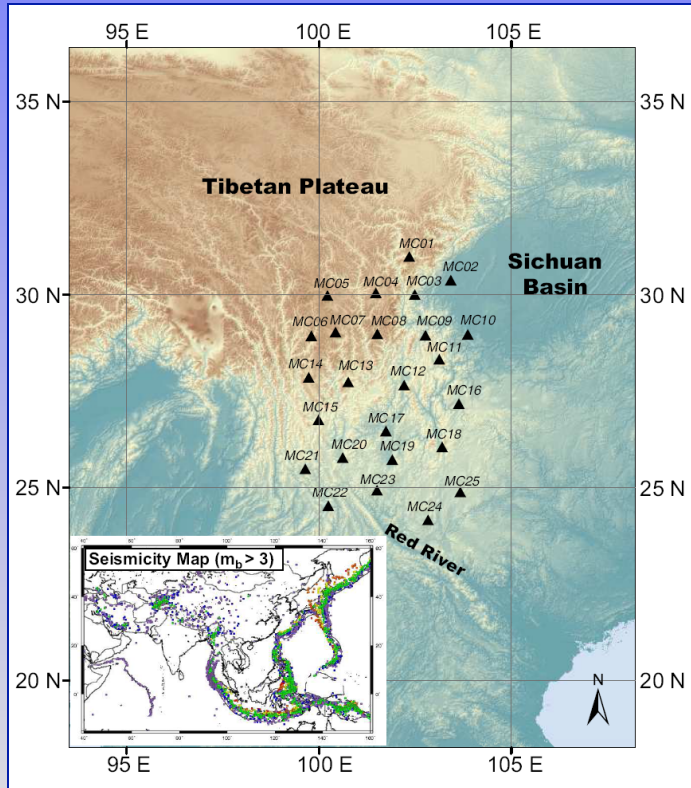
Interferometry:

long-term noise correlation \rightarrow new data
for crustal tomography

(simple in concept, but devil is in the detail ...)

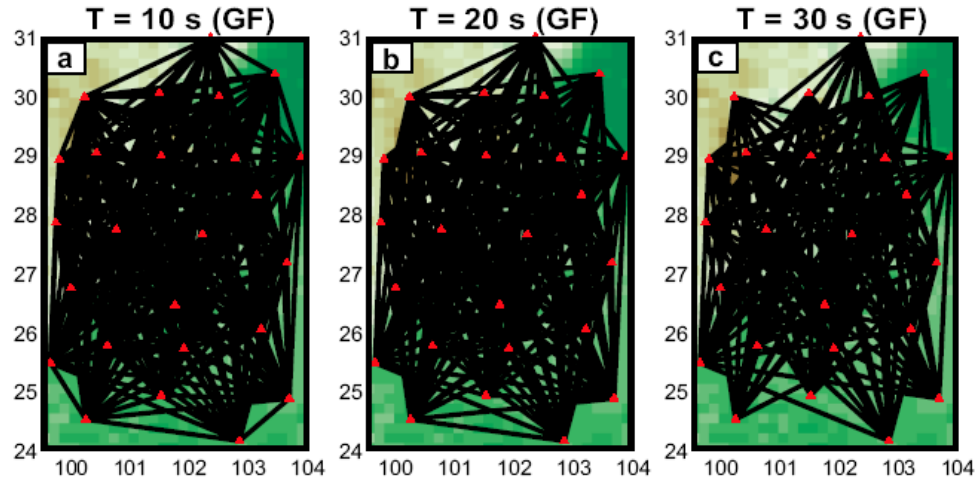


Crust and Lithosphere: Multi-resolution surface wave tomography



Seismic interferometry → estimate data from background “noise”
(NB we ignore asymmetry and sum causal and a-causal signals)

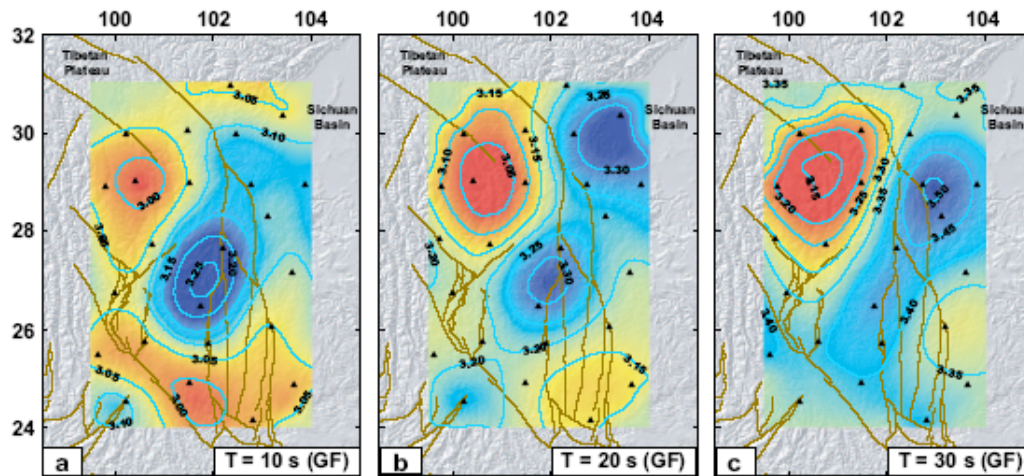
Example: “ambient noise” surface wave tomography



“source”-receiver pairs at different periods

Interferometry (scattering) → works well for relatively short periods (high frequency)

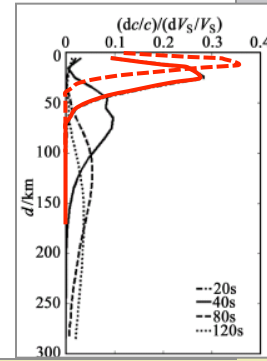
Example: “ambient noise” surface wave tomography



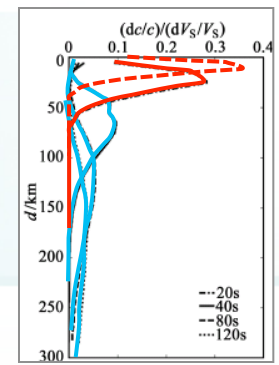
Phase velocity maps at different periods

Interferometry (scattering) → relatively short periods (high frequency)

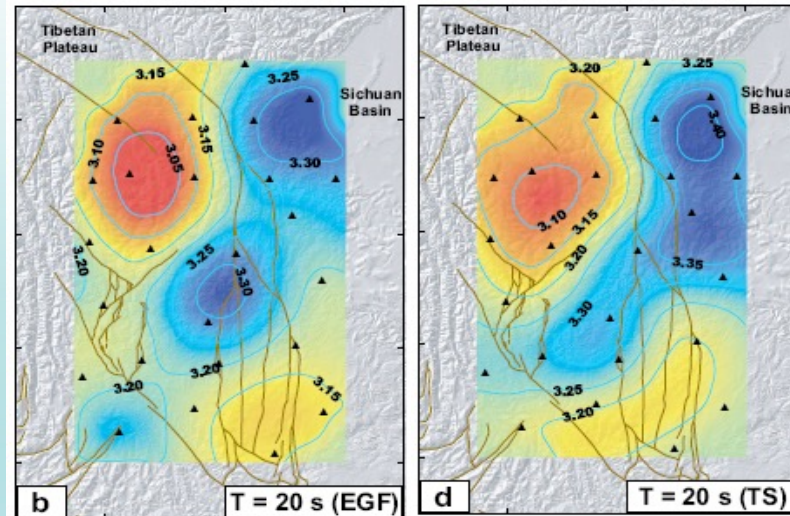
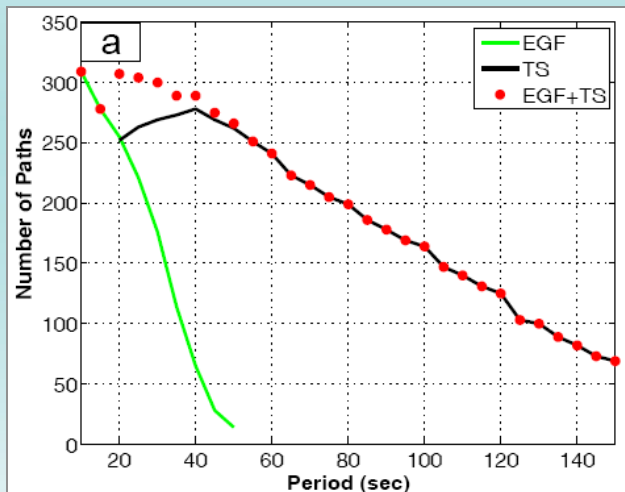
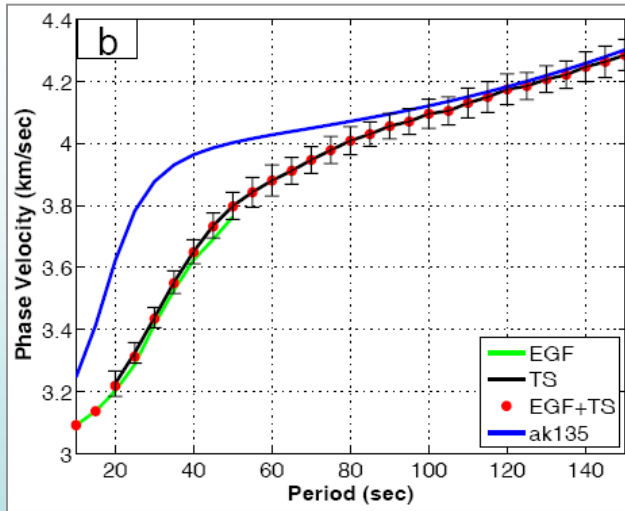
For surface wave tomography that means: “shallow” sub-surface



Combination of ambient noise and earthquake data: extend frequency range \rightarrow extend depth range

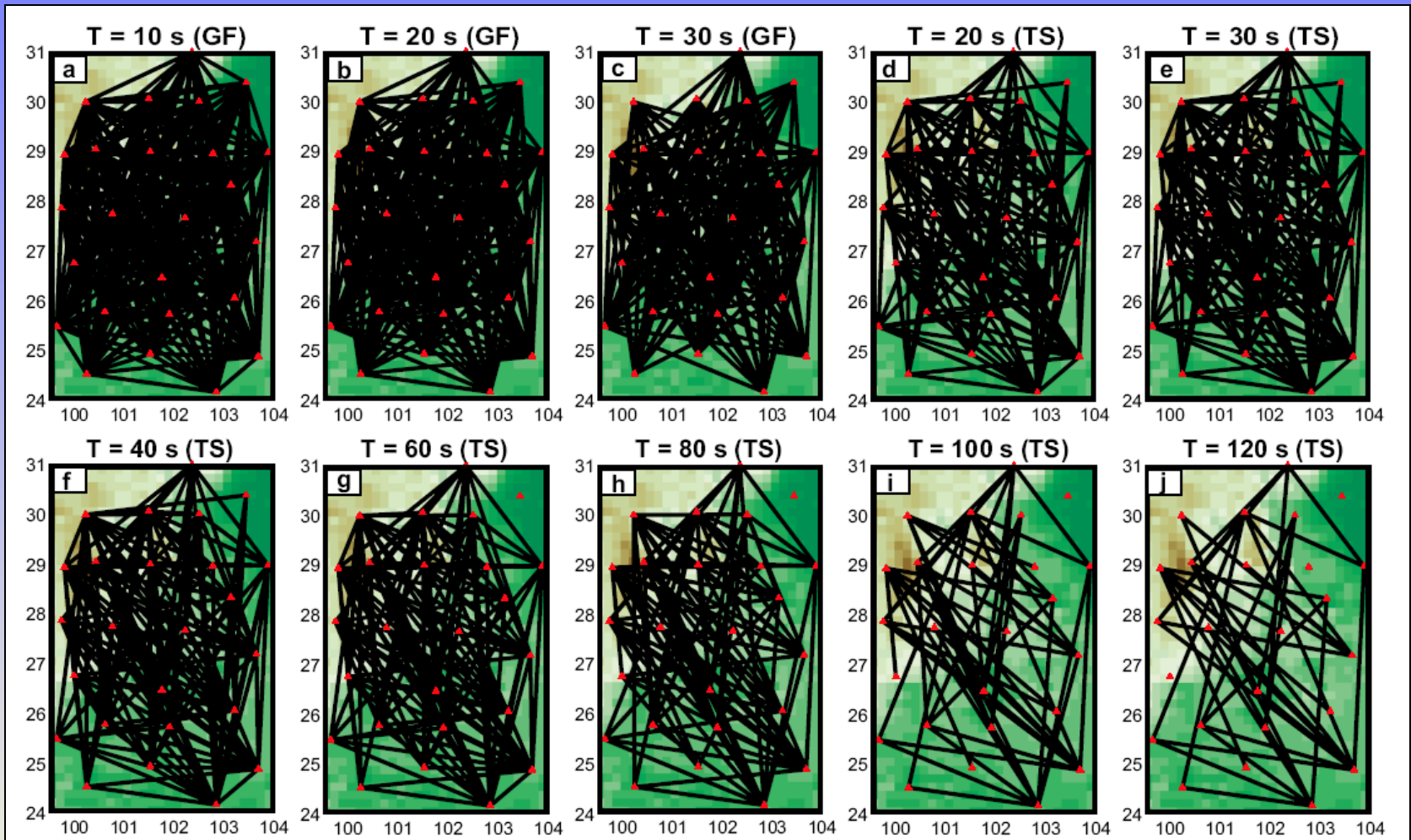


At overlapping periods, Rayleigh wave phase velocities from EGF (from 10 months Z-comp. data) and TS analyses are similar

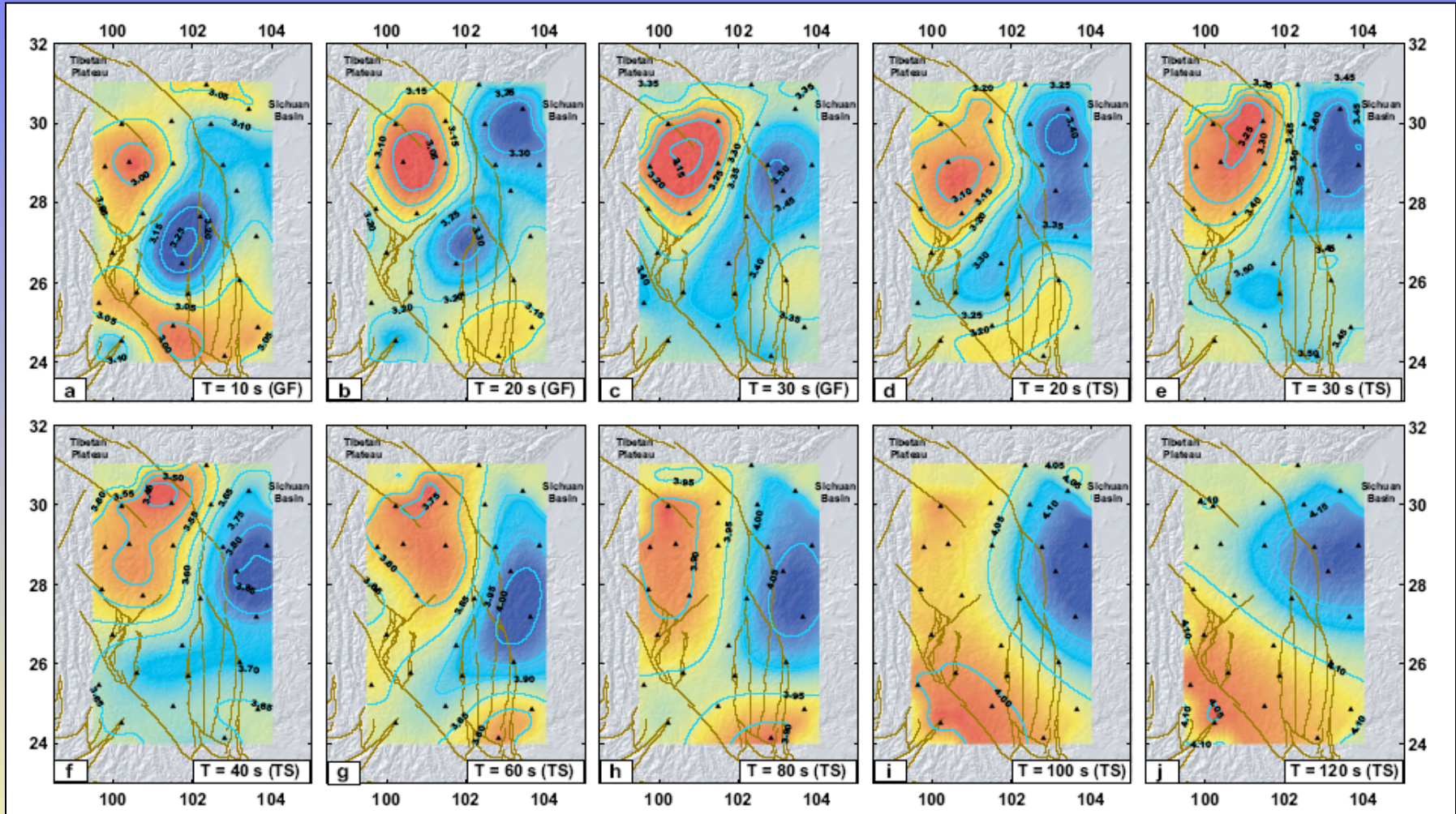


- TS slightly higher ($< 0.7\%$) due to differences in finite frequency effect
- Difference \ll medium perturbations ($< 10\%$)

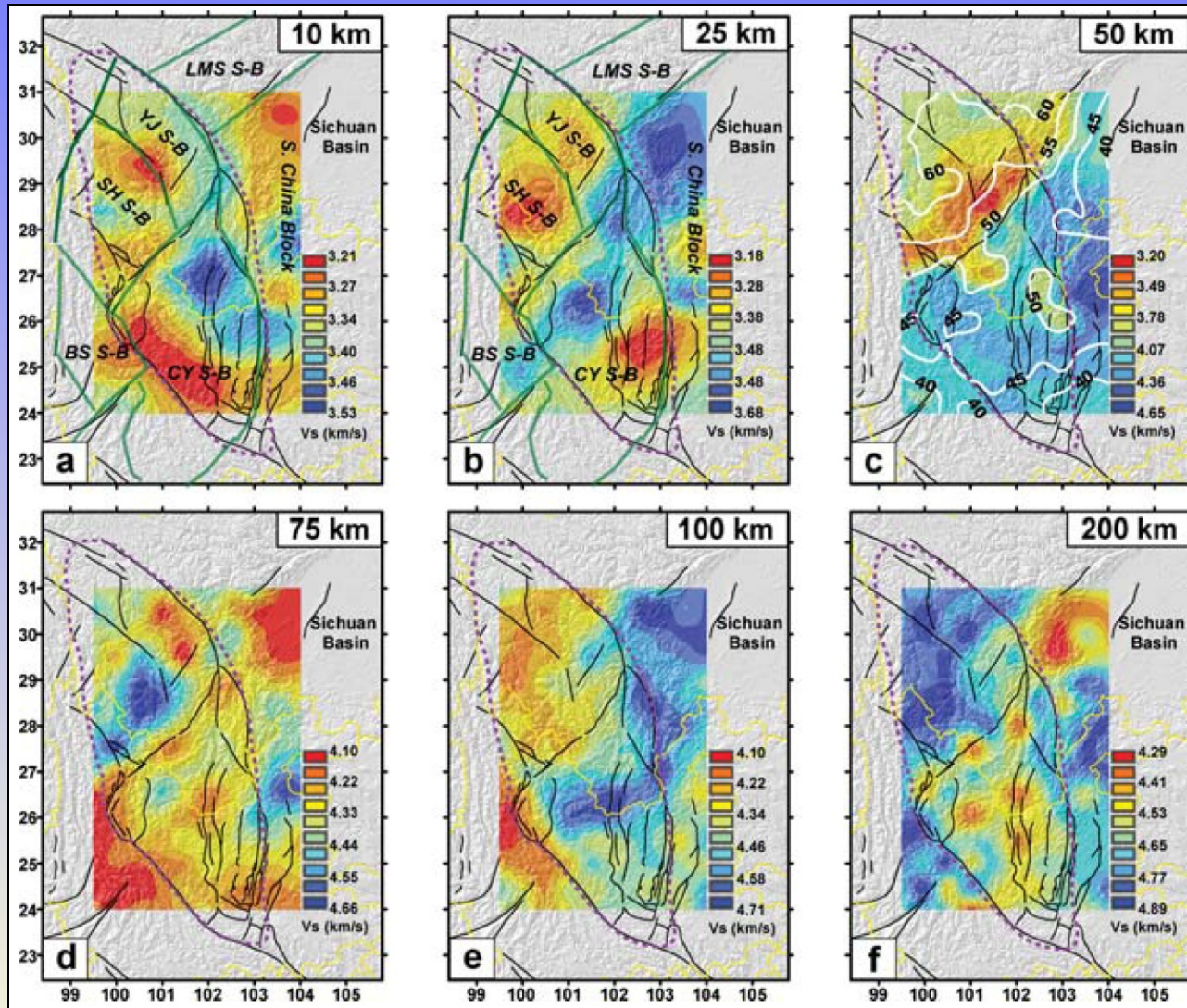
Multi-resolution surface wave tomography



Phase velocity maps at different periods



Multi-resolution surface wave tomography



Anisotropy I: Azimuthal Anisotropy

(i.e., dependence of wavespeed on direction of propagation in horizontal plane)

- Step 1: inter-station phase velocities from **EGF** → azimuthally anisotropic phase velocity maps

$$c(\omega, \psi) = c_0(\omega) [1 + a_0(\omega) + a_1(\omega) \cos 2\psi + a_2(\omega) \sin 2\psi]$$

- Step 2: phase velocity maps → shear wave speed & anisotropy

$$\delta c_R(x, y, \omega, \psi) \approx \int_0^H \left[\frac{\partial c_R}{\partial L} (\delta L + G_c \cos 2\psi + G_s \sin 2\psi) \right] \frac{dz}{\Delta h}$$

At each point (x,y), the reference crustal thickness is constrained from receiver functions (Xu et al., 2007; Zurek et al, 2005)

$$\hat{\beta}_{SV} \approx \beta_{SV} \left(1 + \frac{G_c}{2L} \cos 2\psi + \frac{G_s}{2L} \sin 2\psi \right)$$

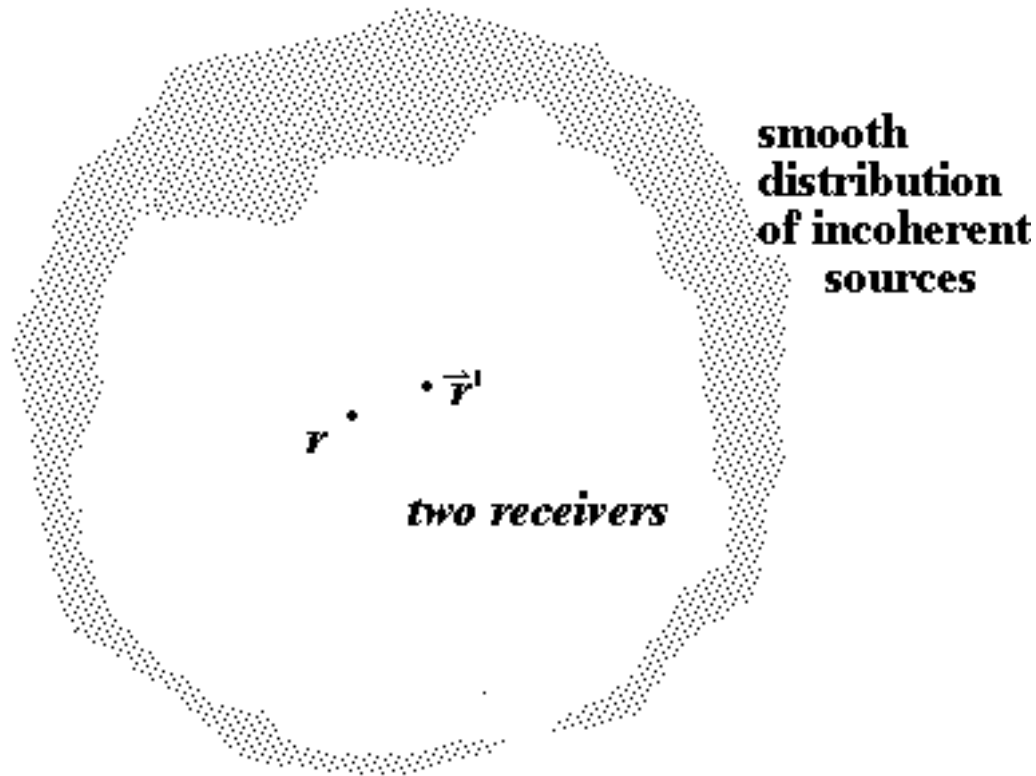
Transverse isotropic v_{SV} : $\beta_{SV} = \sqrt{L/\rho}$

Magnitude of azimuthal aniso $A_{SV} = \frac{1}{2L} \sqrt{(G_c)^2 + (G_s)^2}$

Fast axis of azimuthal aniso: $\phi = \frac{1}{2} \tan^{-1}(G_s/G_c)$

"Ponderosity" (i.e. angular weighting of incident intensity)

What is the effect of uneven noise distribution on estimates of elastic anisotropy?
That is, what happens if the intensity of incident field itself is anisotropic?

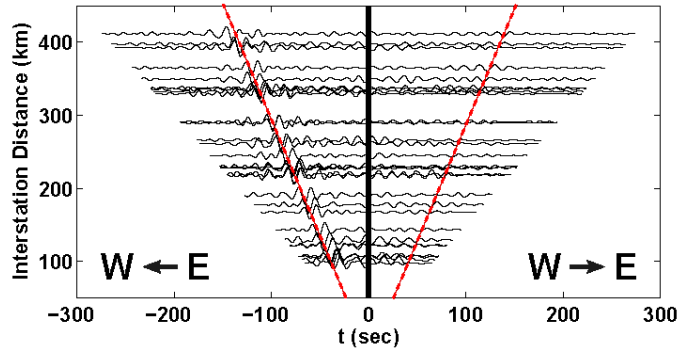


Courtesy: Weaver (Cargese, 2011)
Froment et al. (2009)

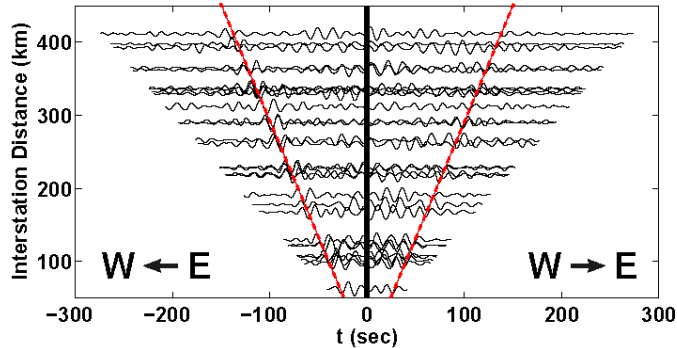
Recovery of surface wave GF in SE Tibet from ambient noise

(onebit) cross-correlation of monthly continuous data (10-20s)

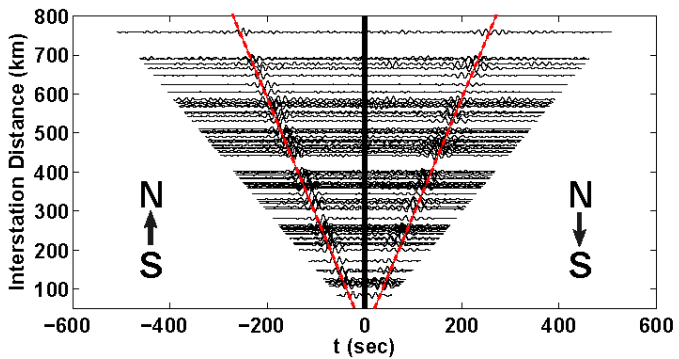
(a) Jan 2004 (E-W)



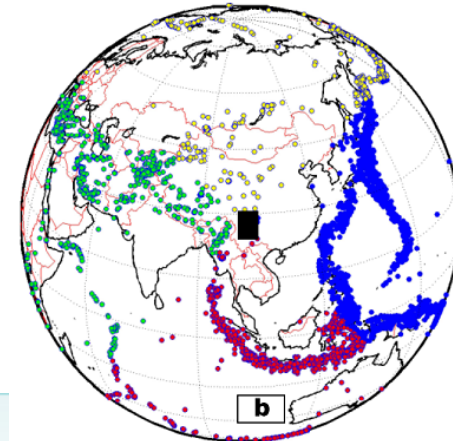
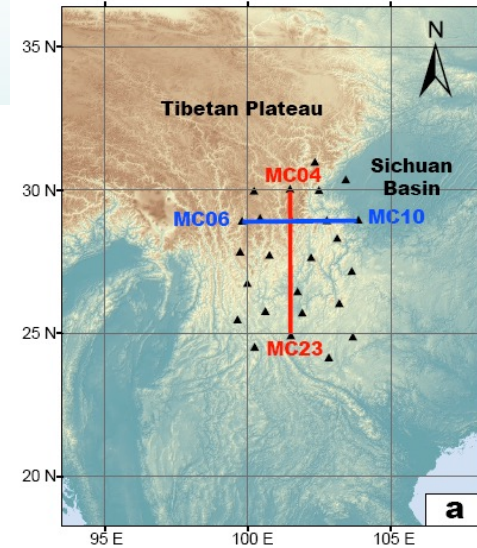
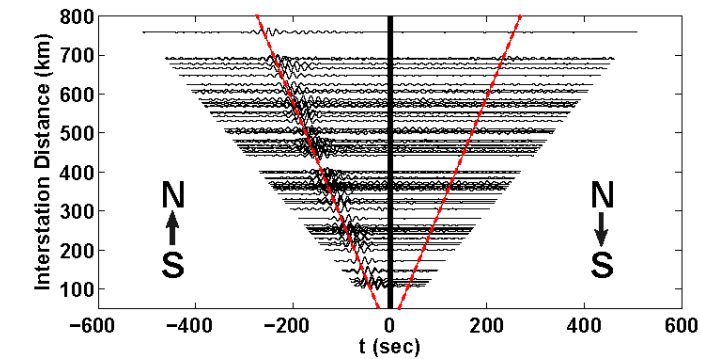
(b) July 2004 (E-W)



(c) Jan 2004 (S-N)



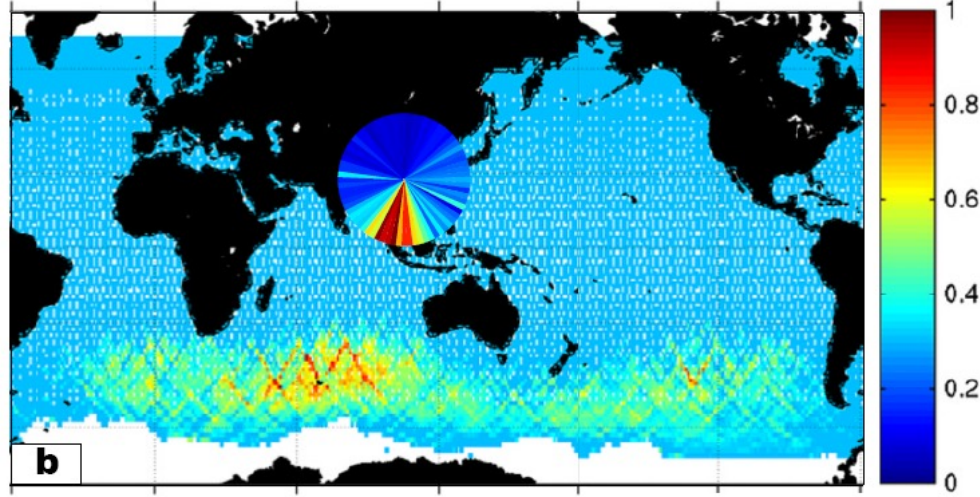
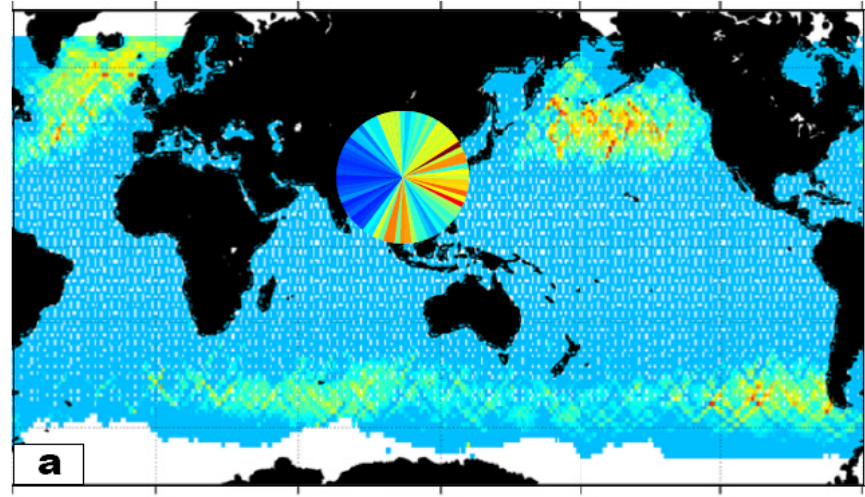
(d) July 2004 (S-N)



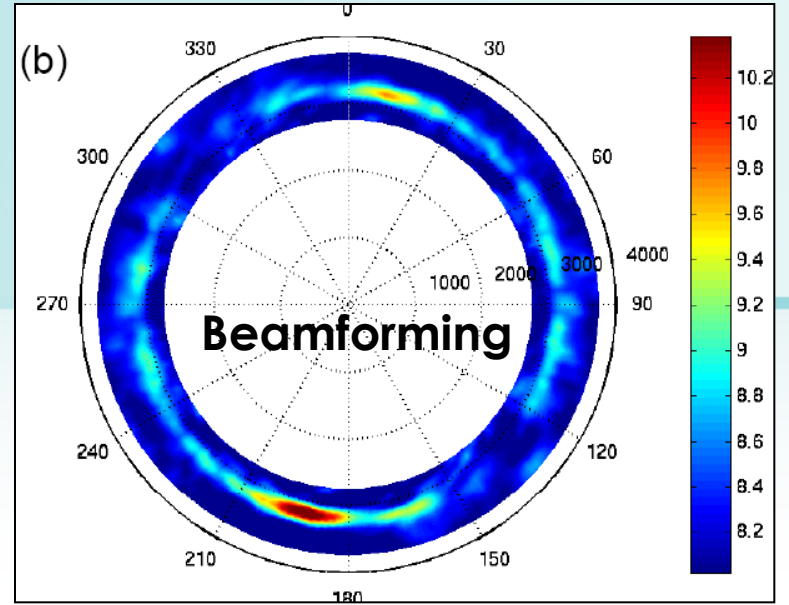
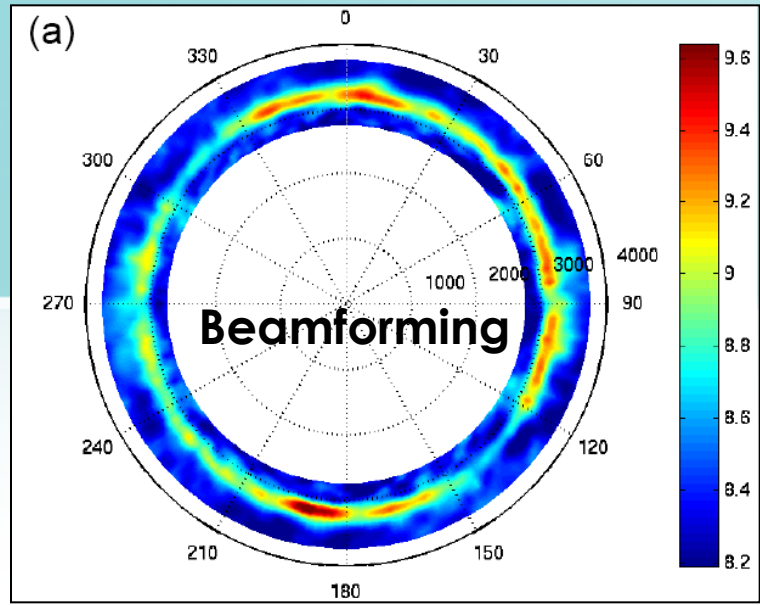
Seasonal variation of ambient noise energy (10-20s)

Jan 2004

July 2004

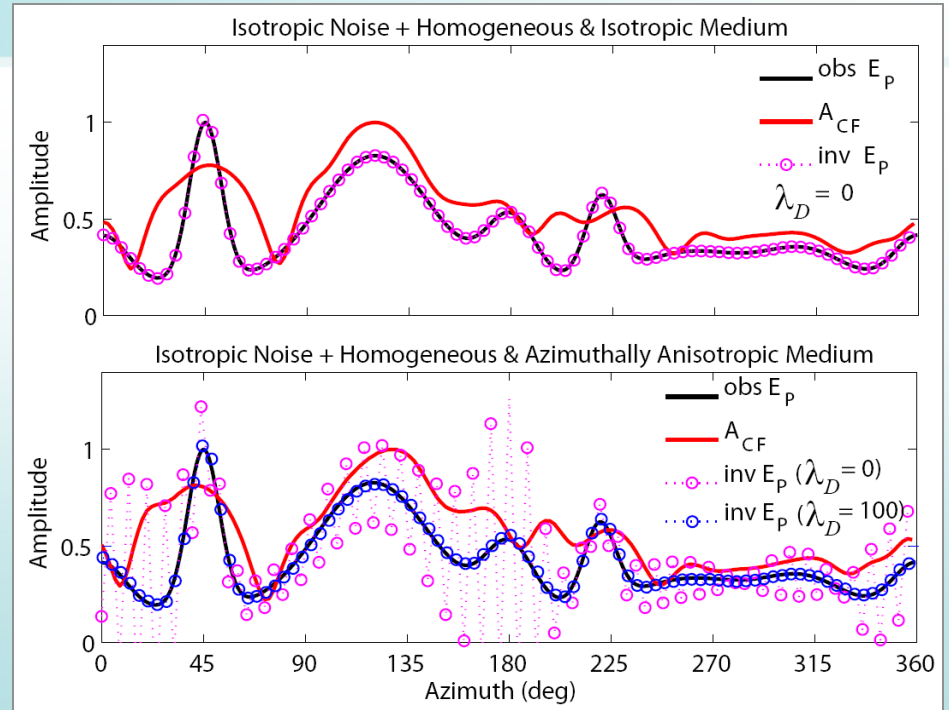
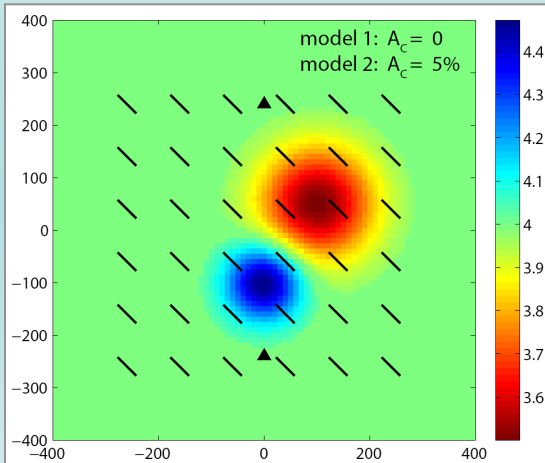
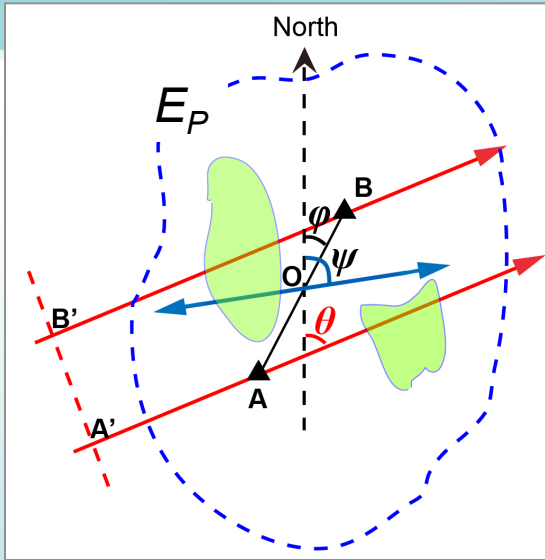


- **Correlation of ambient noise energy (10-20s) with ocean wave activity**
(background image: normalized global ocean wave height in winter time (a) and in summer time (b), modified from Stehly et al., 2006)



Uneven noise energy distribution + medium heterogeneity/anisotropy

imperfect recovery of \mathbf{G} \rightarrow bias in dispersion measurement.



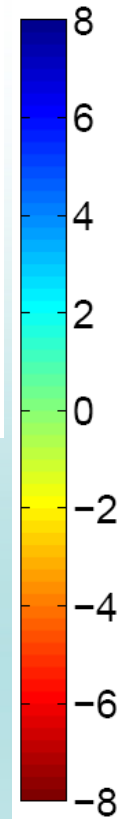
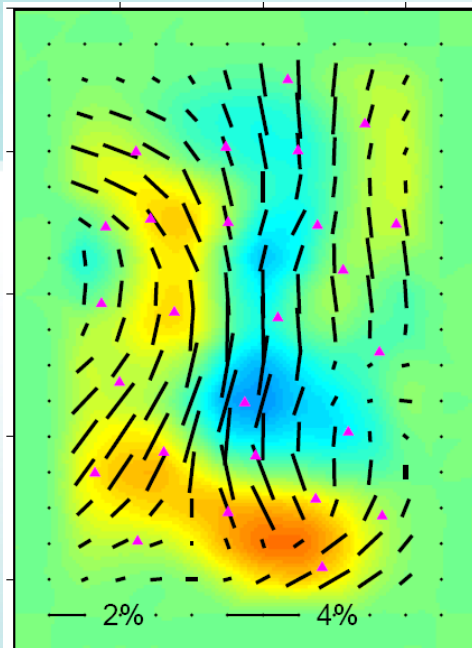
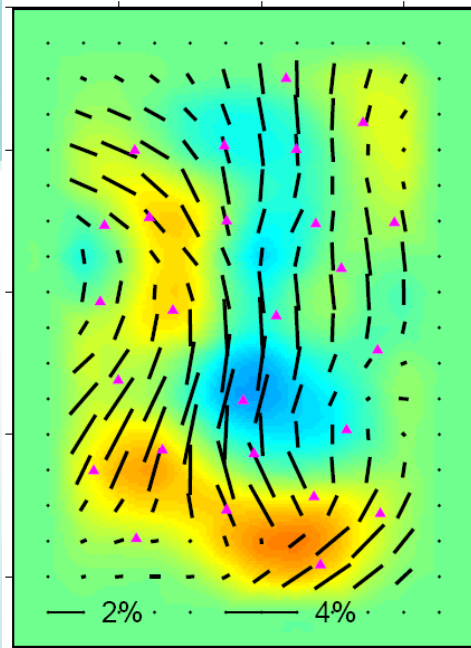
$$C_{AB}(\omega, t) = \int_0^{2\pi} E_P(\omega, \theta) \cos[\omega(t - \delta t)] H(t, \delta t) d\theta$$

Incoming plane wave
(ambient noise) energy

Before bias correction

After bias correction

10 s

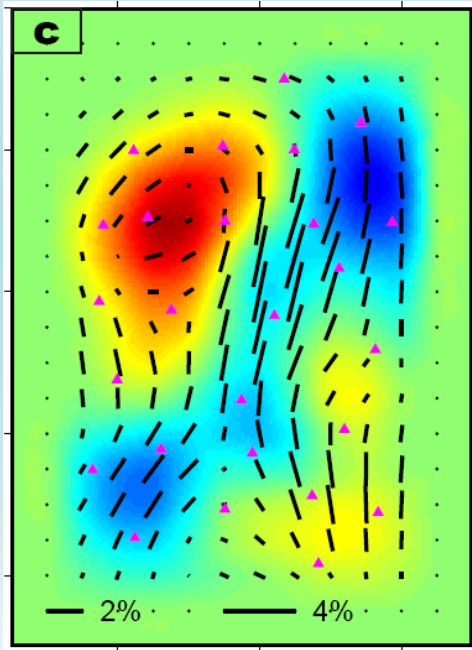
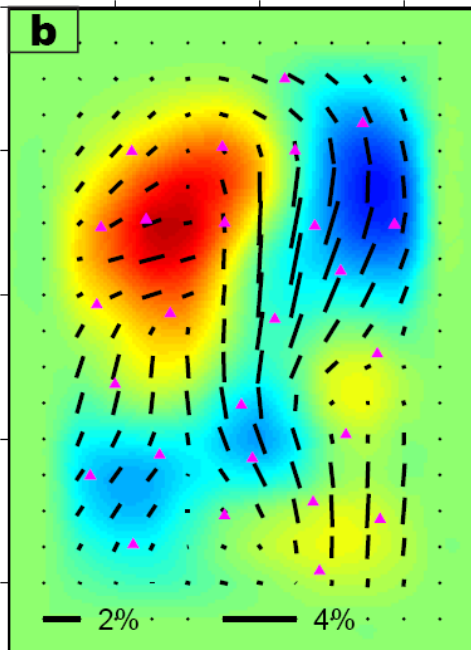


Effect on phase velocity is small ...

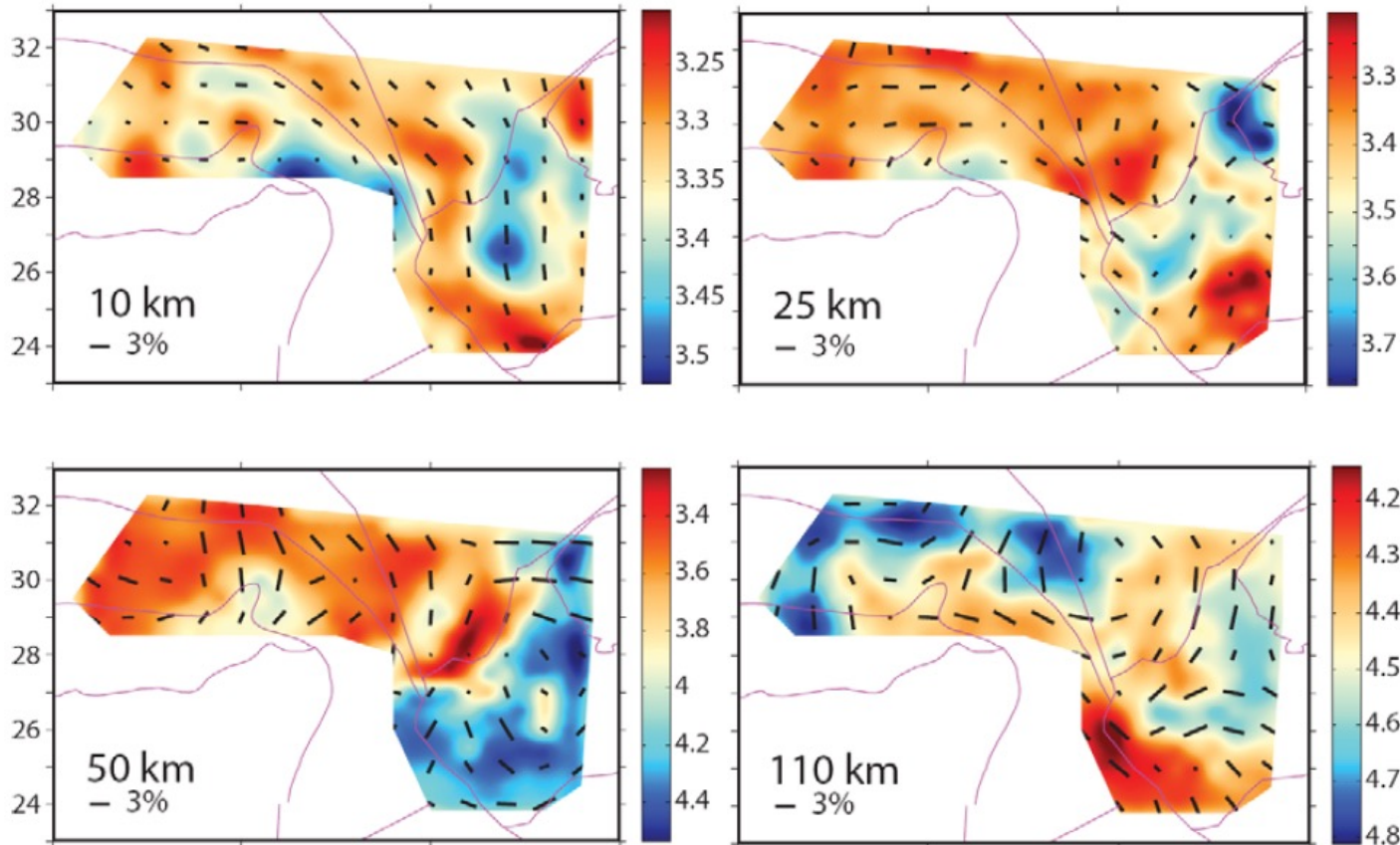
(see also remarks by Weaver, last Monday)

... and will be neglected

25 s



3D lithospheric heterogeneity & azimuthal anisotropy

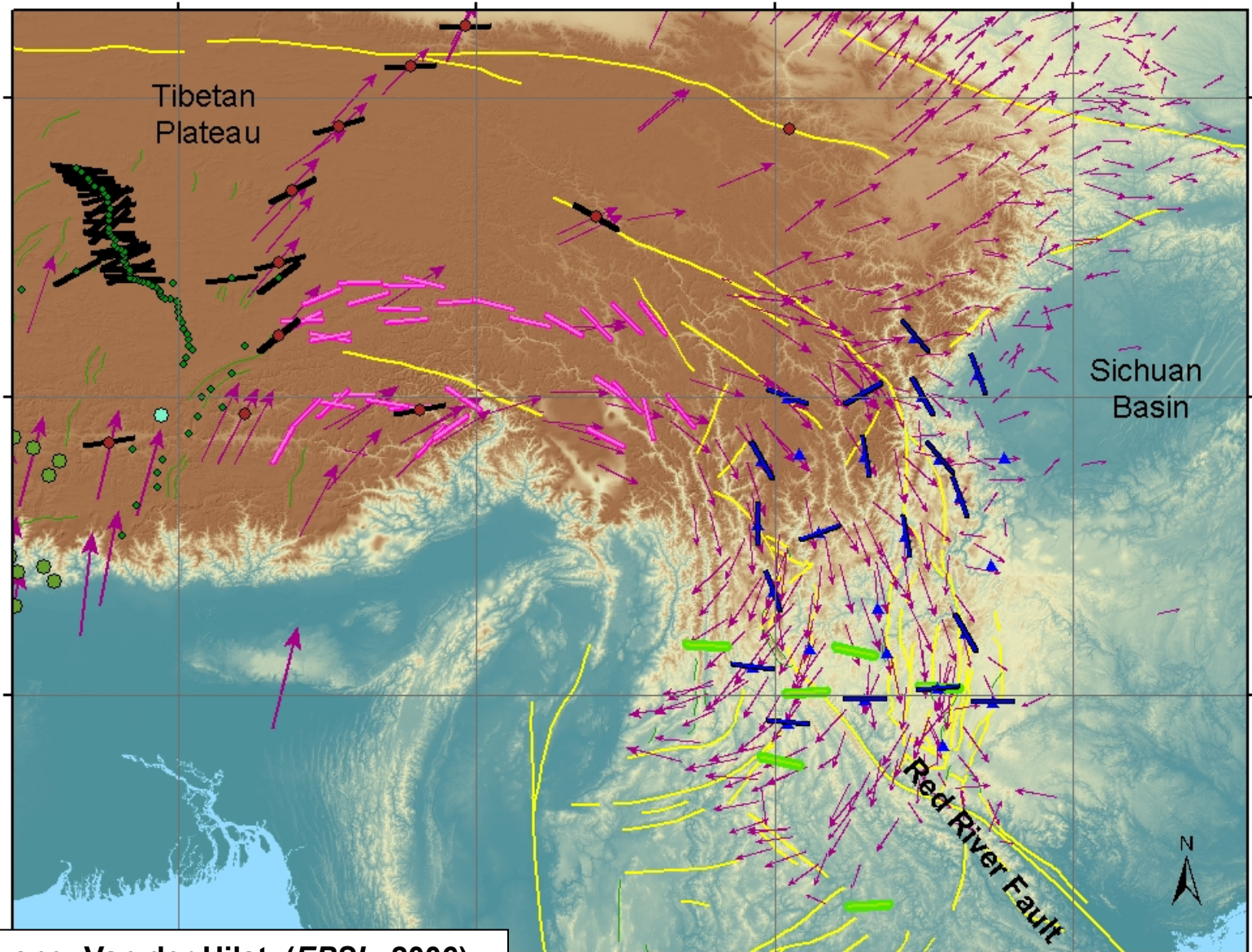


Complicated deformation pattern:

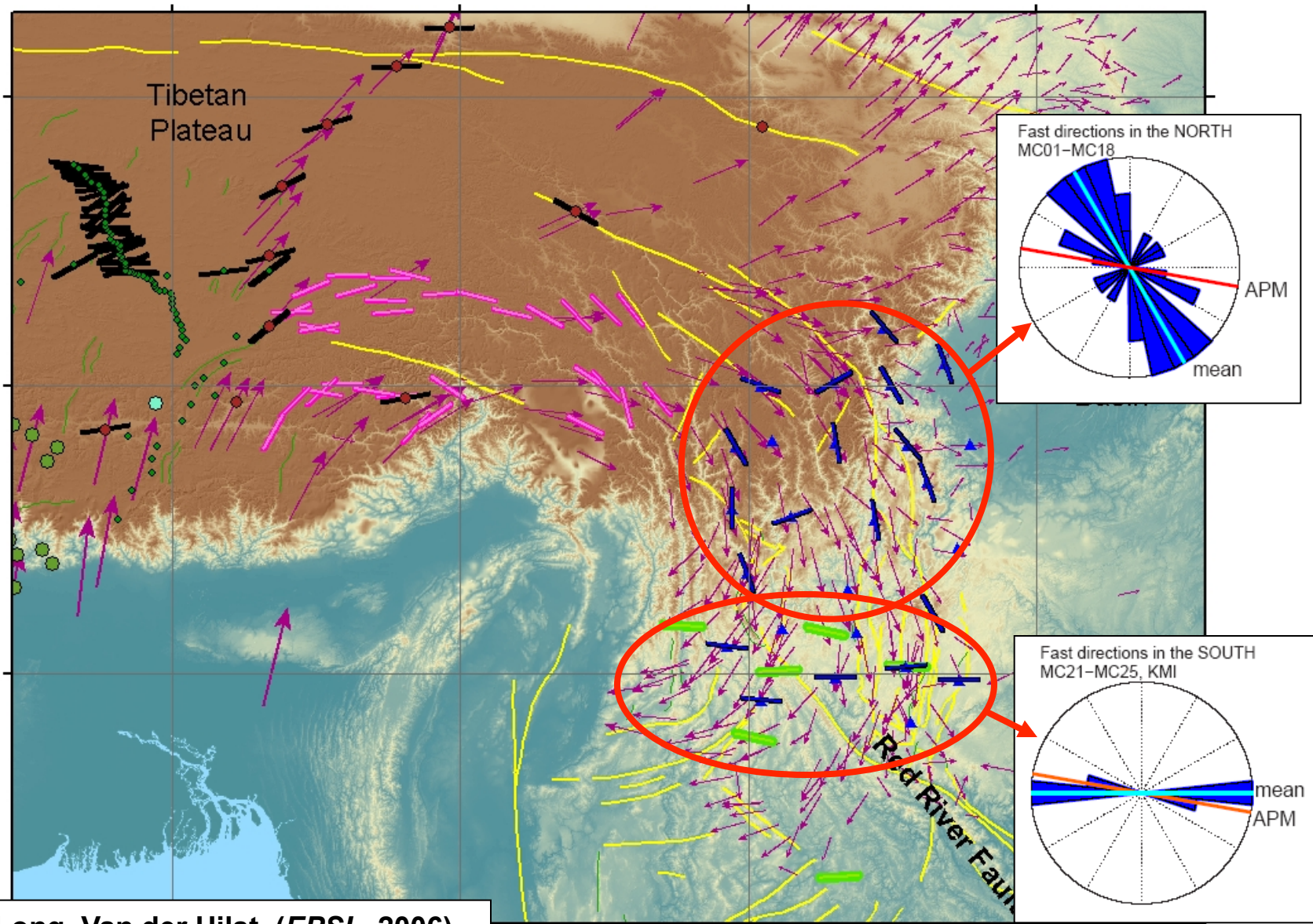
Upper crust: consistent with clockwise rotation (GPS)

Uppermost mantle: fast direction along the LVZ of the margin of Yangtze block

SKS splitting (~ azimuthal anisotropy) and GPS (purple arrows)

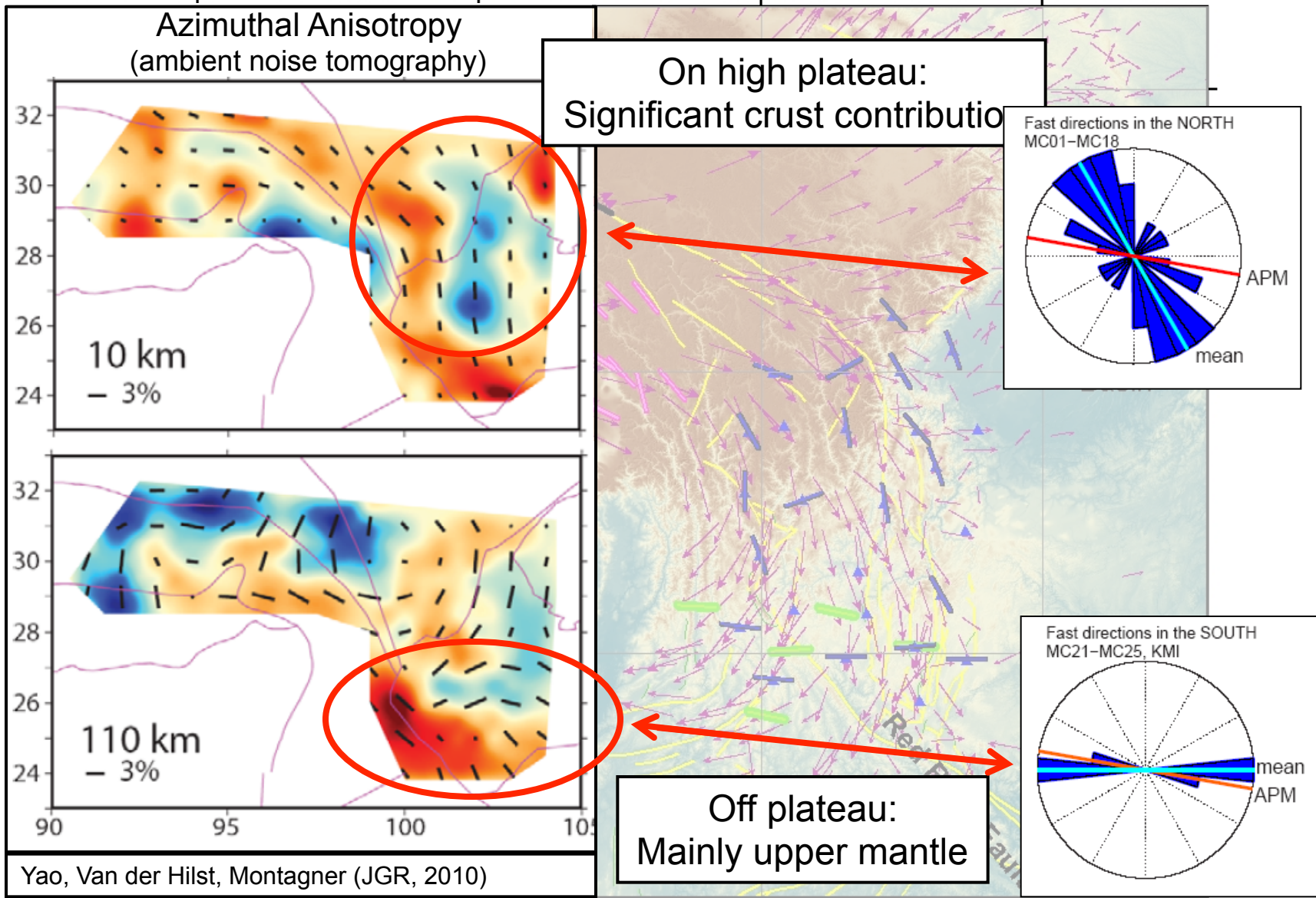


Lev, Long, Van der Hilst (*EPSL*, 2006)
Sol et al. (*Geology*, 2007)

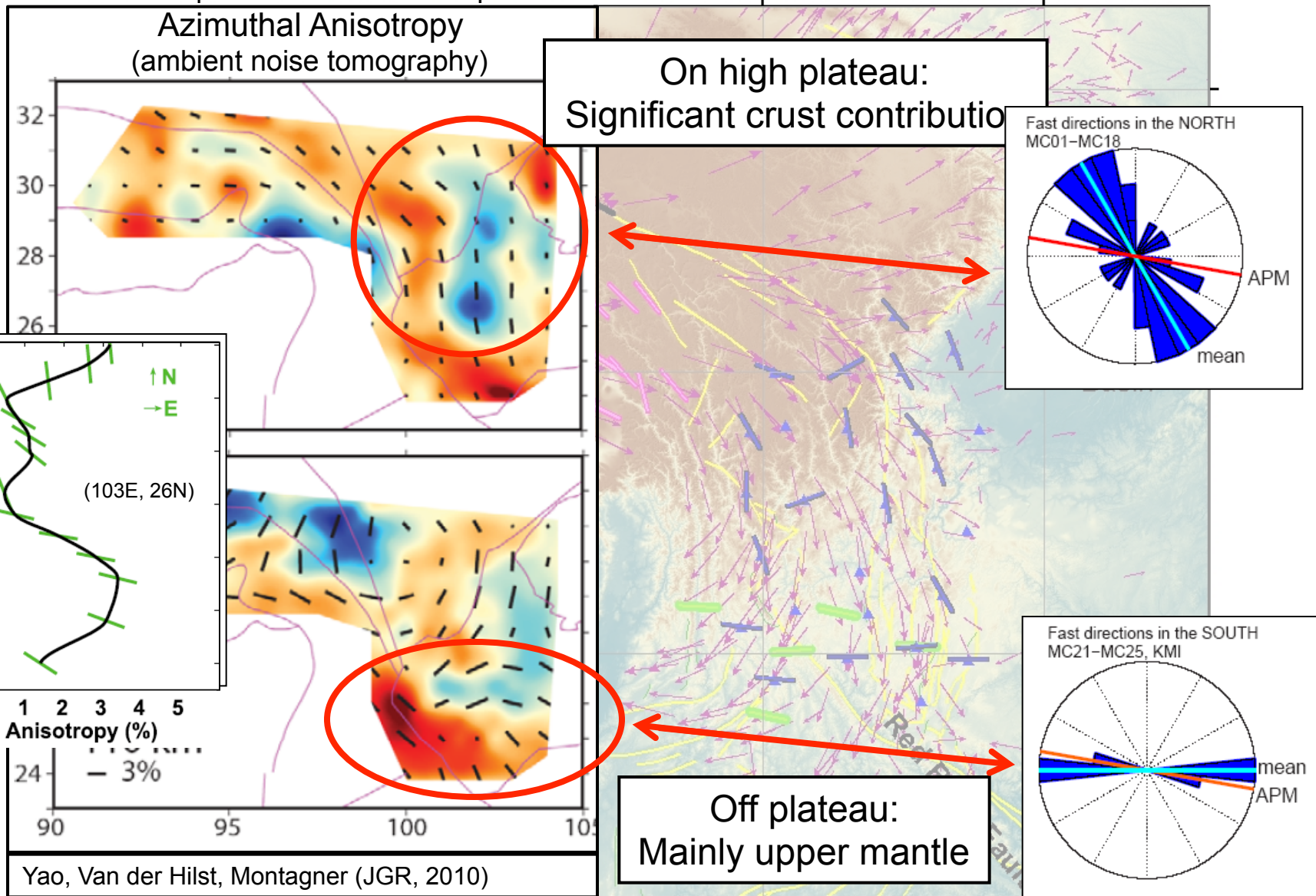


Lev, Long, Van der Hilst (*EPSL*, 2006)
 Sol et al. (*Geology*, 2007)

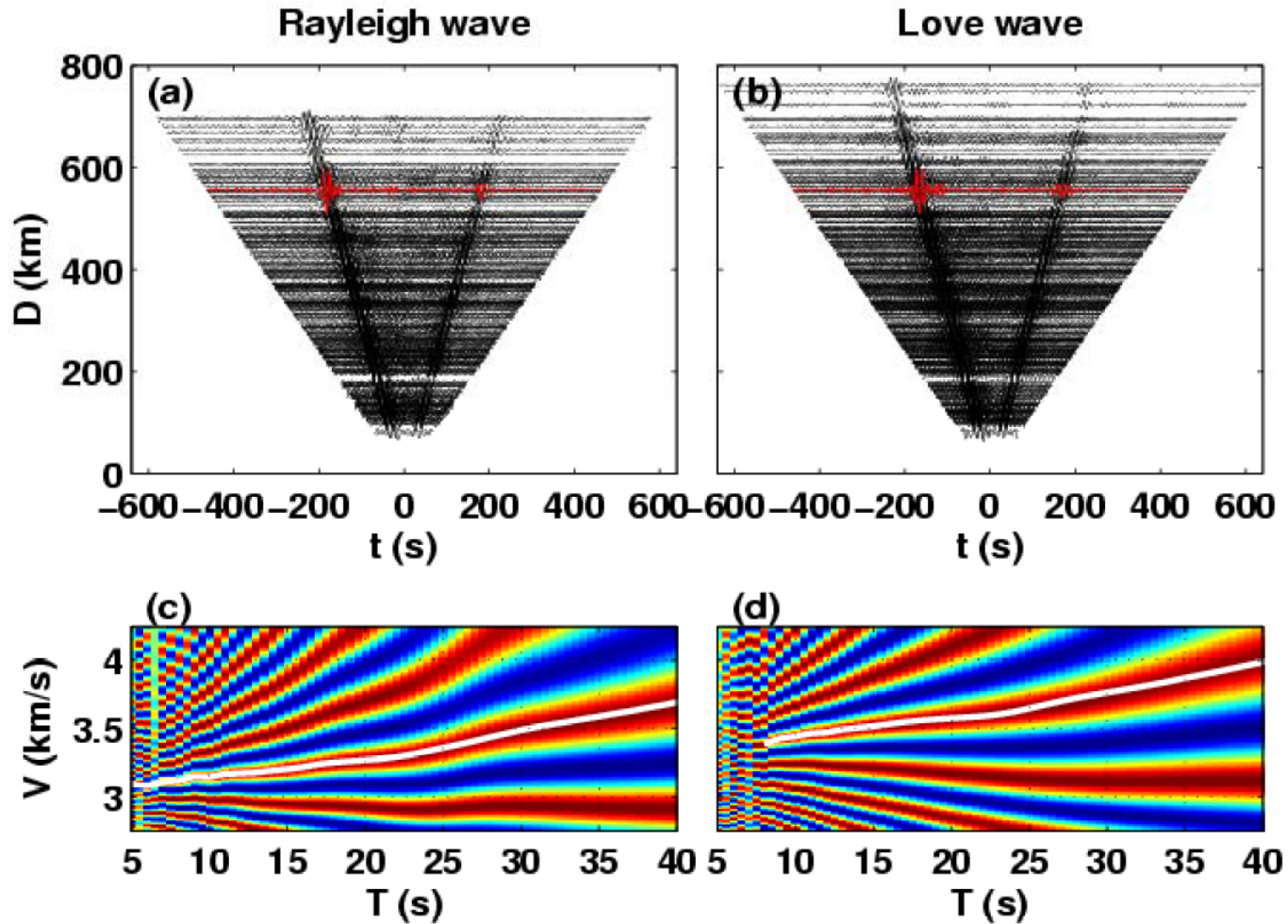
strong variation of azimuthal anisotropy with depth



strong variation of azimuthal anisotropy with depth



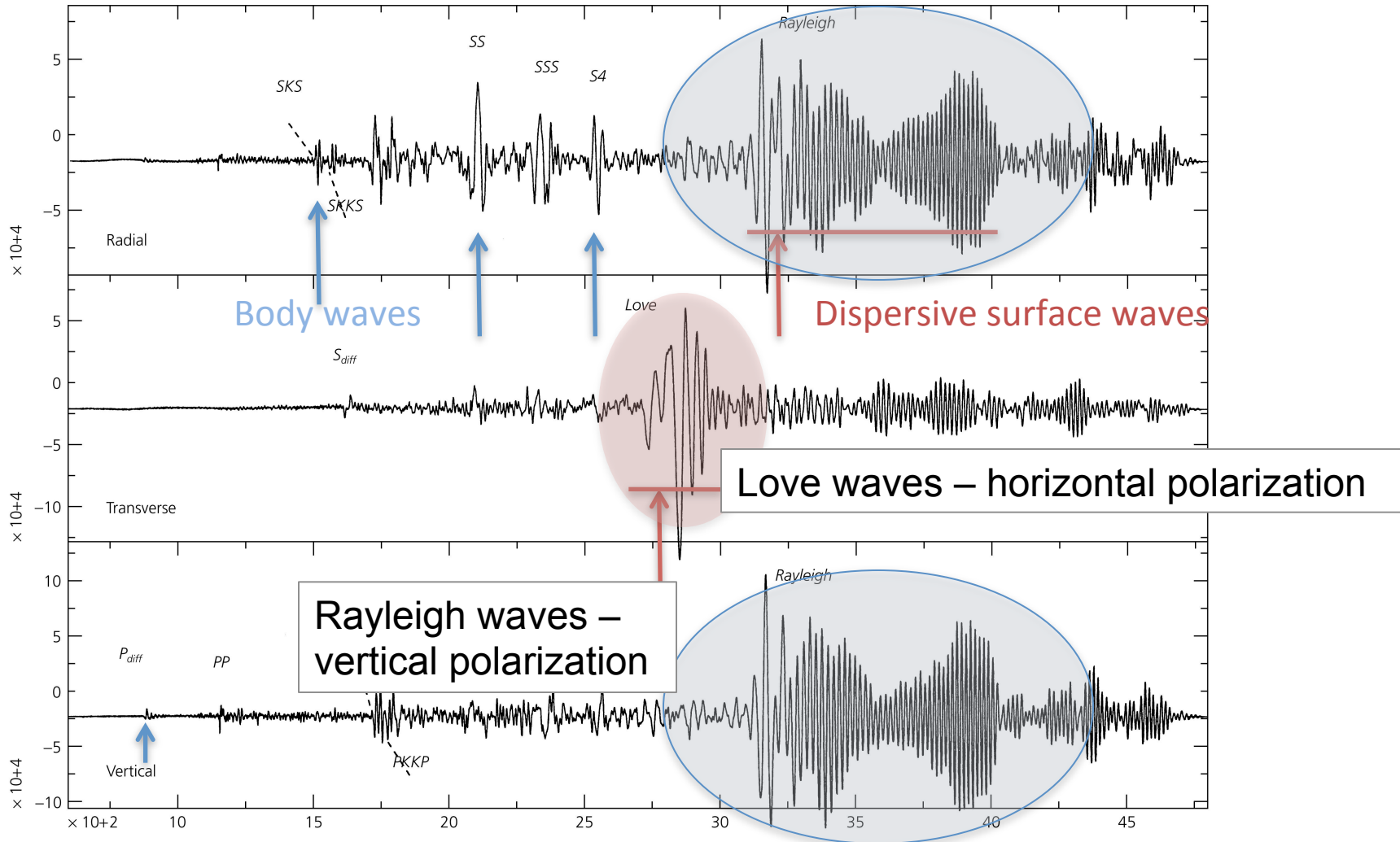
Anisotropy II: Radial Anisotropy from joint inversion of Love and Rayleigh wave dispersion (empirical Green's functions for noise correlation).



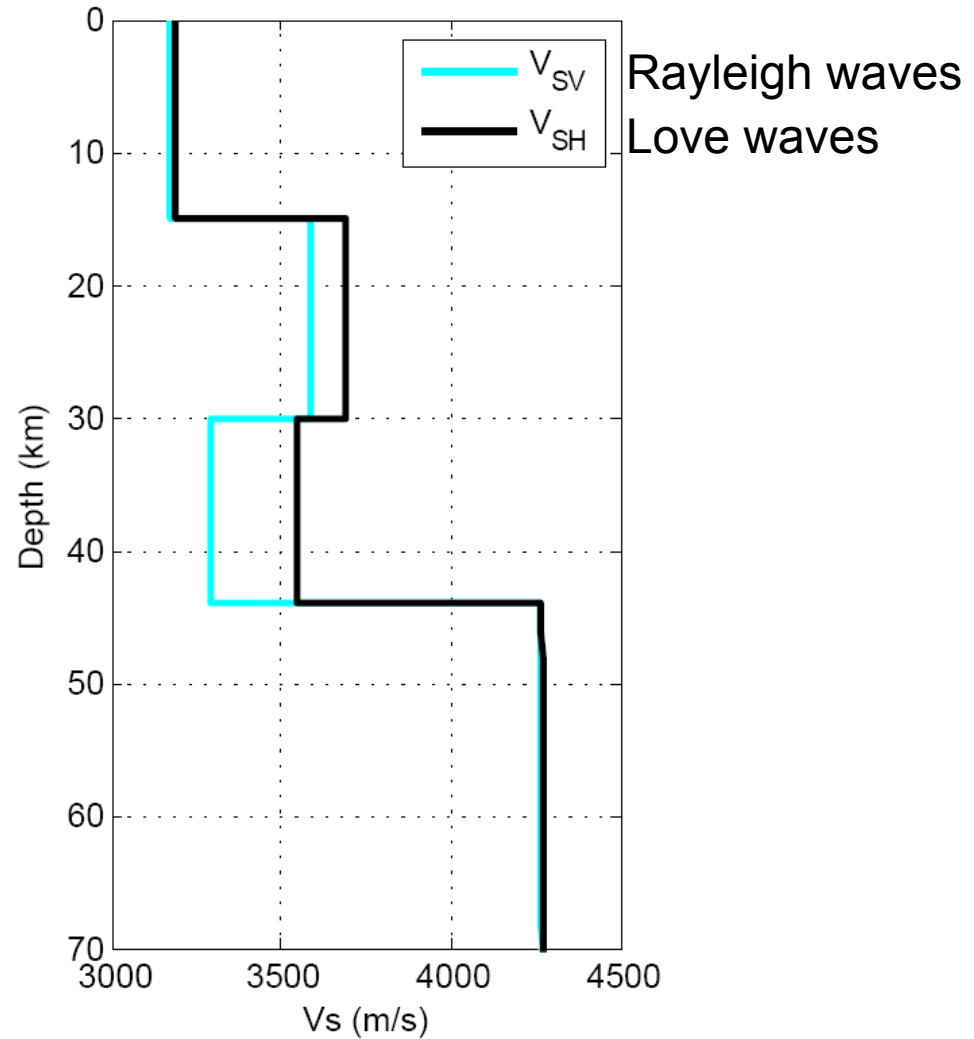
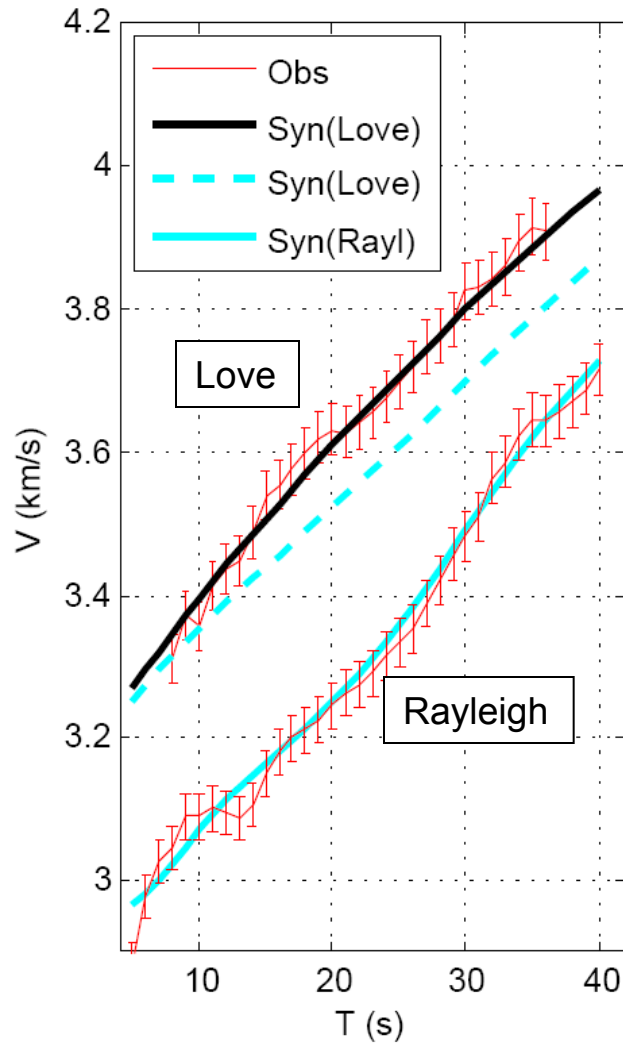
Huang, Yao, and Van der Hilst (GRL, 2010)

Anisotropy II: Radial Anisotropy (or: transverse isotropy)

(i.e., difference between wavespeed of horizontally and vertically polarized waves)

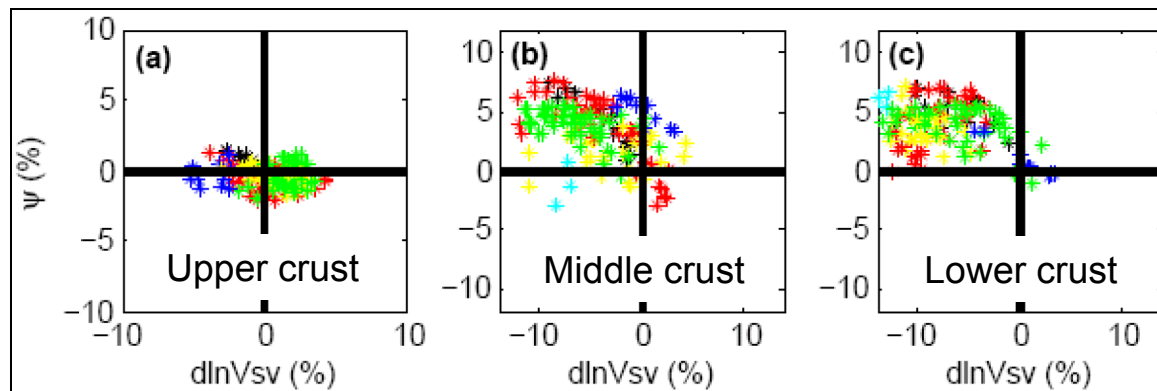
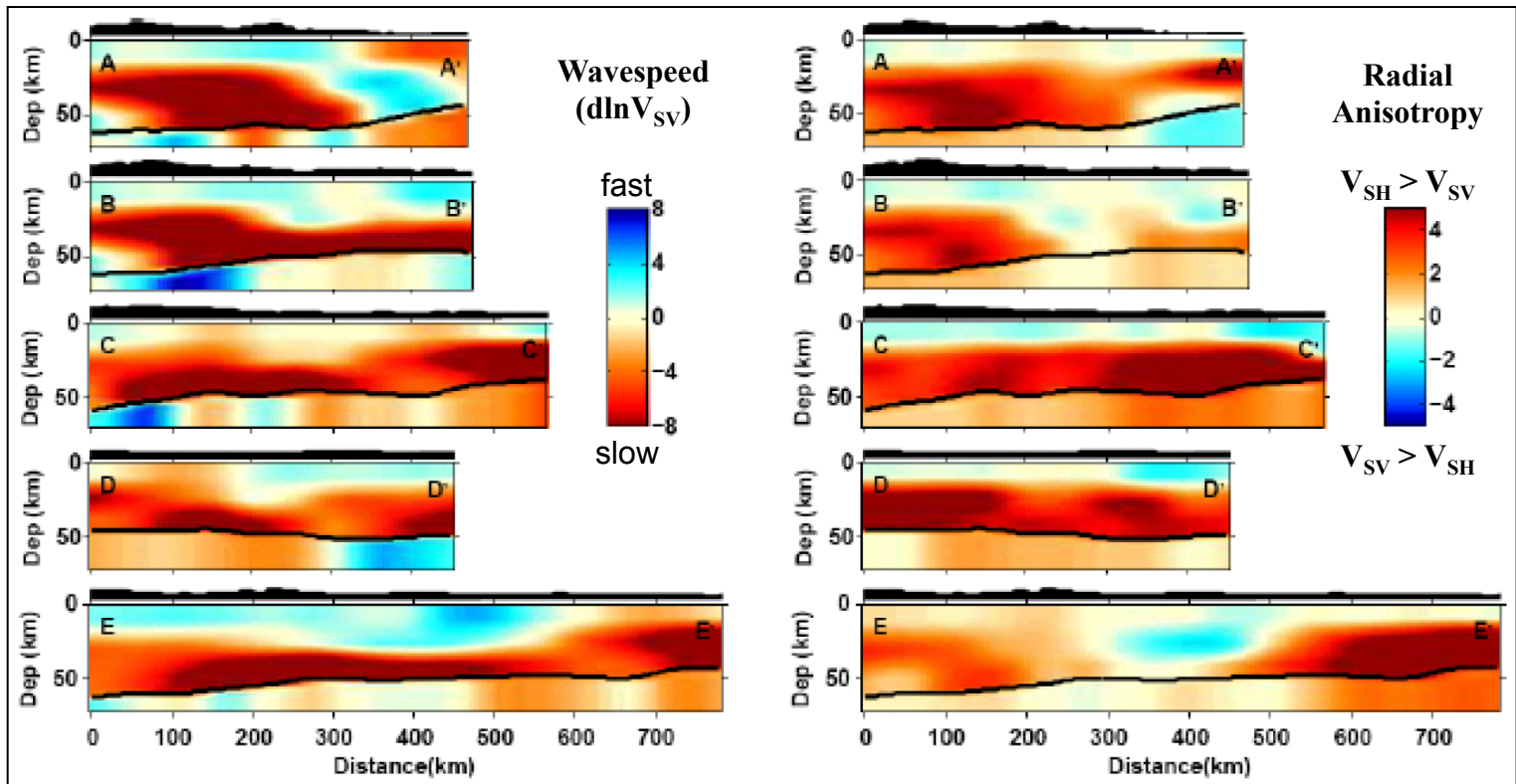


Radial Anisotropy (from Love and Rayleigh wave dispersion)

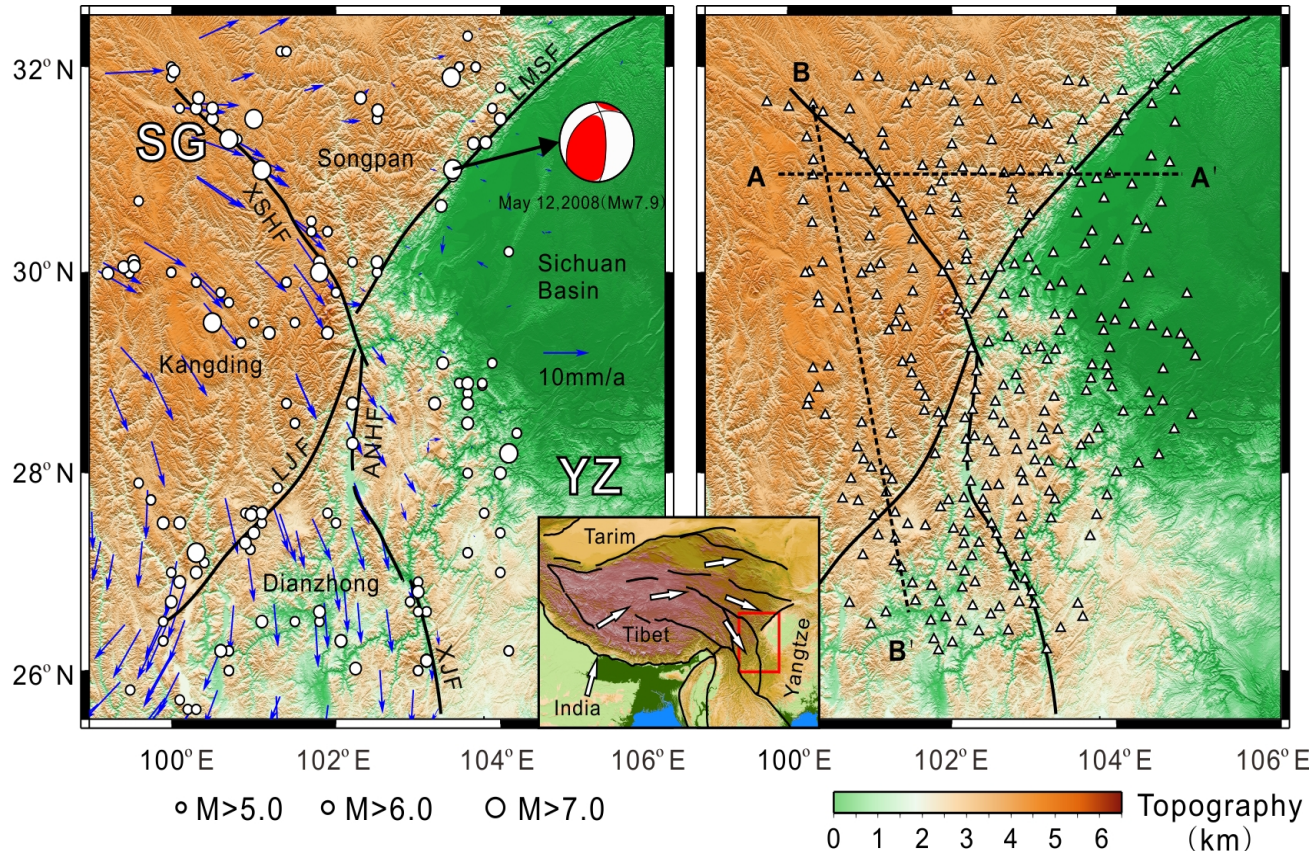


Huang, Yao, and Van der Hilst (GRL, 2010)

Strong correlation with LVZs → horizontal flow in weak zones?



High resolution studies with dense seismograph arrays



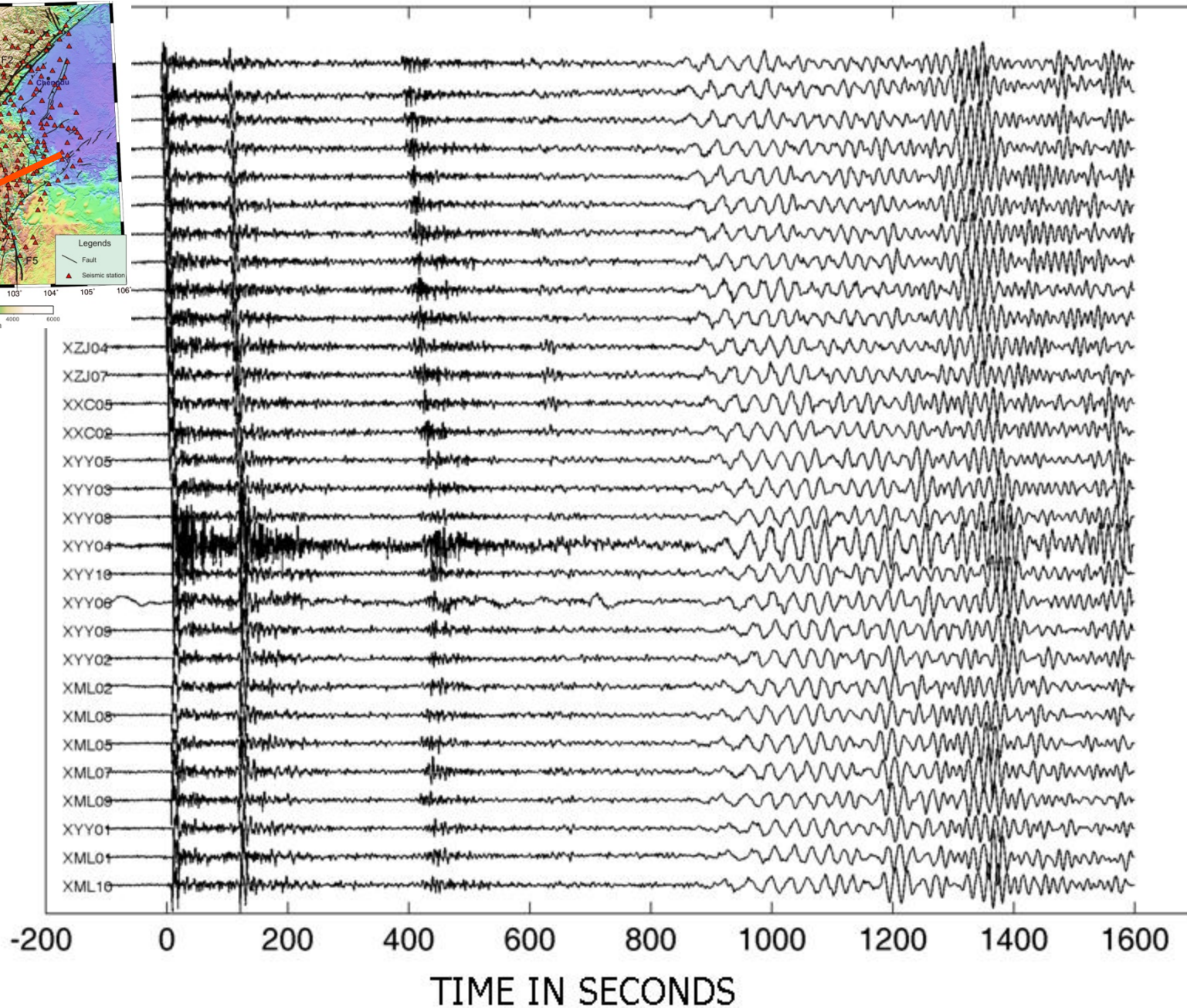
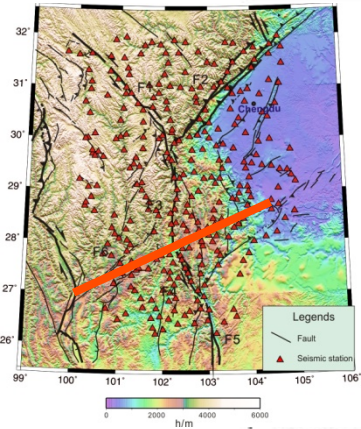
Geological setting and station map of the movable dense seismograph array in western Sichuan (State Key Laboratory of Earthquake Dynamics, Institute of Geology, China Earthquake Administration). Black solid lines: major faults; blue triangles: stations; yellow circles: earthquakes ($M_s \geq 5.0$, 1901-2010, 2008 Wenchuan focal mechanism); blue arrows: crustal motion relative to the Yangtze craton from GPS; red dash lines: seismic profile.

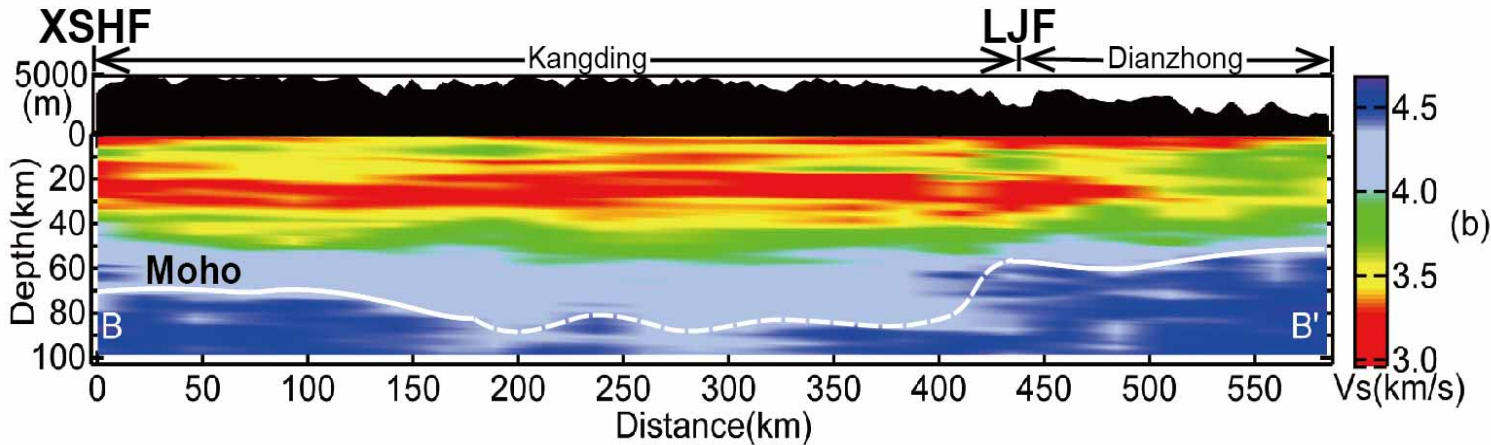
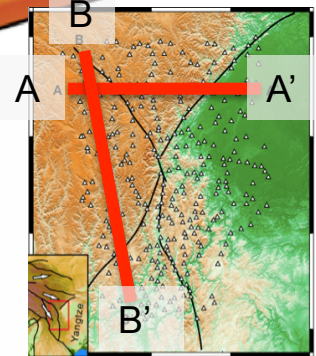
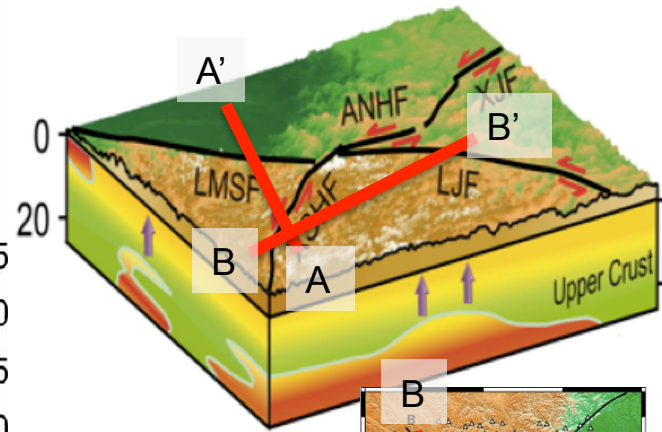
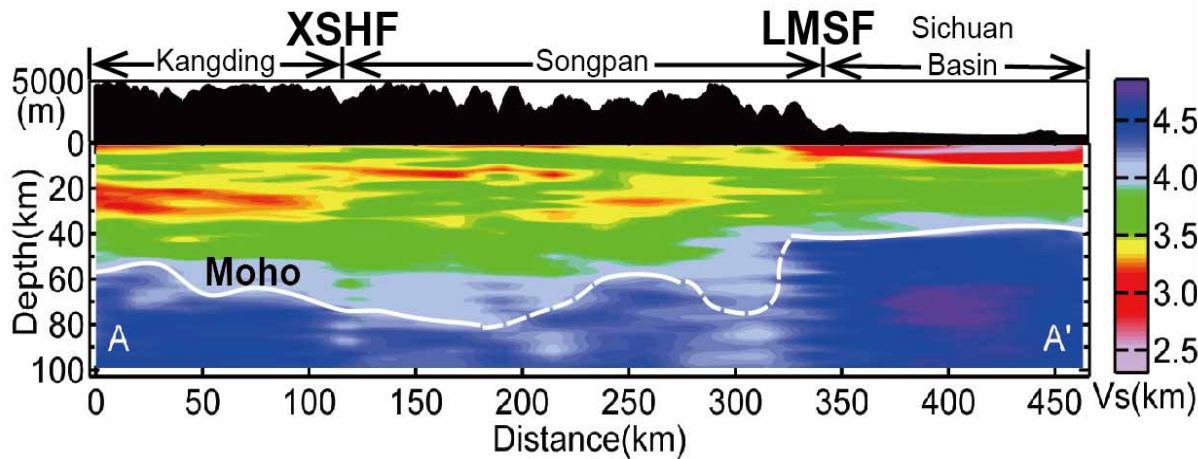
[SB=Sichuan Basin; YZ=Yangtze block; CD=Chundian unit; SG= Songpan-Ganze unit]
 [XSH=Xiangshuihe; LMS=Longmen Shan; ANH=Anninghe; LJ=Lijiang fault]

January 13, 2007 04h23m21.16s

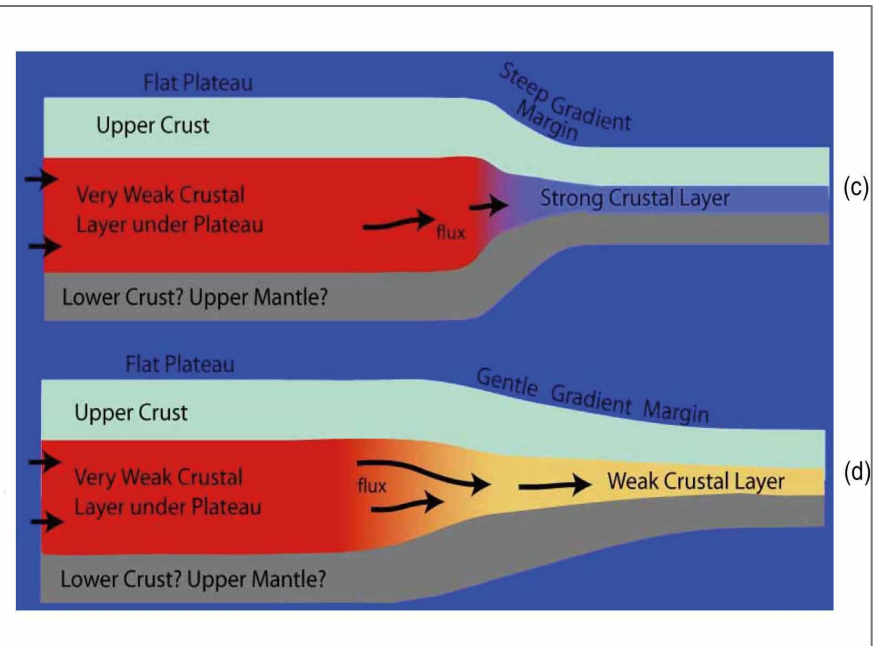
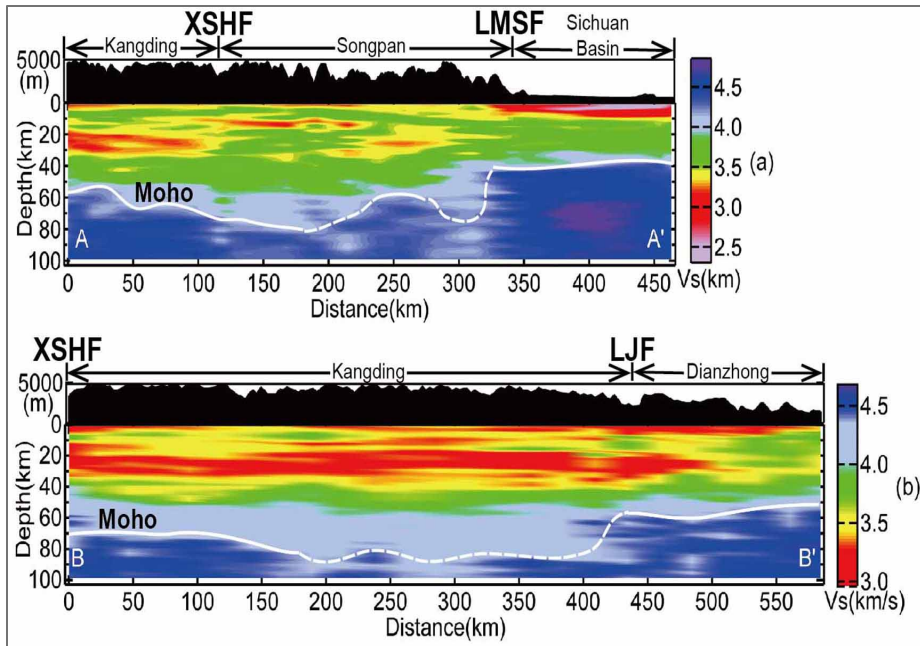
MB 7.3

Location: 46.243° N, 154.524° E





Topography and shear wavespeed variations from joint inversion of P-receiver functions and Ambient Noise (Rayleigh wave) Tomography across region of steep relief (A-A'; top) and gentle topographic gradient (B-B'; bottom).



Crustal structure constrained by waveform data obtained by a dense seismography array in western Sichuan.

Concept: canonical channel flow model. (Figure courtesy of L. Royden, MIT).

Overview of lecture:

1. **Introduction/background**

2. **Ambient noise and surface wave tomography (MIT, 2005-2015)**

- Traditional transmission tomography:

- combining ambient noise and earthquake data
- quantifying and correcting for uneven noise distribution
- azimuthal anisotropy
- radial anisotropy

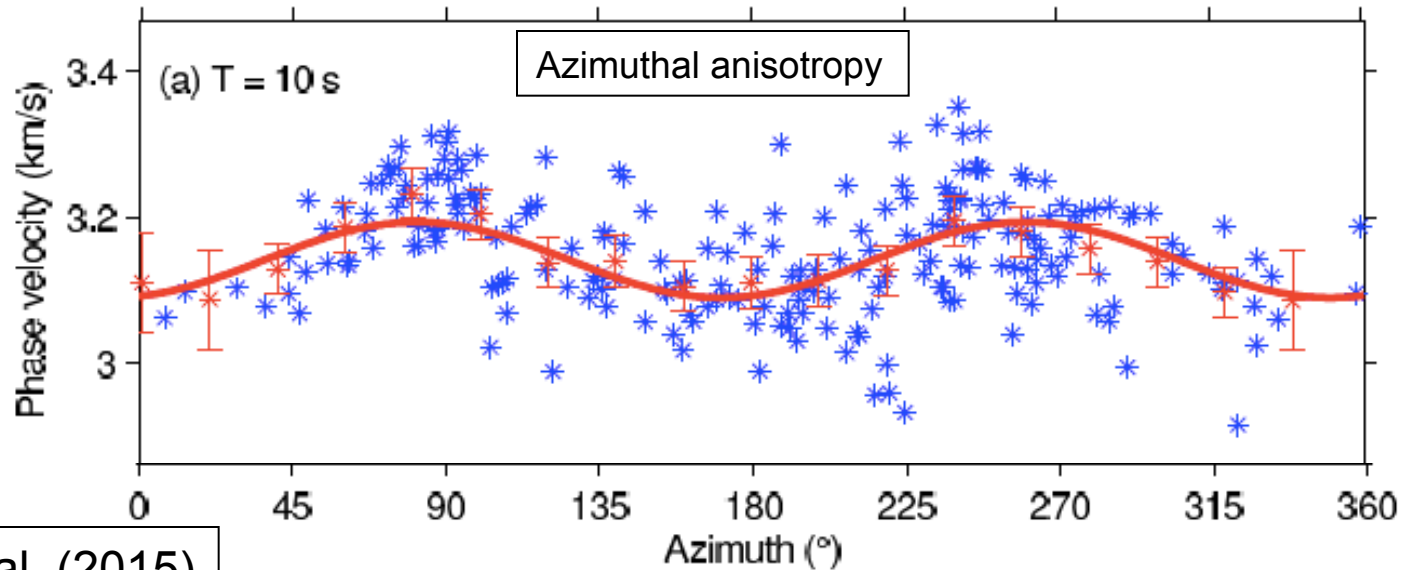
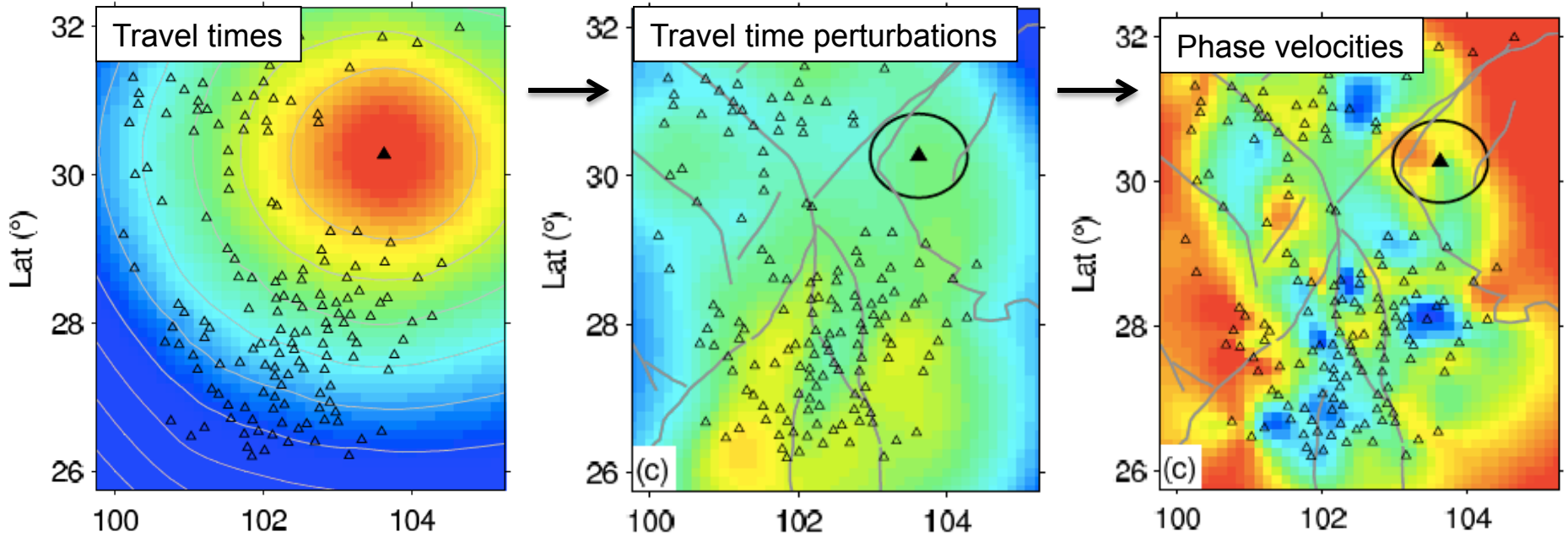
- **Eikonal tomography**

- Adjoint tomography with ambient noise data

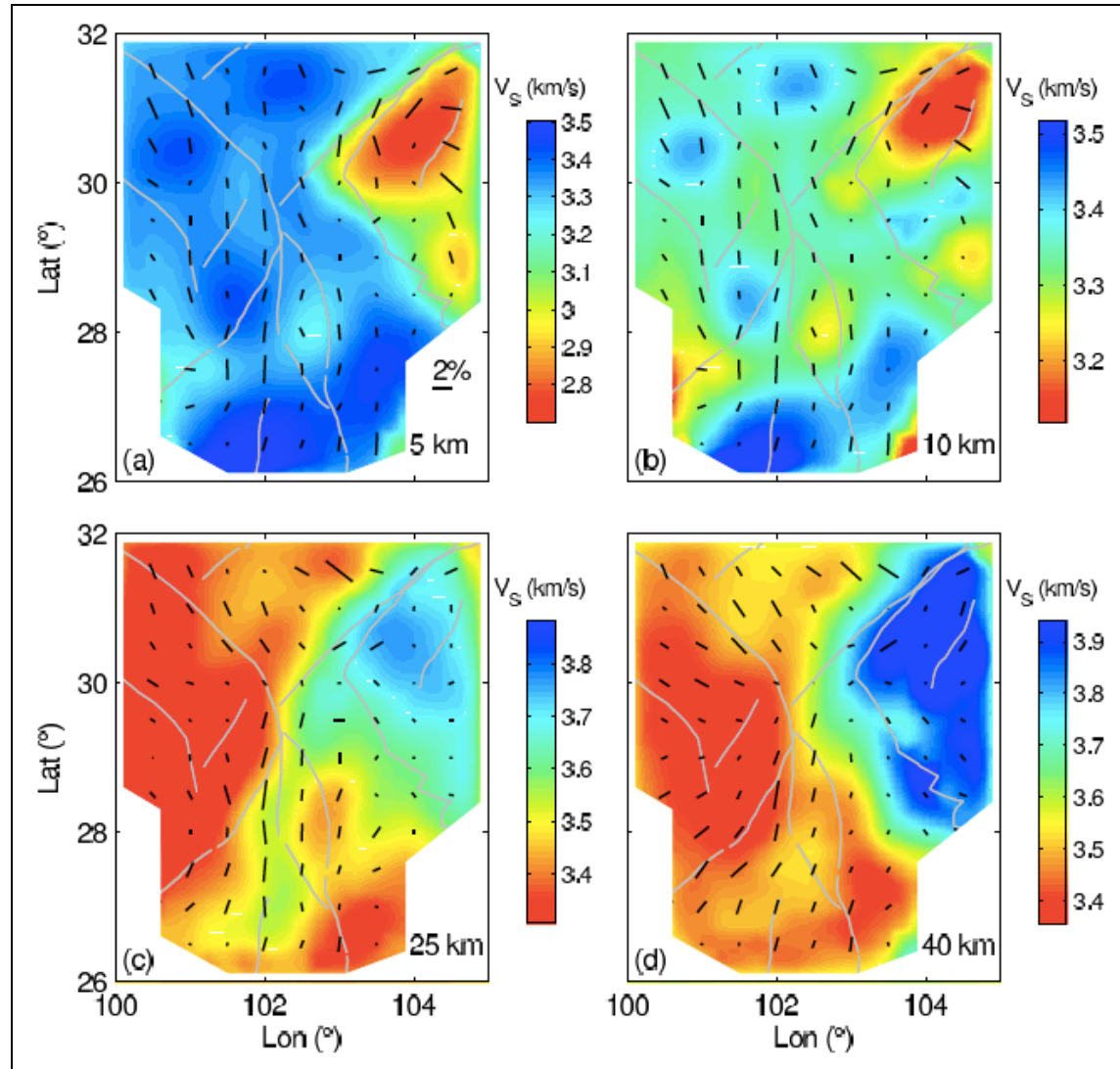
3. **Interferometry of teleseismic body waves**

4. **Imaging with multiples**

Eikonal Tomography: interpolation of travel time *perturbations* instead of travel times

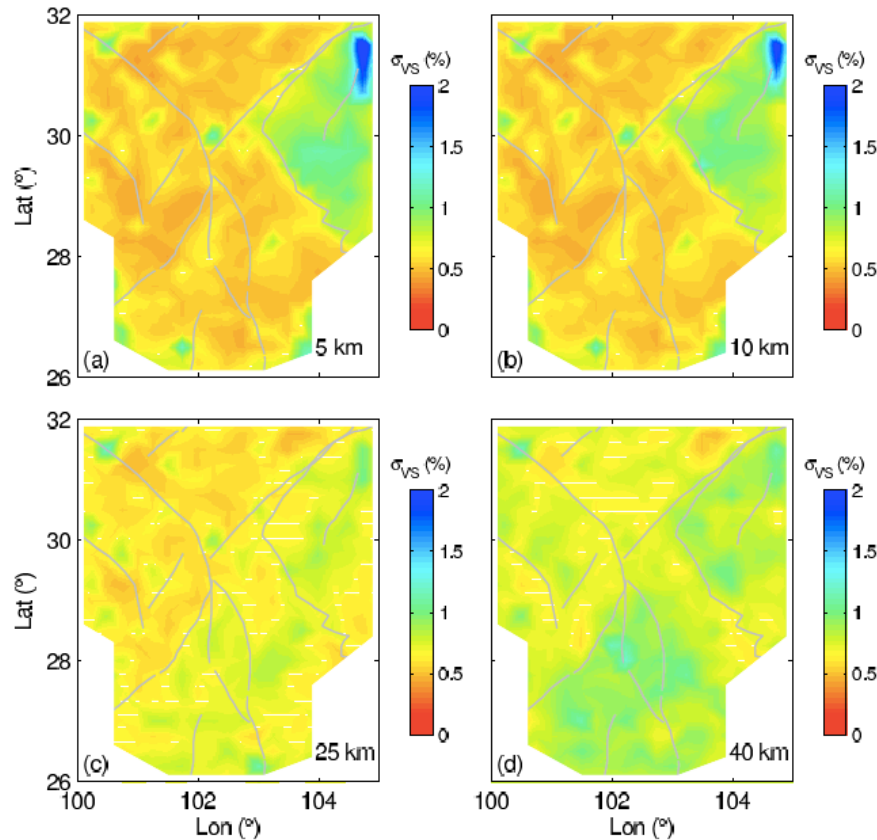


Eikonal Tomography: interpolation of travel time *perturbations* instead of travel times

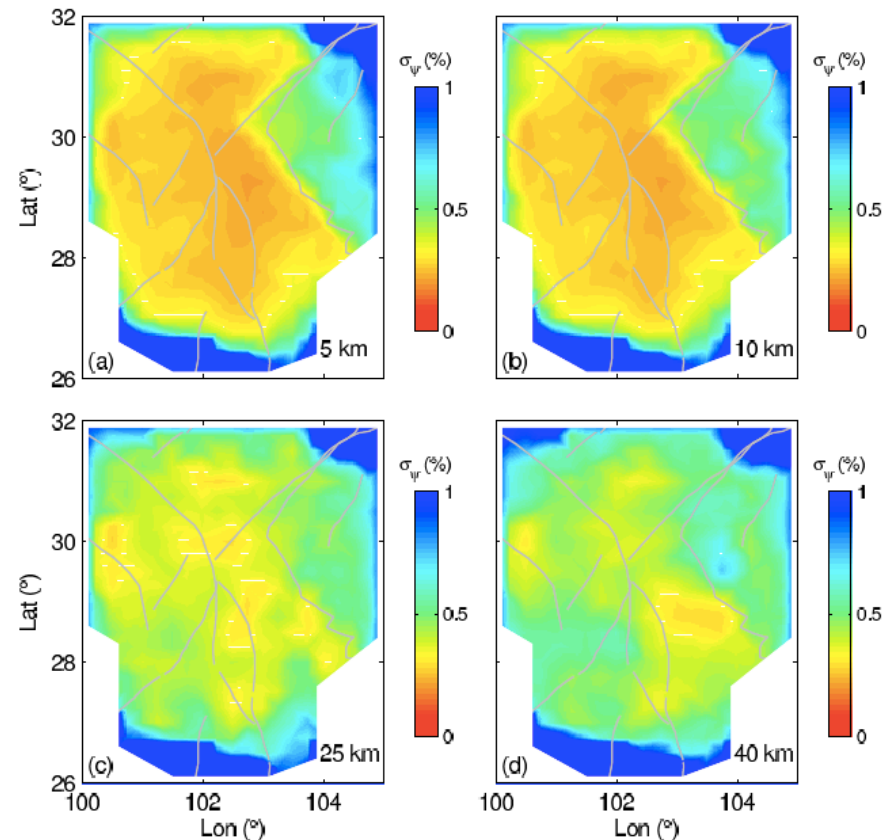


Eikonal Tomography: interpolation of travel time *perturbations* instead of travel times

Standard errors for Vs



Standard errors for anisotropy



Robust estimation of heterogeneity and (azimuthal) anisotropy,
but lower spatial resolution than traditional tomography due to interpolation

Overview of lecture:

1. **Introduction/background**

2. **Ambient noise and surface wave tomography (MIT, 2005-2015)**

- Traditional transmission tomography:

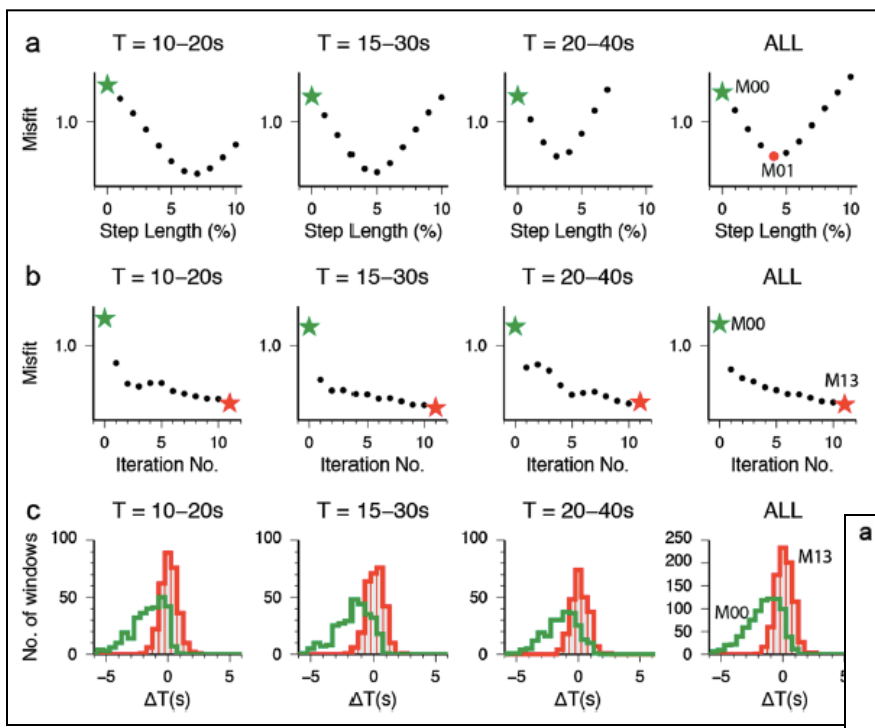
- combining ambient noise and earthquake data
- quantifying and correcting for uneven noise distribution
- azimuthal anisotropy
- radial anisotropy

- Eikonal tomography

- **Adjoint tomography with ambient noise data**

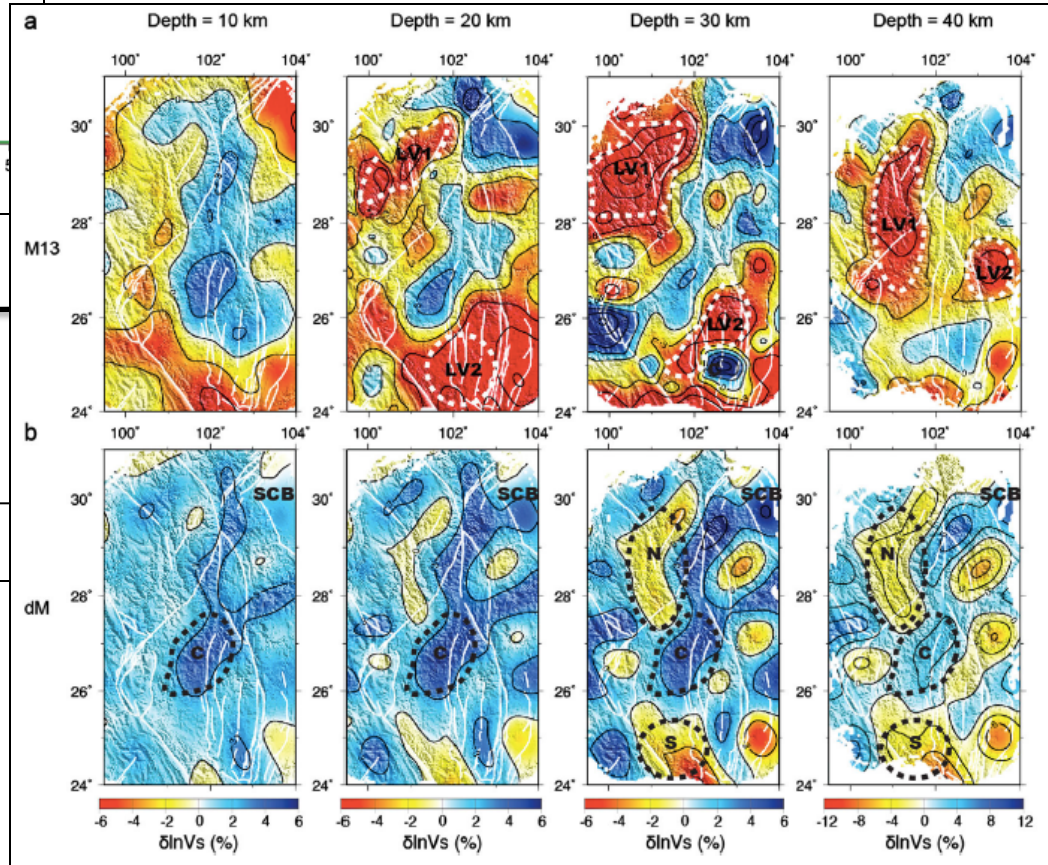
3. **Interferometry of teleseismic body waves**

4. **Imaging with multiples**



Result after 13 iterations

Difference from starting model



Overview of lecture:

1. Introduction/background

2. Ambient noise and surface wave tomography (MIT, 2005-2015)

- Traditional transmission tomography:

- combining ambient noise and earthquake data
- quantifying and correcting for uneven noise distribution
- azimuthal anisotropy
- radial anisotropy

- Eikonal tomography

- Adjoint tomography with ambient noise data

3. Interferometry of teleseismic body waves – concept

4. Imaging with multiples

Teleseismic wave-equation reflection tomography using free surface reflected phases

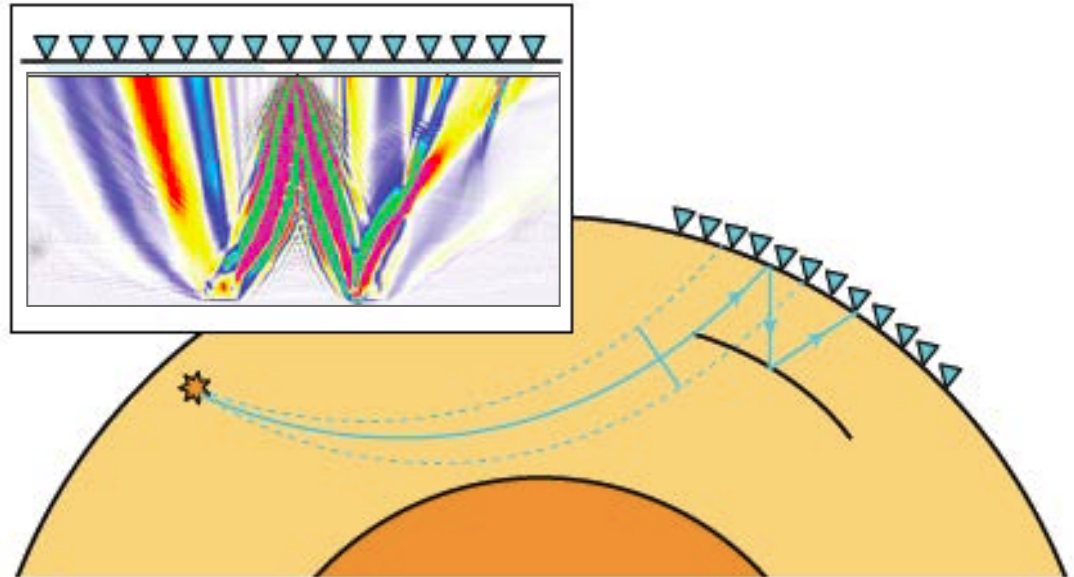
S. Burdick¹, M. V. de Hoop², S. Wang², R. D. van der Hilst¹

¹ Department of Earth, Atmospheric, and Planetary Sciences, Massachusetts Institute of Technology Cambridge, MA 02139, USA

² Department of Mathematics, Purdue University

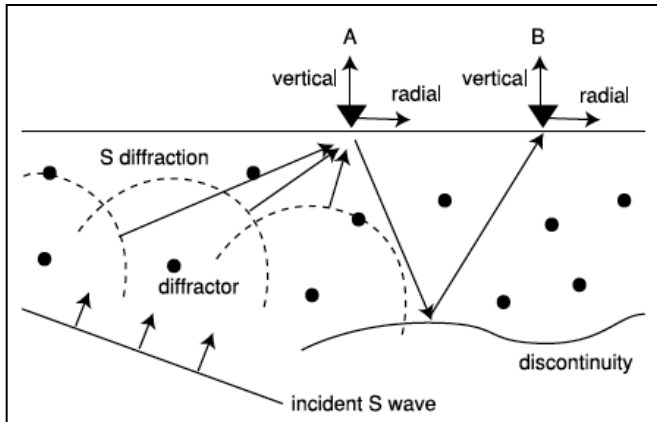
“Remote sensing”

Estimating wavespeed variations beneath an array using waves coming from distant sources.



Construct images from converted and multiply-reflected teleseismic phases (NB the source can be ‘ambient noise’)

For instance, imaging of the slab interface



Seismic interferometry of teleseismic S-wave coda for retrieval of body waves: an application to the Philippine Sea slab underneath the Japanese Islands

Takashi Tonegawa,¹ Kiwamu Nishida,¹ Toshiki Watanabe² and Katsuhiko Shiomi³

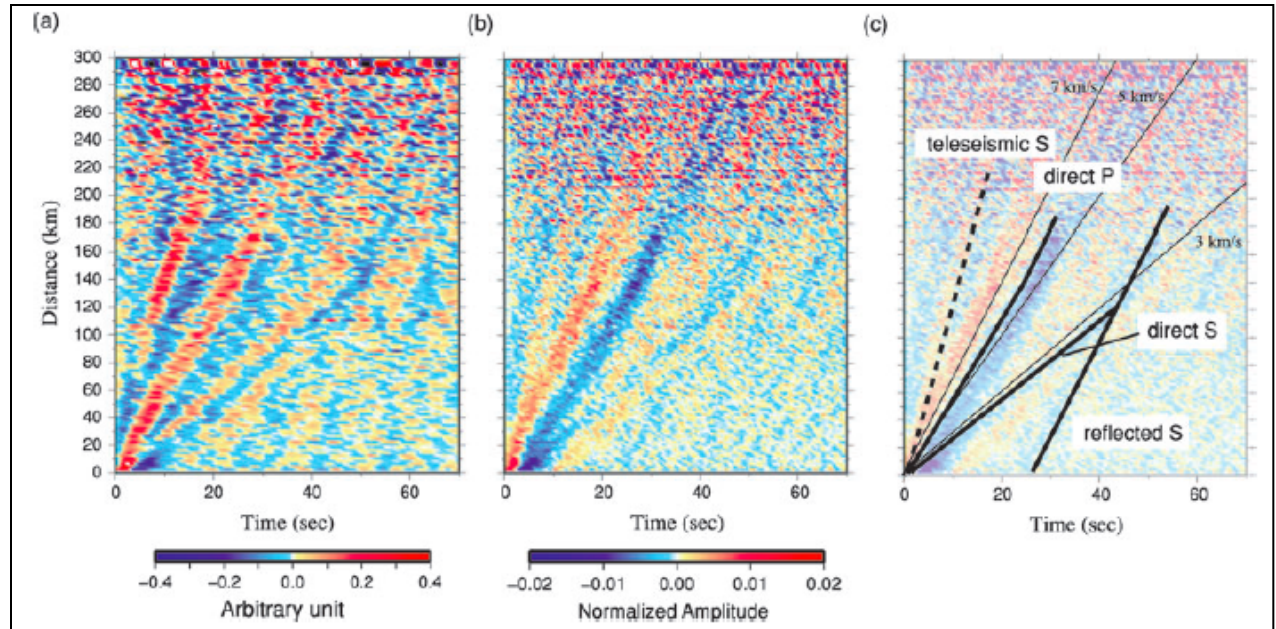
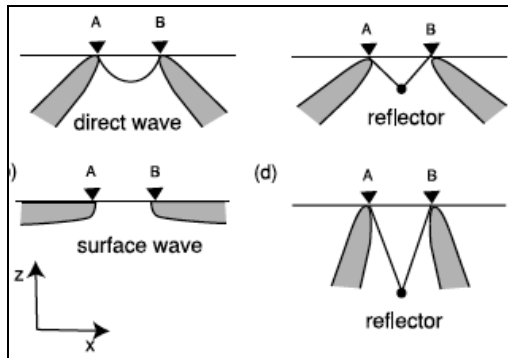
¹Earthquake Research Institute, Univ. of Tokyo, 1-1-1, Yayoi, Bunkyo-ku, Tokyo 113-0032, Japan. E-mail: tonegawa@eri.u-tokyo.ac.jp

²Graduate School of Environmental Studies, Nagoya University, Furo-cho, Chikusa-ku, Nagoya 464-8602, Japan

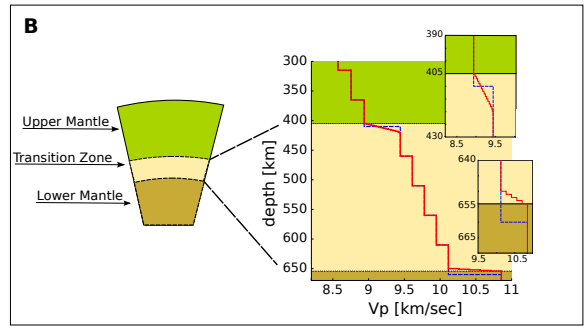
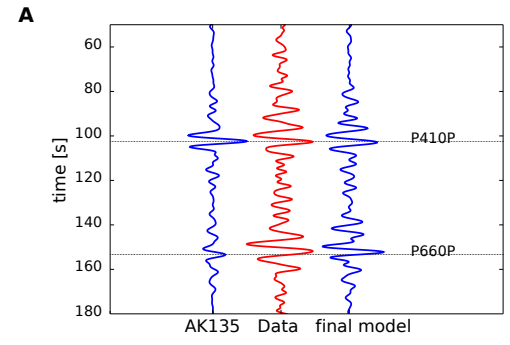
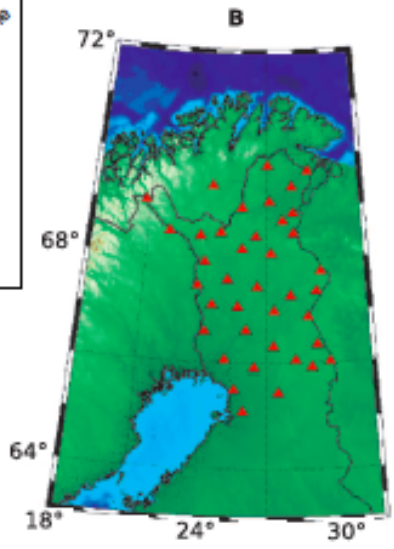
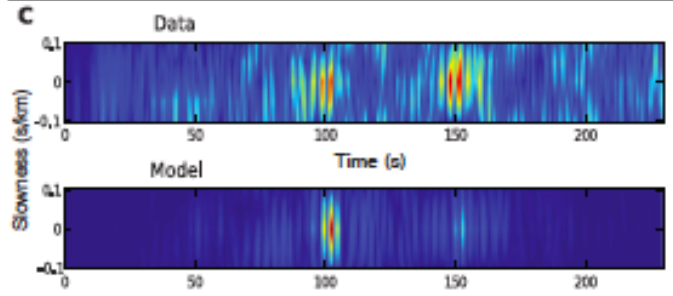
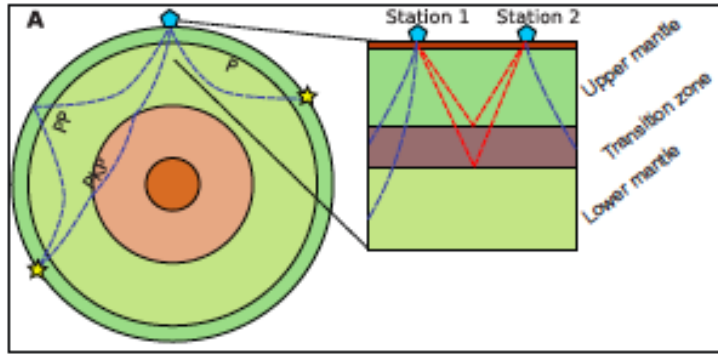
³National Research Institute for Earth Science and Disaster Prevention, 3-1, Tennodai, Tsukuba, Ibaraki 305-0006, Japan

Accepted 2009 May 11. Received 2009 April 20; in original form 2009 January 22

Tonegawa et al. (GJI, 2009)

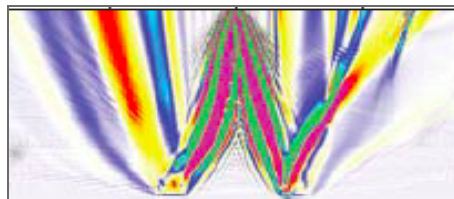
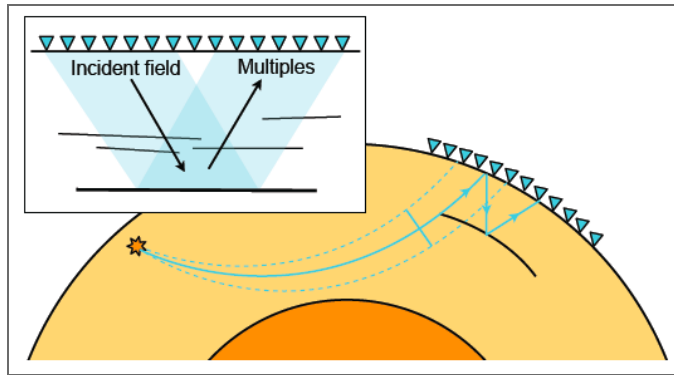


Or passive imaging: Earth's mantle discontinuities from ambient seismic noise.



Poli et al. (Science, 2012)

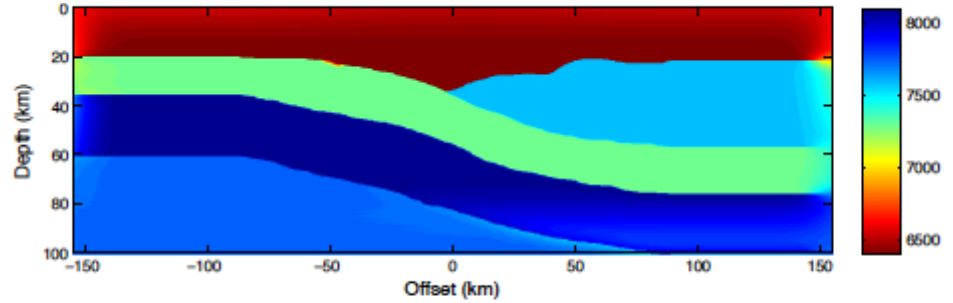
Construct images from converted and multiply-reflected teleseismic phases



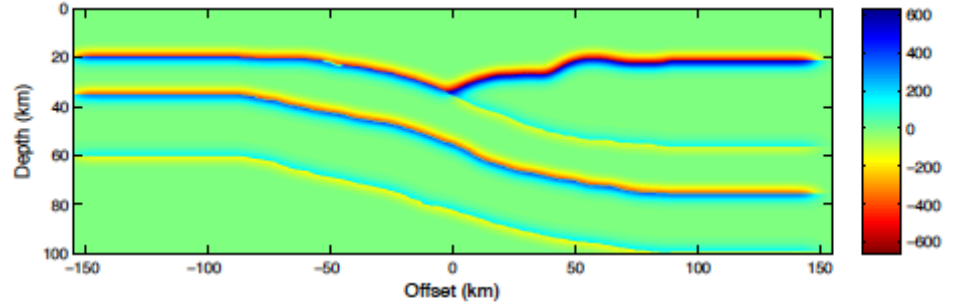
Wave-equation reflection tomography → full finite frequency (De Hoop et al., (GJI, 2006))

Burdick et al. (GJI, 2014)

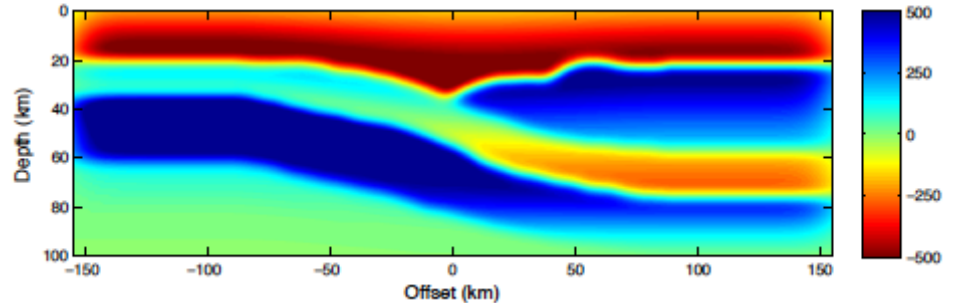
Actual model (used to create synthetic data)



Reflectivity (singular part of model)

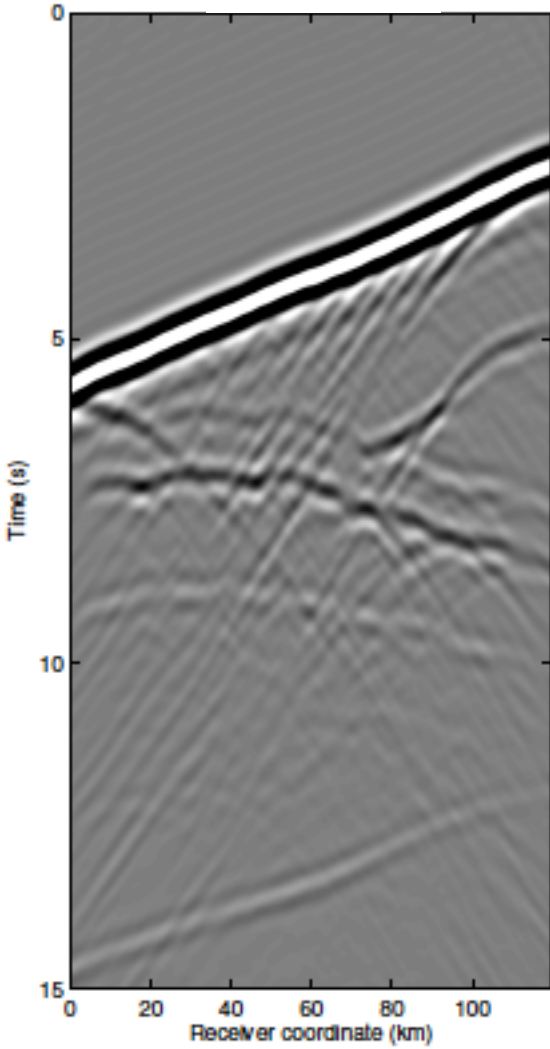


Wavespeed perturbation (smooth part of model)

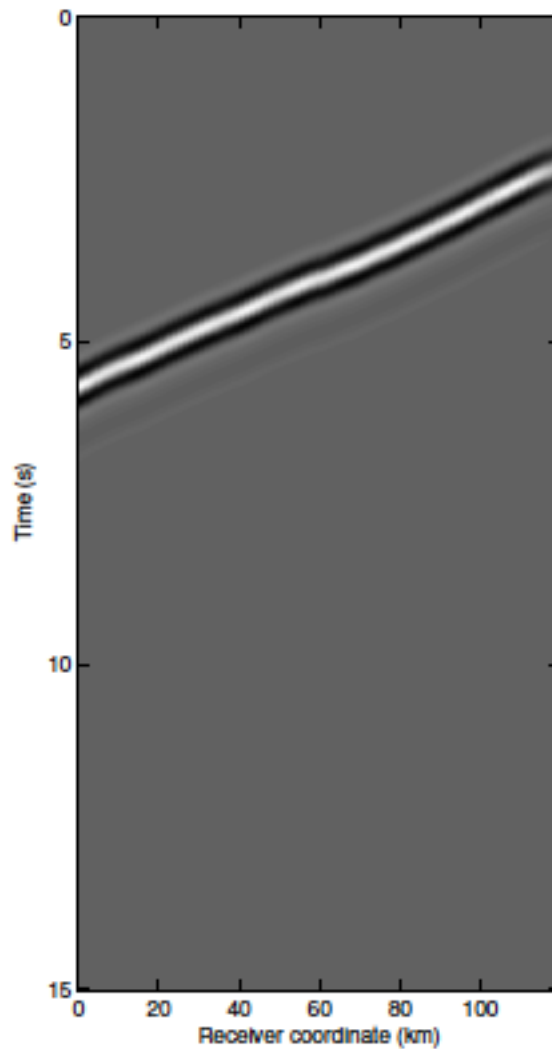


Separation of the direct and multiple fields: interferometry/cross-correlation

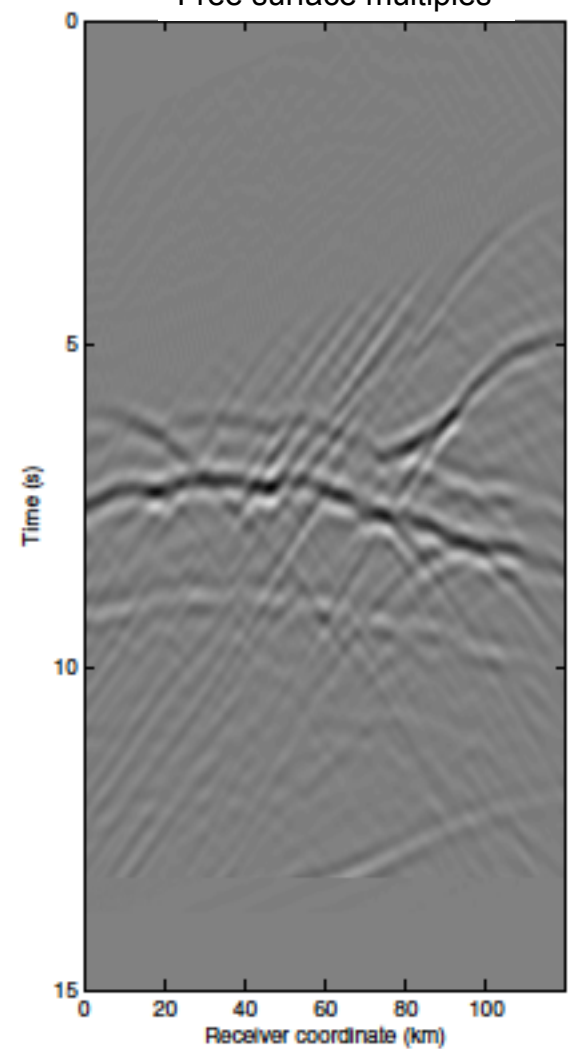
Full wavefield



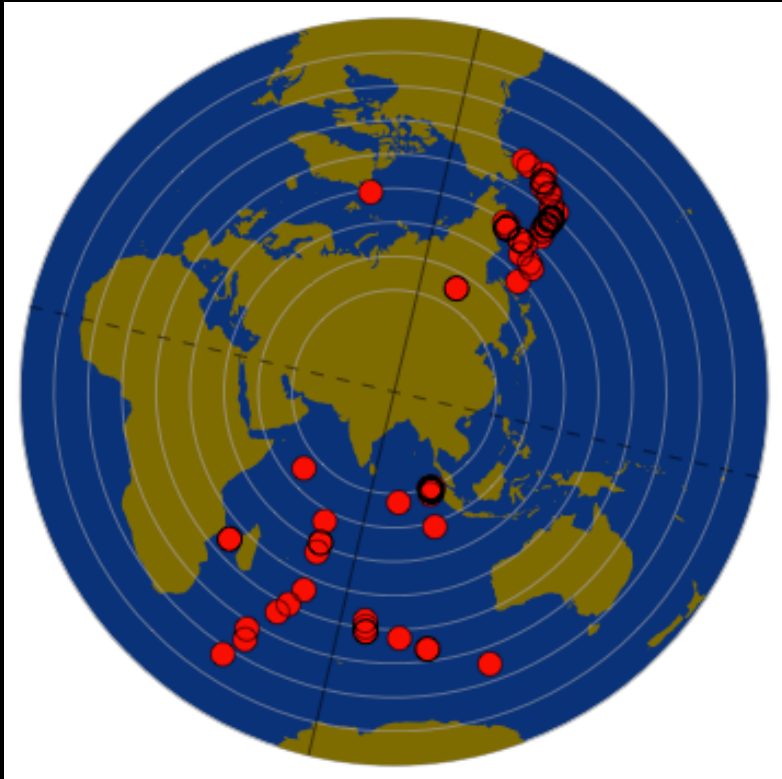
Incident wavefield



Free surface multiples



Challenges of teleseismic data

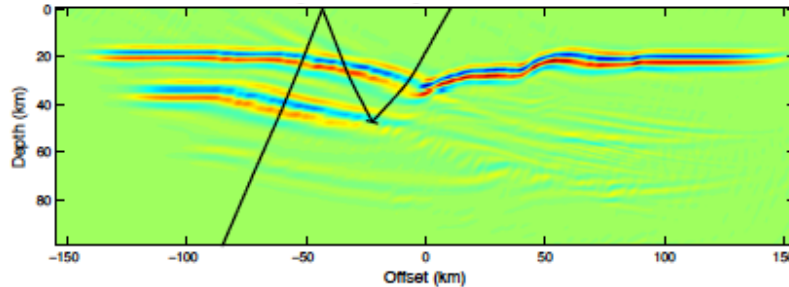


Events magnitude > 5.0
 $< 30^\circ$ from great circle arc

- 1) Limited global seismicity & irregular array configurations \rightarrow limited angular and azimuthal data \rightarrow **Angle domain annihilation not effective**

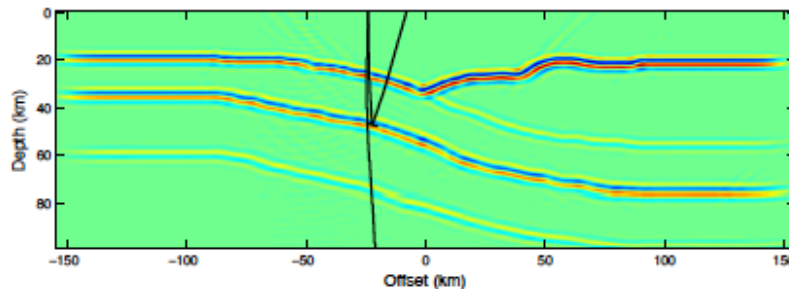
Single source images formed using inverse scattering for teleseismic sources arriving from different directions

Single source image for 23.7 deg incidence



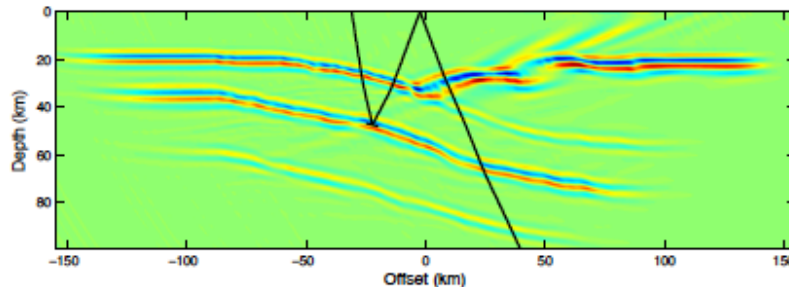
(a)

Single source image for 1.3 deg incidence



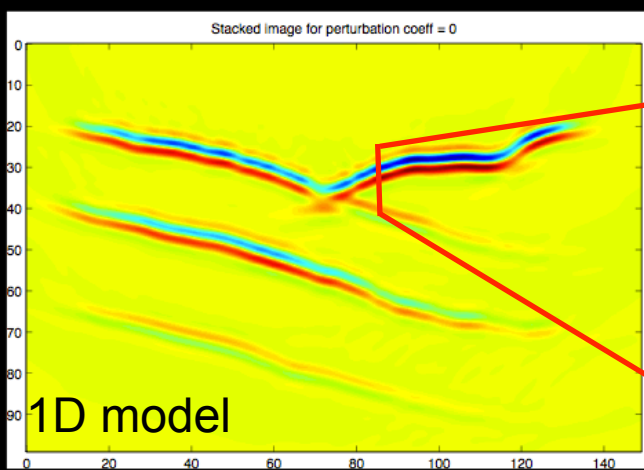
(b)

Single source image for -22.7 deg incidence

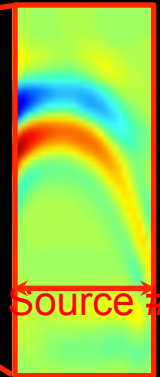


Power norm error function

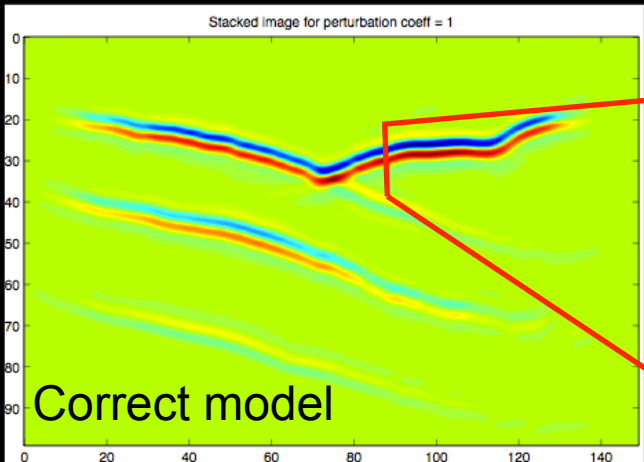
- **correlation of images** sources → **maximum correlation gives best optimal velocity model**
- More robust than error function based on depth move-out (angle domain annihilation)



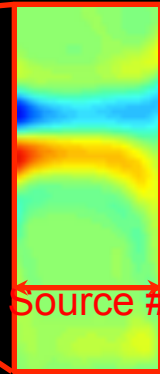
Too fast



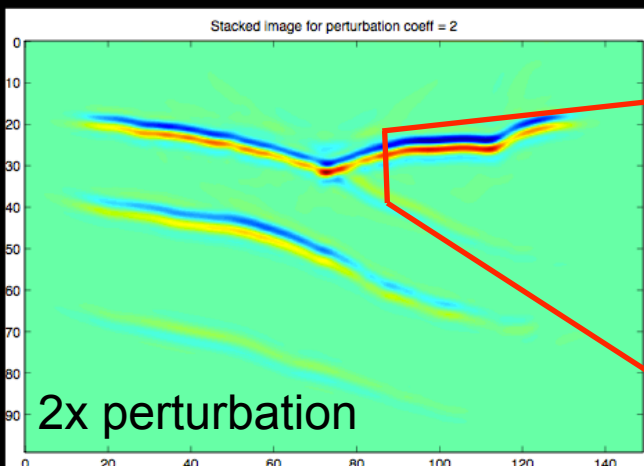
Residual moveout in source-index image gathers



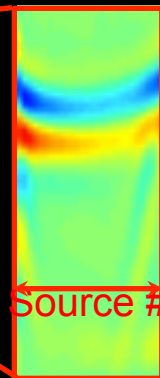
Just right



Incorrect model creates measurable moveout in single-source images



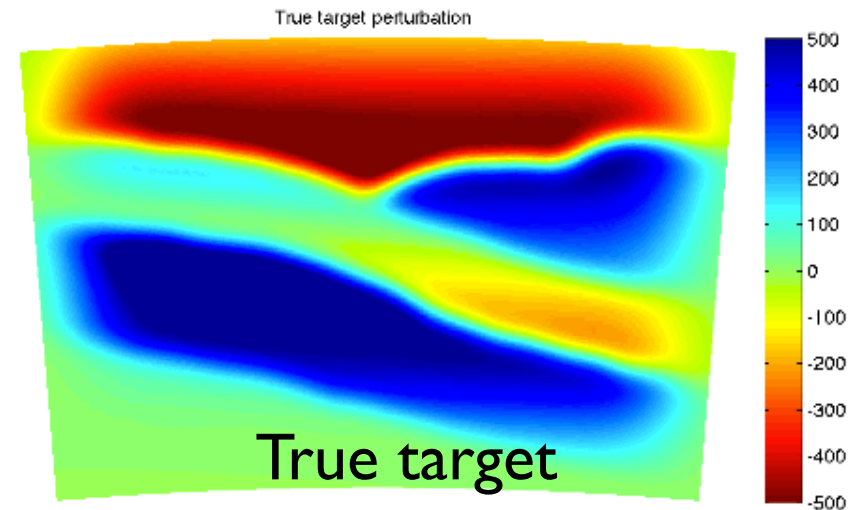
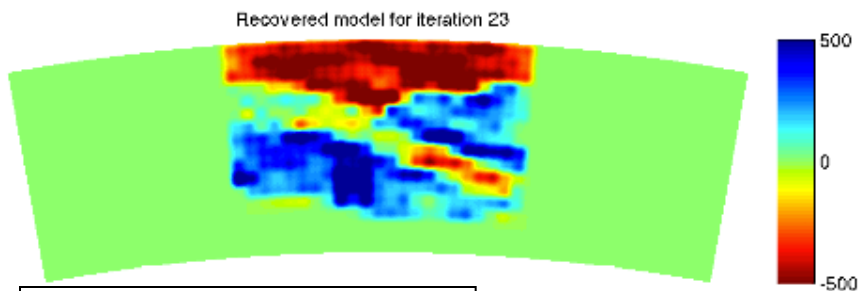
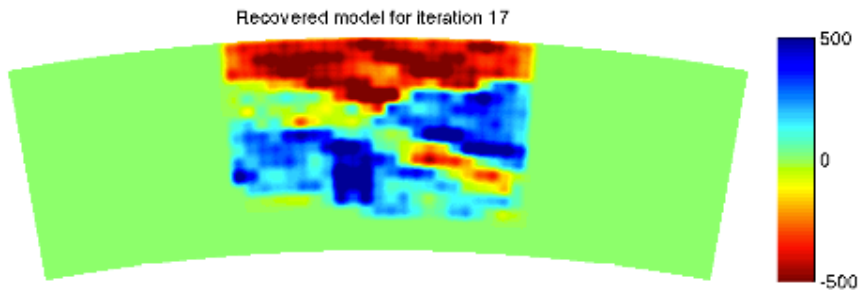
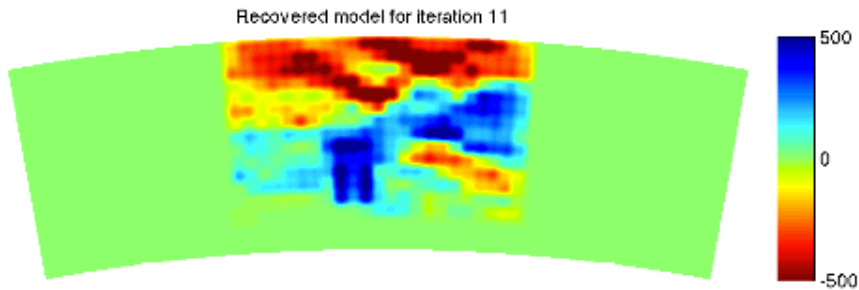
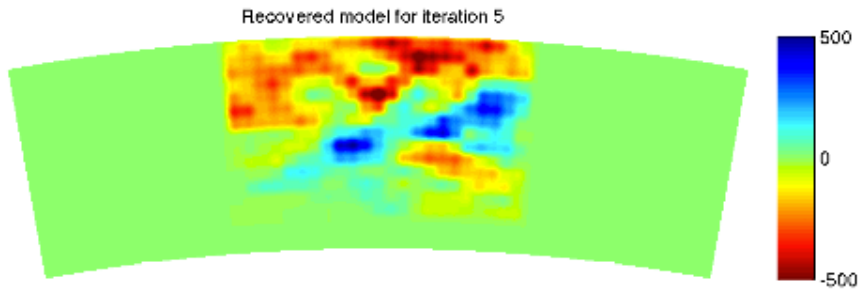
Too slow



Best way to quantify error? → misfit criterion

Preliminary results

Inversion with fine basis,
spherical coordinates



Overview of lecture:

1. Introduction/background

2. Ambient noise and surface wave tomography (MIT, 2005-2015)

- Traditional transmission tomography:

- combining ambient noise and earthquake data
- quantifying and correcting for uneven noise distribution
- azimuthal anisotropy
- radial anisotropy

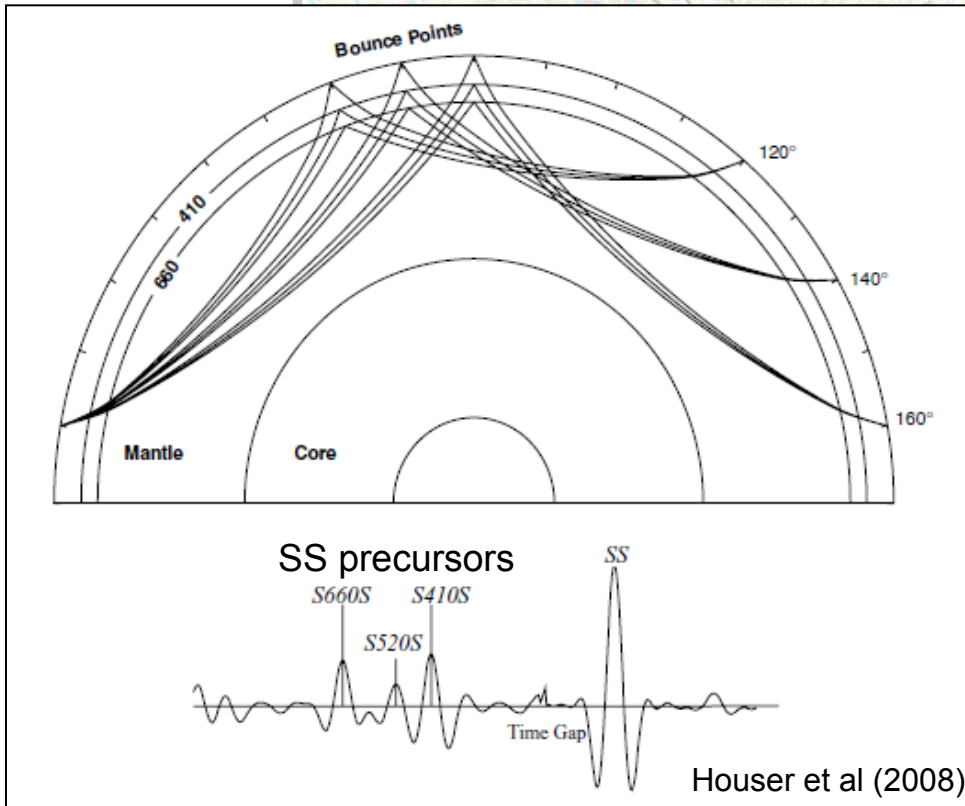
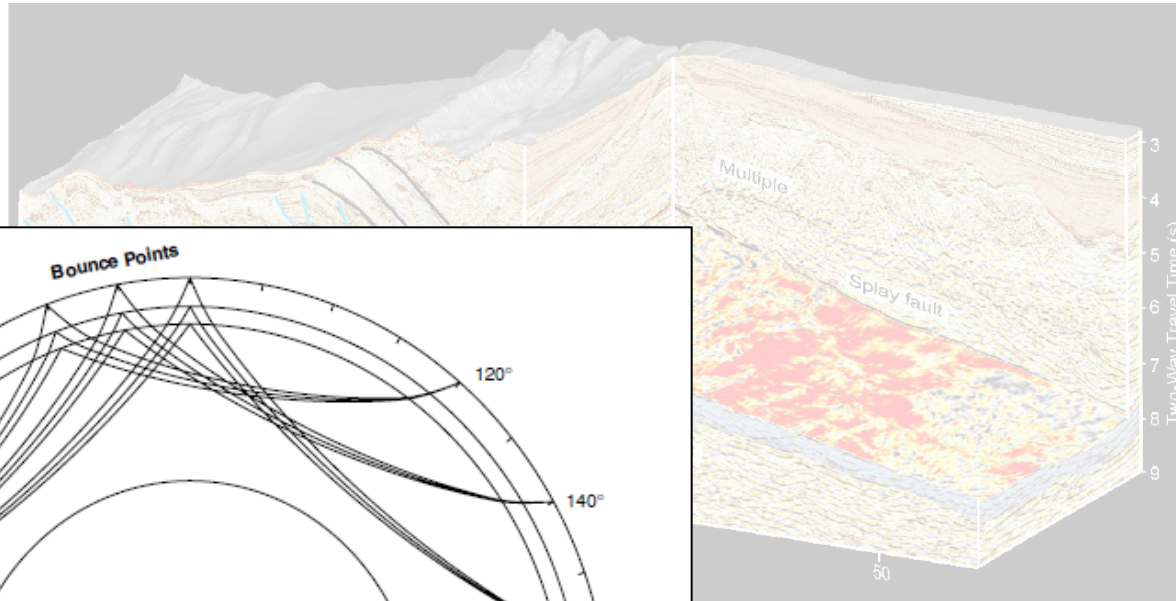
- Eikonal tomography

- Adjoint tomography with ambient noise data

3. Interferometry of teleseismic body waves

4. Imaging with multiples – just some thoughts

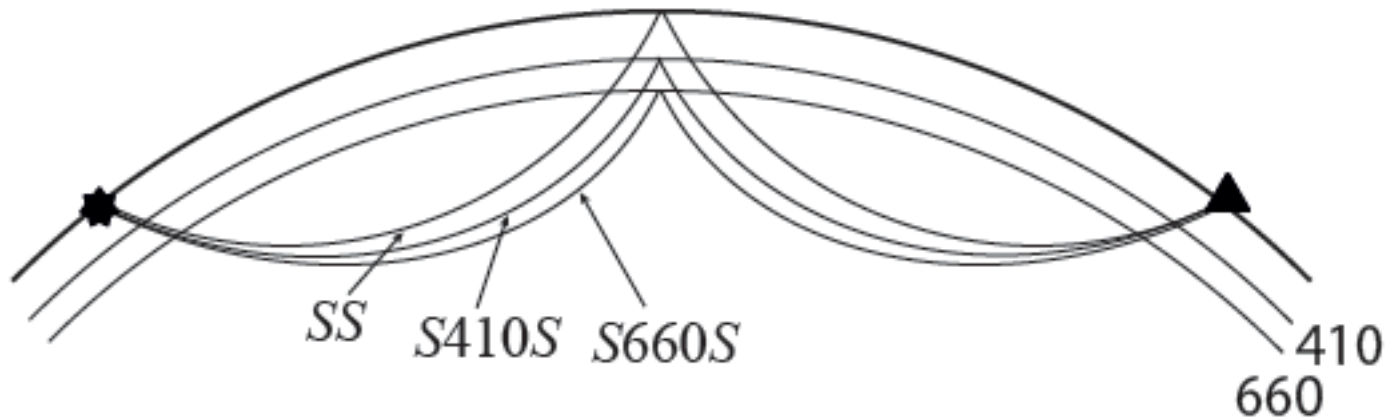
With the many terabytes of seismic data from global networks ...
... can we do high-resolution exploration seismics in the mantle?



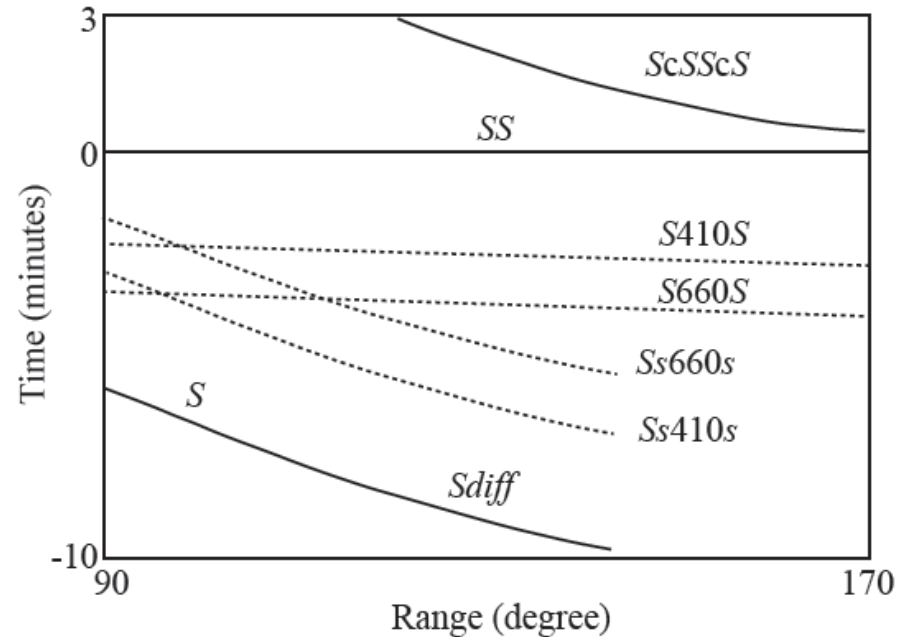
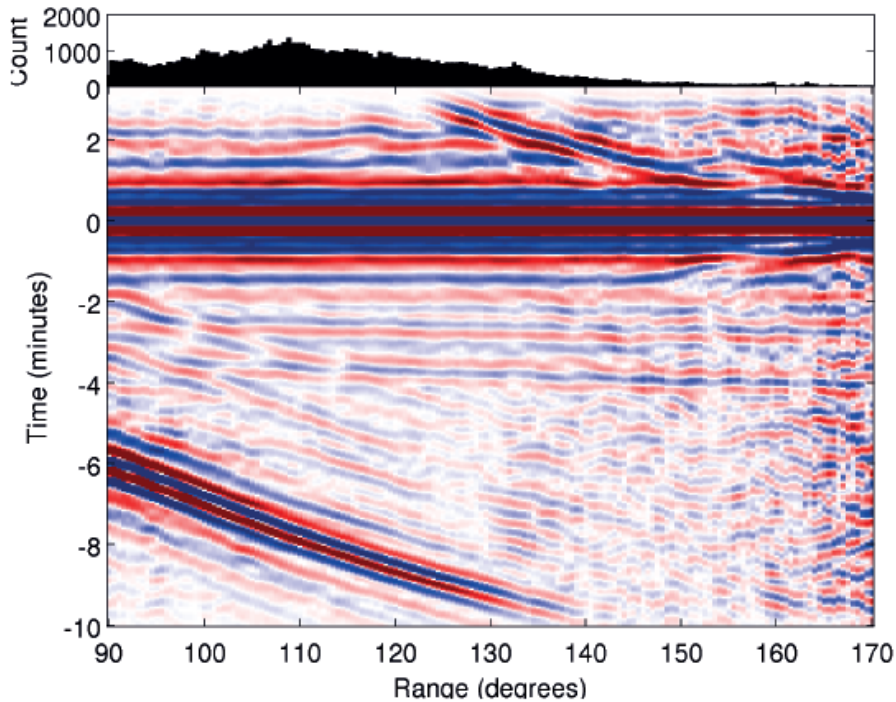
**Imaging the Transition Zone
with the SS wavefield
(i.e., underside reflections)**

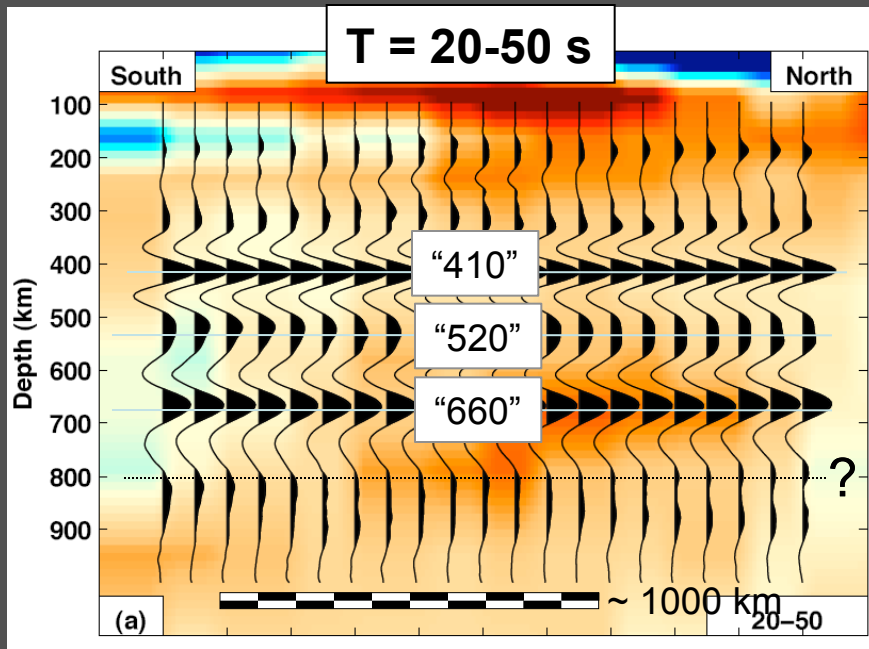
PhD Research: Cao Qin, Yu Chunquan
(supported by CSEDI and CMG Programs of National Science Foundation)

Transition zone imaging with SS precursors

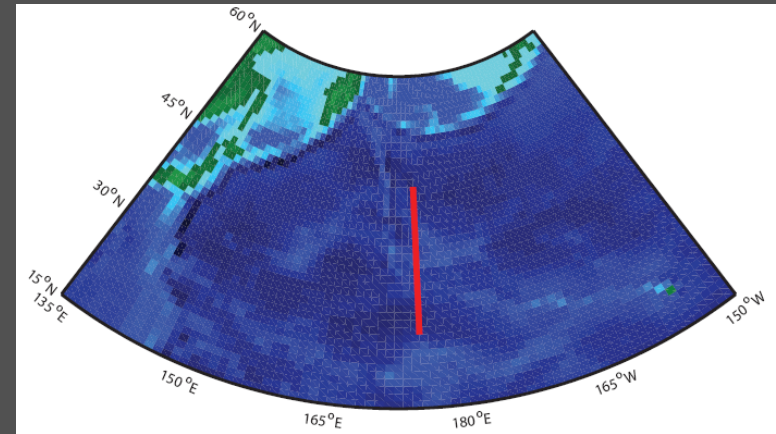


SS stacks





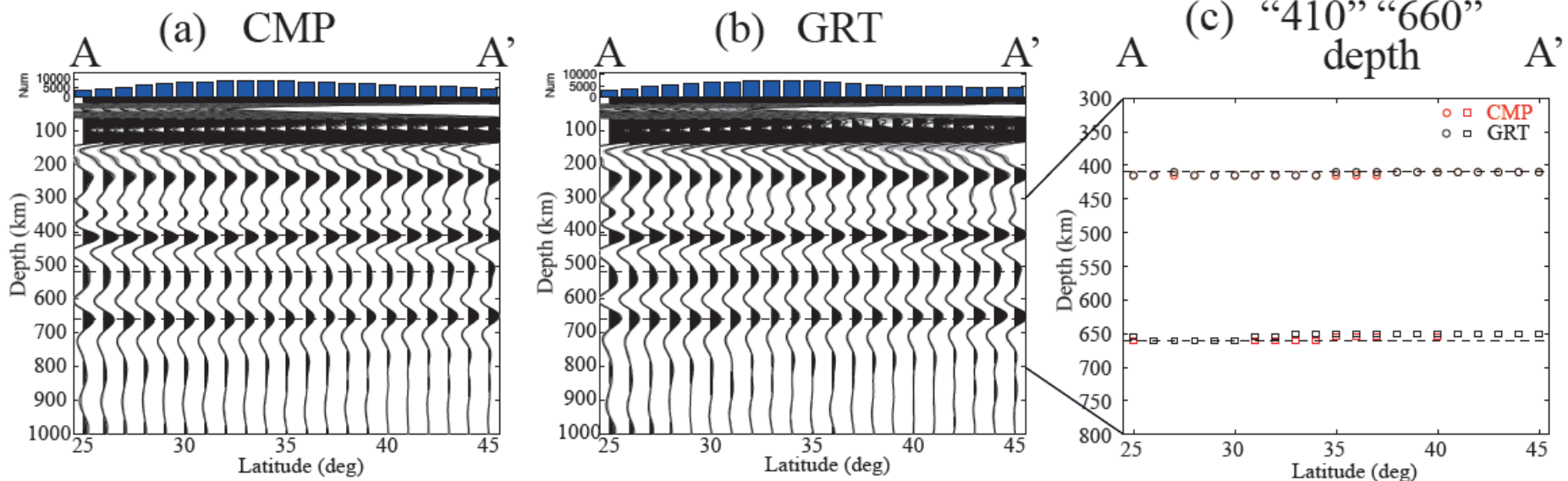
reflection seismology with SS data

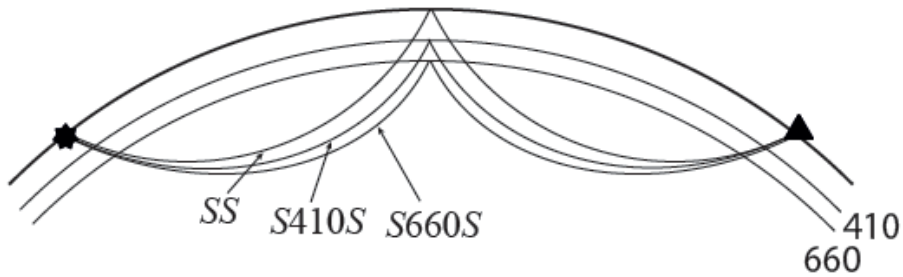


Cao et al. (PEPI, 2010)

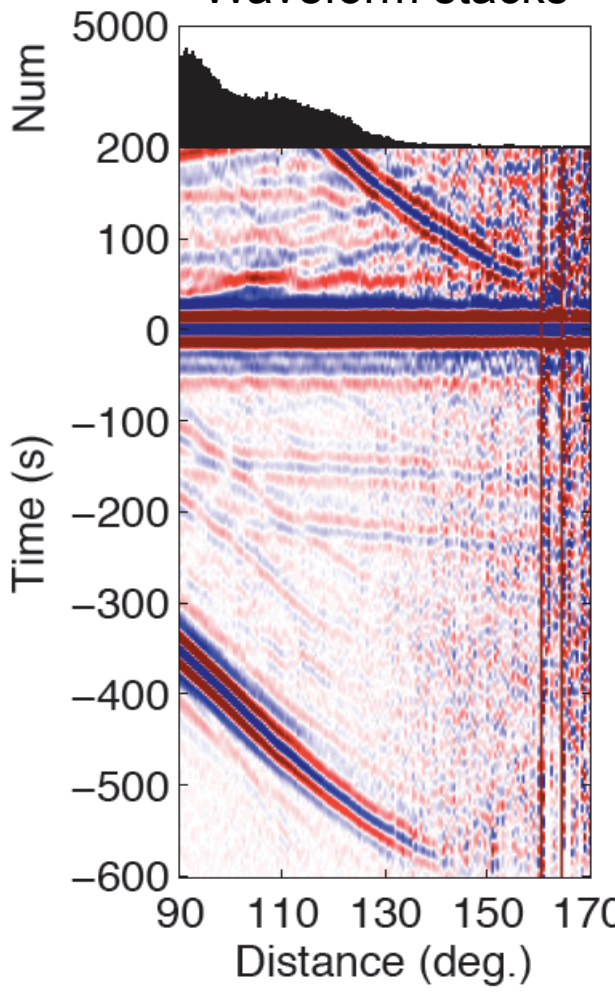
(data - IRIS-DMC)

Shang et al (in prep)

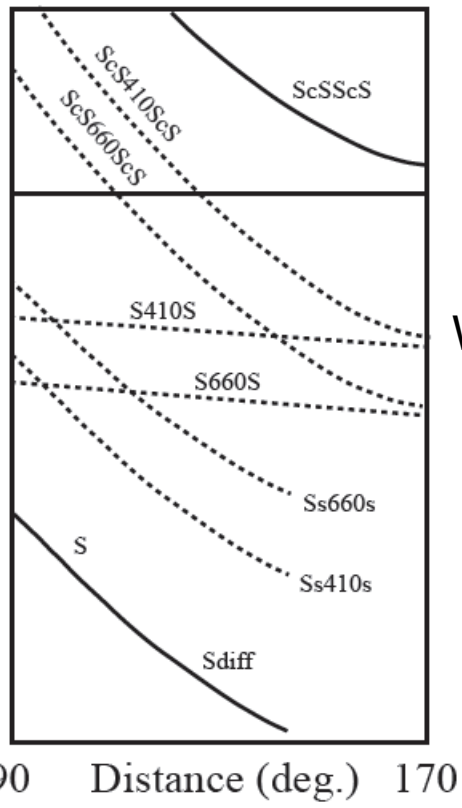




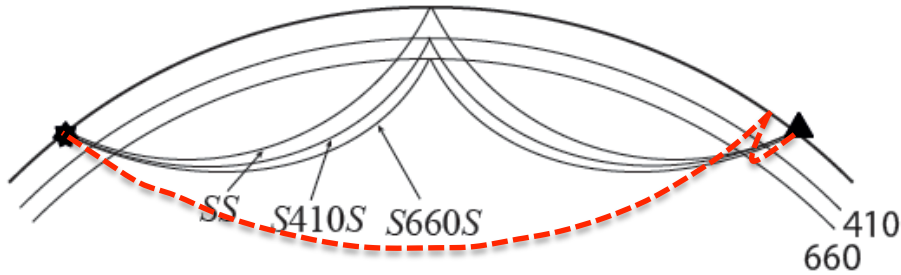
Waveform stacks



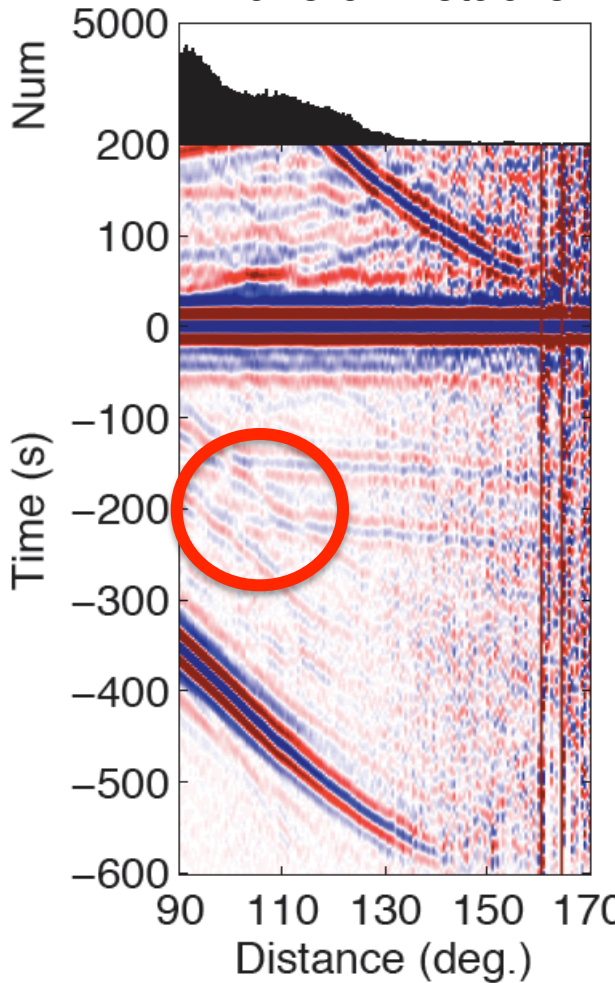
Travel times



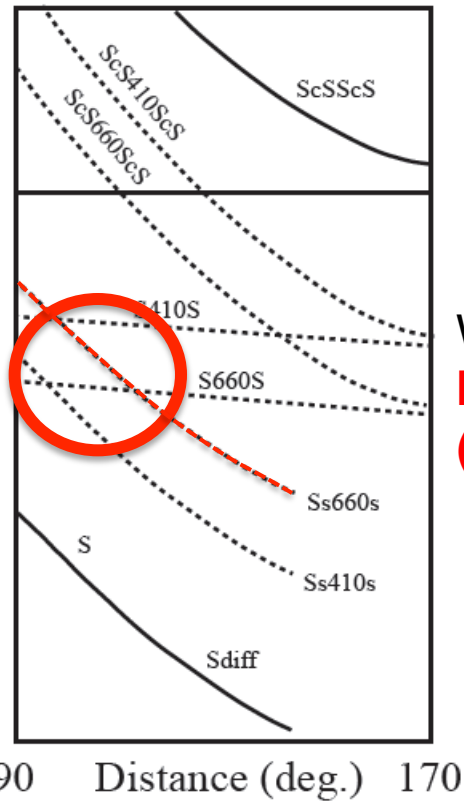
What can go wrong?



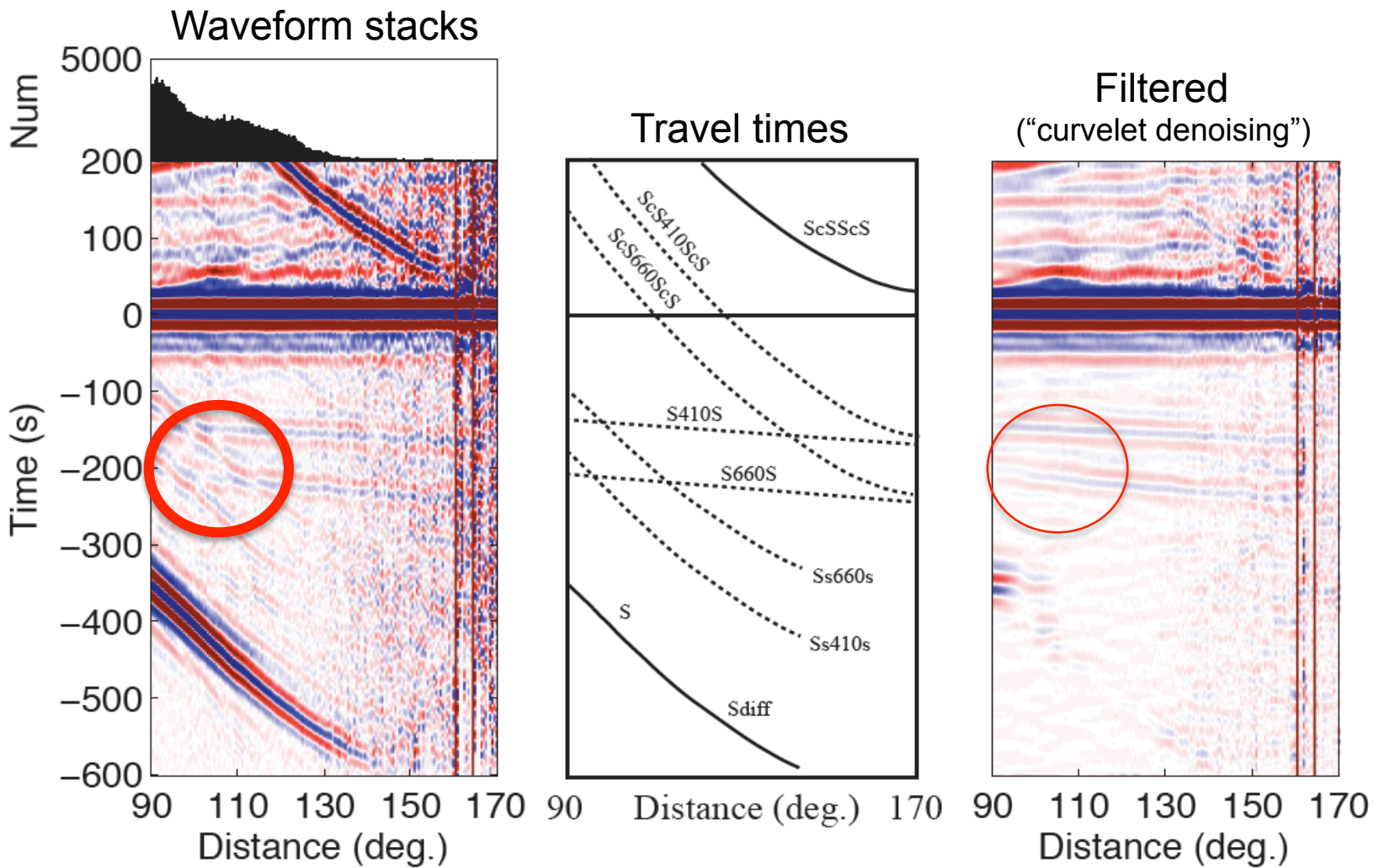
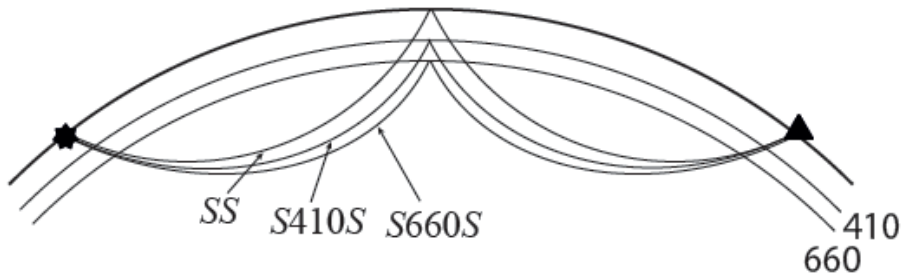
Waveform stacks

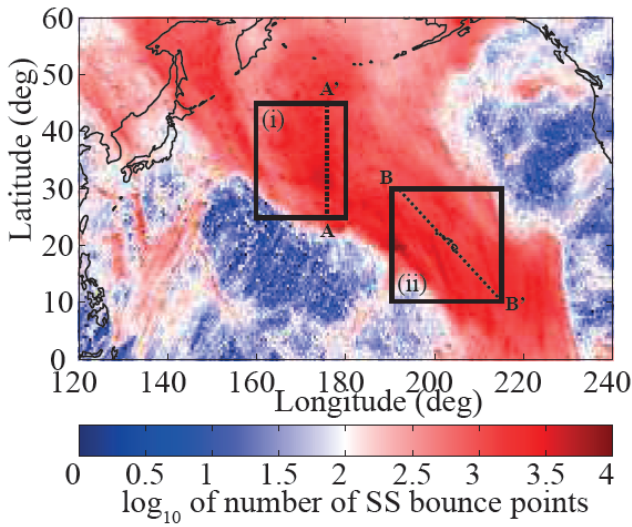


Travel times

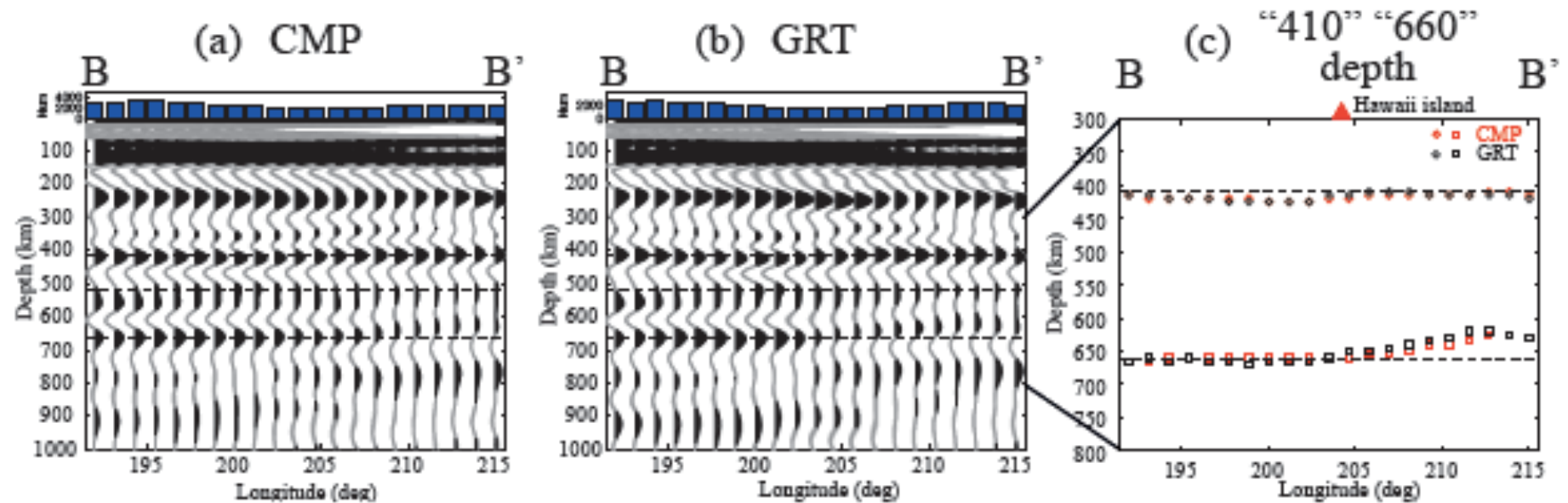


What can go wrong?
Interfering phases!
(e.g. multiples)



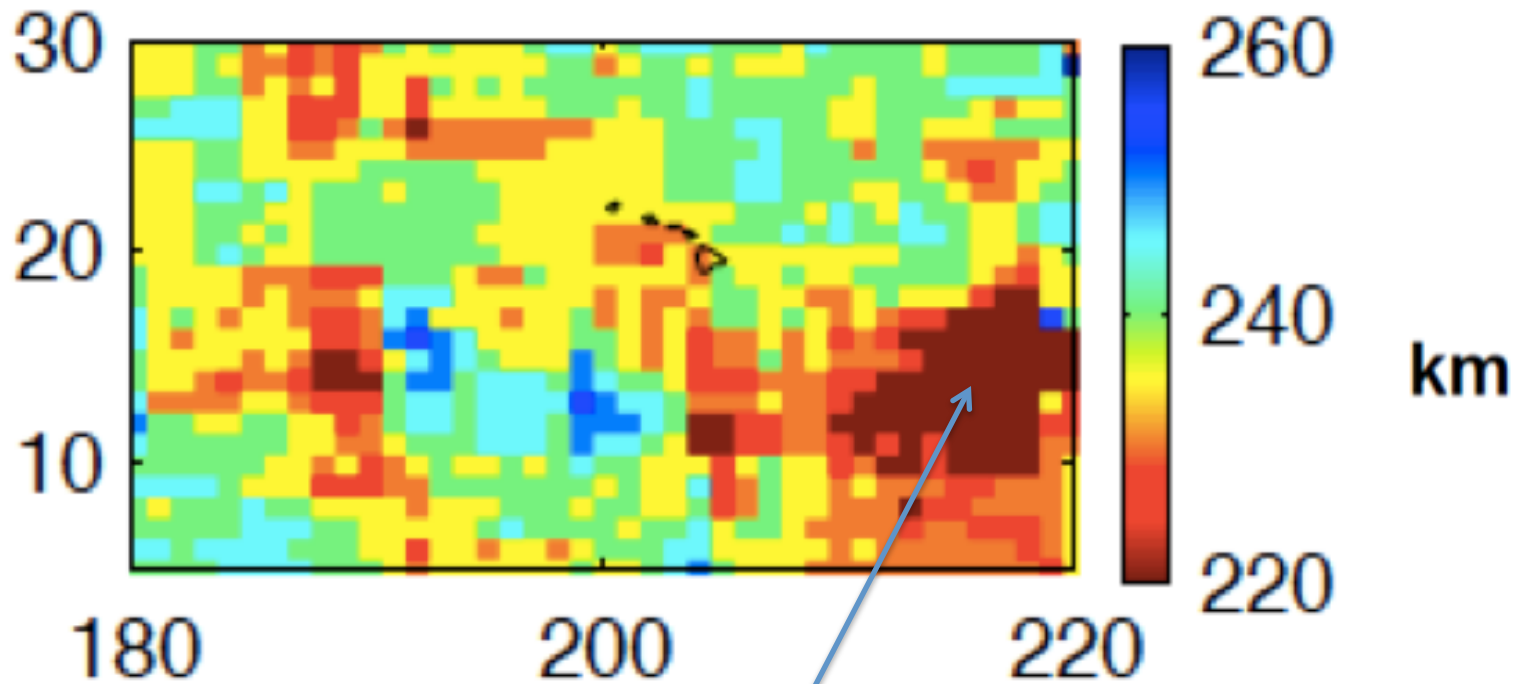


Latest results for Hawaii
(Chunquan Yu, MIT)



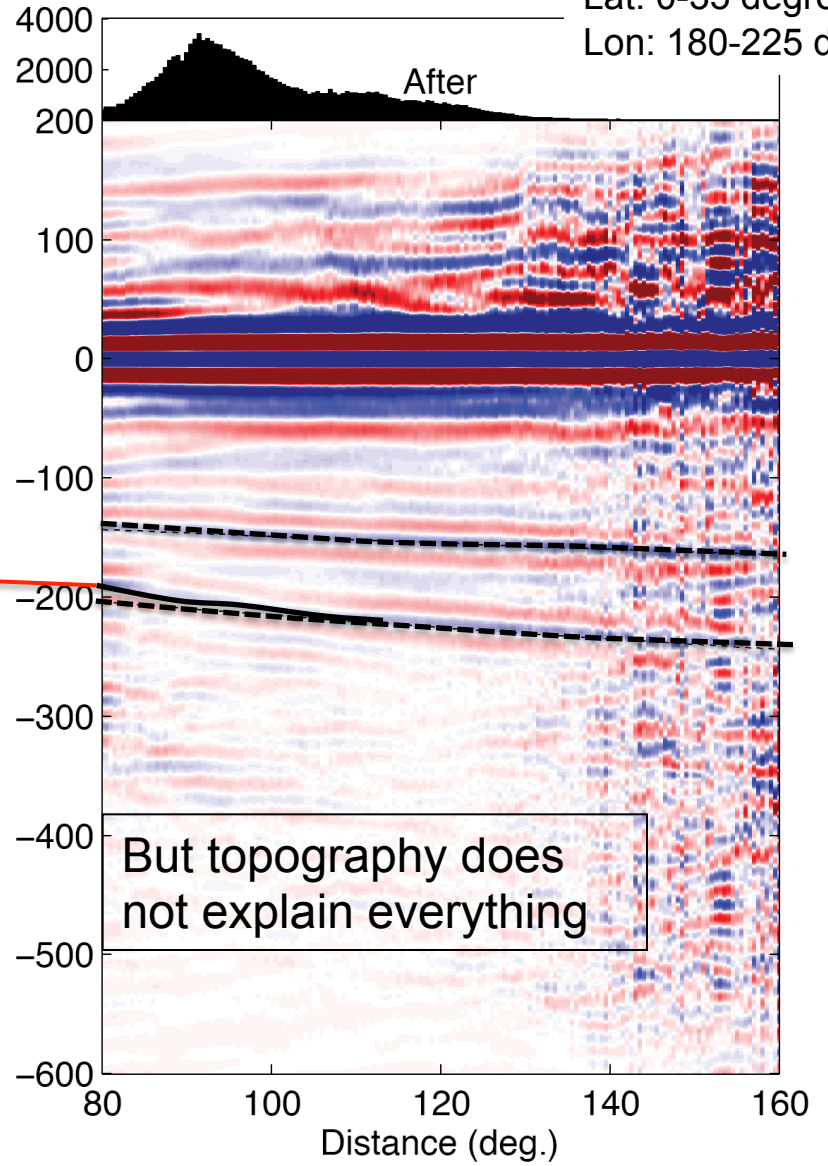
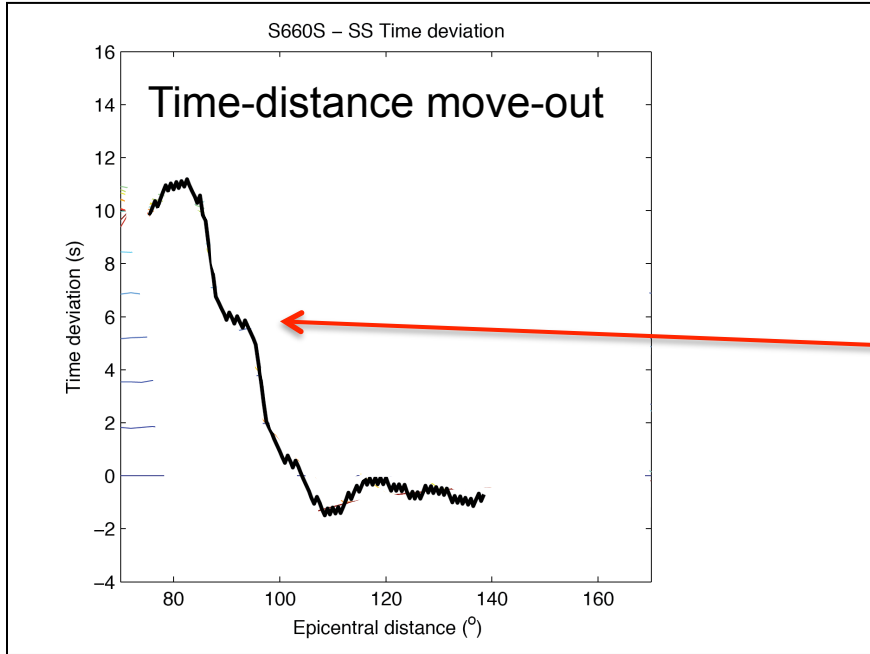
B-B': Hawaii – Central Pacific

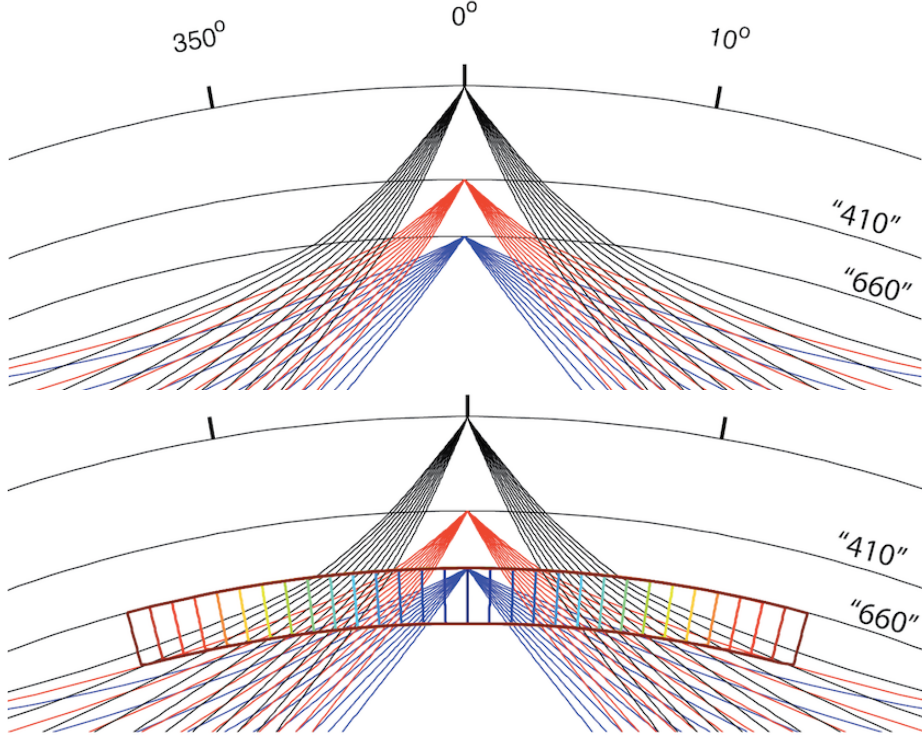
Preliminary result: Yu Chunquan (MIT)



Thin transition zone SE of Hawaii → high temperatures?

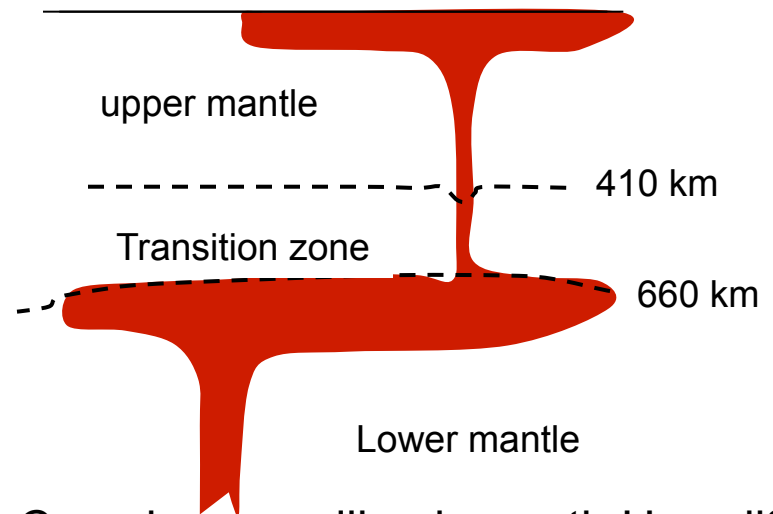
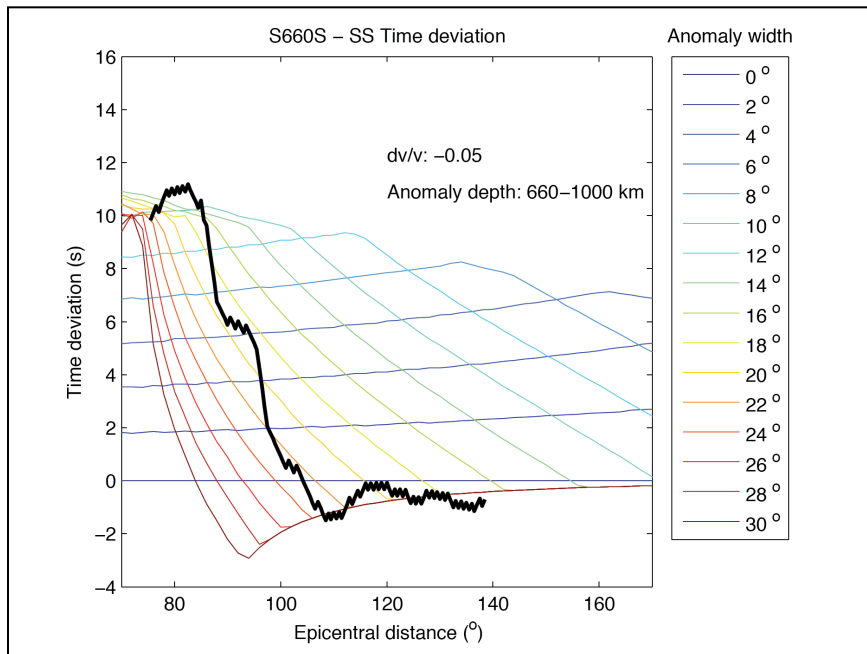
Stack area:
Lat: 0-35 degrees
Lon: 180-225 degrees



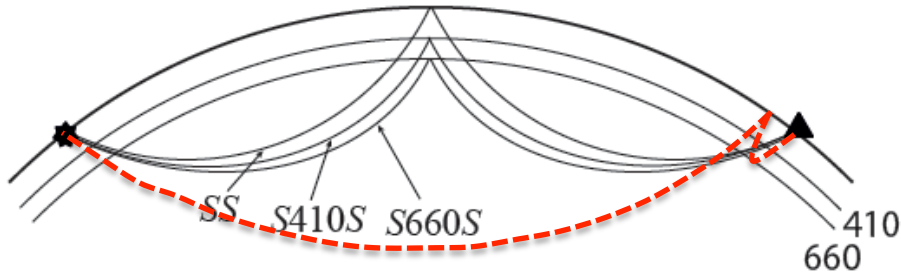


Move-out in exploration seismics?
 → Find the move-out velocity!

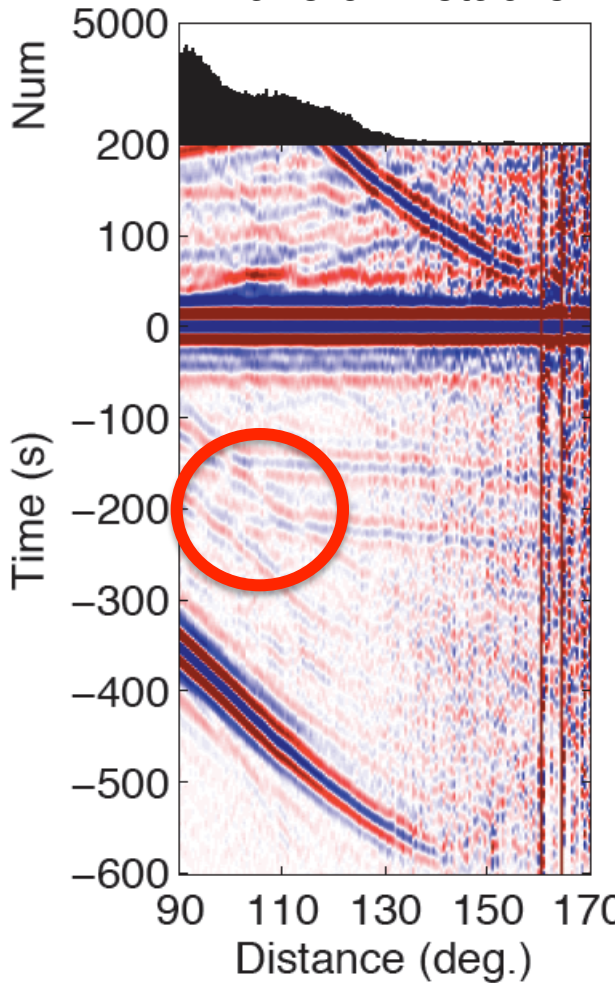
→ Low velocity zone below “660”
 (of varying horizontal extent)



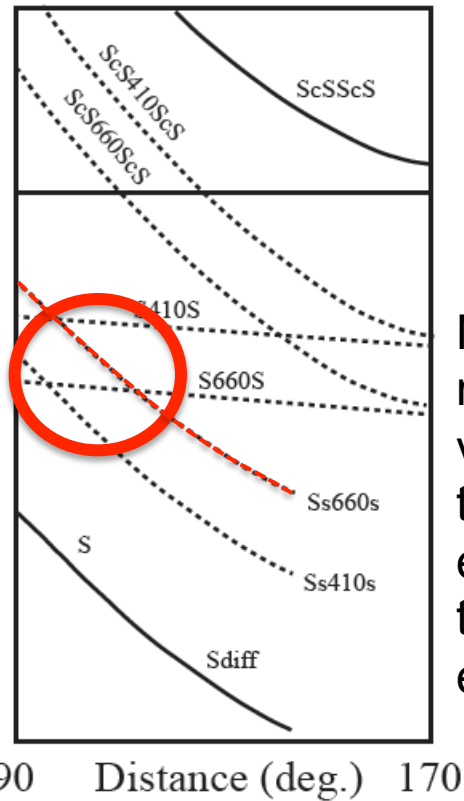
Complex upwelling beneath Hawaii?



Waveform stacks

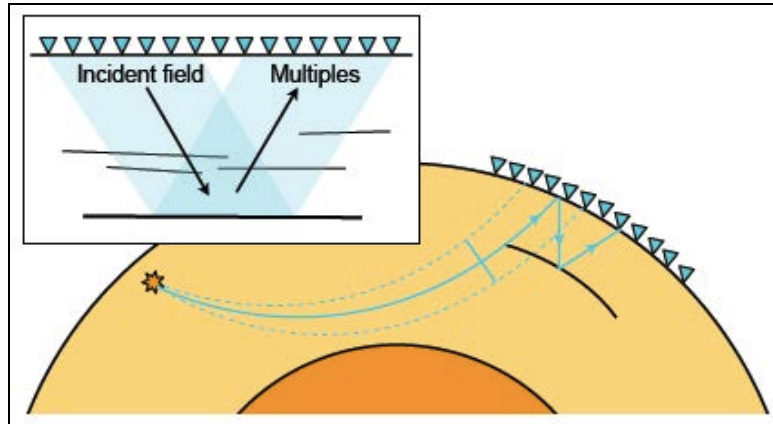


Travel times



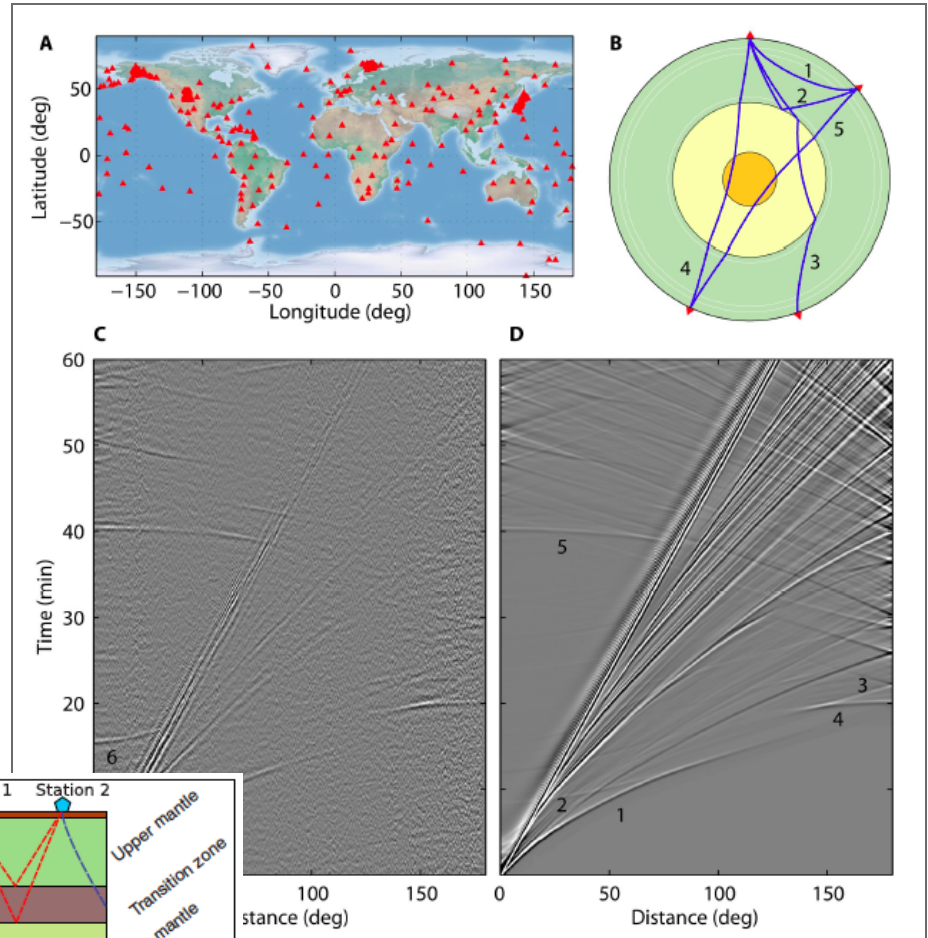
Next step: use the multiples for imaging or velocity analysis (e.g. using the method for wave equation reflection tomography due to Burdick et al. (GJI, 2014))

Cargese ~~2015~~ (or 2017)?

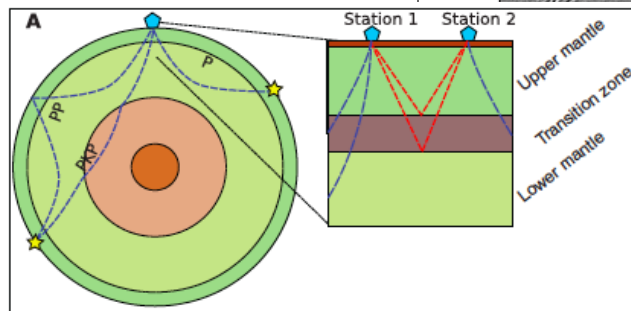


Burdick et al (GJI, submitted)

+



Poli et al (Science, 2012)



Boué et al. (2014)